NIST-GCR-92-604

Ignition and Flame Propagation Studies Over a Flat Fuel Surface

Bryan Thomas Amos

United States Department of Commerce
Technology Administration
National Institute of Standards and Technology

NIST-GCR-92-604

Ignition and Flame Propagation Studies Over a Flat Fuel Surface

Bryan Thomas Amos

University of Californiay
Department of Mechanical Engineering
Berkeley, CA 94720

Issued March 1992

Sponsored by:
U.S. Department of Commerce
Barbara Hackman Franklin, *Secretary*
Technology Administration
Robert M. White, *Under Secretary for Technology*
National Institute of Standards and Technology
John W. Lyons, *Director*

Notice

This report was prepared for the Building and Fire Research Laboratory of the National Institute of Standards and Technology under grant number 60NANB7D737. The statements and conclusions contained in this report are those of the authors and do not necessarily reflect the views of the National Institute of Standards and Technology or the Building and Fire Research Laboratory.

Ignition and Flame Propagation Studies
Over a Flat Fuel Surface

By

Bryan Thomas Amos
B.M.E. (Georgia Institute of Technology) 1980
M.S. (University of California) 1983

DISSERTATION

Submitted in partial satisfaction of the requirements for the degree of

DOCTOR OF PHILOSOPHY

in

ENGINEERING

in the

GRADUATE DIVISION

OF THE

UNIVERSITY OF CALIFORNIA, BERKELEY

Approved: A. C. F. Vella 8/26/87
Chairman Date

R. B. Williamson 9/9/87

Patrick J. Pagni 9/23/87

.....

ACKNOWLEDGEMENTS

I would like to express my sincere gratitude to Professor A. C. Fernandez-Pello for his patience, encouragement, and guidance and without whom the completion of this thesis would not have been possible. Also I would like to thank my predecessor, Hisashi Kodama, for his help in my learning about many of the numerical methods employed in this thesis. I would also like to thank Professor R. Brady Williamson, and Professor Patrick J. Pagni for their review of this thesis. Professor Pagni deserves special acknowledgement for his help in the non-dimensionalization of the equations and his suggestions on how to organize the thesis.

Finally several of my fellow graduate students, Roger Rangel, Cory Dunsky and Betsy Cantwell deserve thanks for their suggestions and encouragements.

This work was supported by the Center for Fire Research in the U.S.D.O.C., National Bureau of Standards under Grant No. NB83NADA4020 and by an IBM-DACE Grant.

TABLE OF CONTENTS

Nomenclature

A	Non-dimensional absorption coefficient
a_λ	Dimensional absorption coefficient
B	Frequency factor in the chemical reaction rate expression
b	Coefficient in the discretization equation, defined in Eq. (2.5).
C	Source term in the discretization equation
c_p	Specific heat
D	Diffusion coefficient
Da	Damkohler number
E	Activation energy
F	u/x, defined by Eq. (4.8)
H	Ratio of non-dimensional heat of combustion to non-dimensional heat of vaporization
I	Non-dimensional radiant intensity at outer boundary
i	Intensity of radiation
L_b	Distance from the outer boundary to the fuel surface in the stagnation point problem
L_v	Latent heat of vaporization
Le	Lewis number
MW	Molecular Weight
P	Pressure
P_x	x-direction pressure variable defined in Eq. (4.10)
P_y	y-direction pressure variable defined in Eq. (4.10)
Pec	Numerical Peclet number based on grid size, defined by Eq. (2.6)
PF	Chemical power generation per unit area of fuel surface

Pr	Prandtl number
Q	Heat of combustion
R_μ	Universal gas constant
Re	Reynolds number
S	Non-dimensional fuel-oxygen ratio
T	Temperature
t	Time
u	x-direction velocity
v	y-direction velocity
V_b	y-direction velocity at the outer boundary of the stagnation point flow problem
w	Reaction rate
x	Spatial coordinate parallel to wall
y	Spatial coordinate perpendicular to wall
Y	Mass fraction

Greek Symbols

α	Non-dimensional heat of combustion
β	Non-dimensional activation energy
λ	Thermal conductivity
η	Similiarity variable
ρ	Density
δ_y	Grid size in the y-direction
δ_x	Grid size in the x-direction
ν	Stoichiometric coefficient
μ	Viscosity

Subscripts

b	Quantity evaluated at the outer boundary of the stagnation point problem
c	Denotes characteristic quantity
E	Denotes a quantity on the east side of the grid point under consideration
F	Quantity related to fuel
FT	Refers to the mass fraction of fuel present in the fuel wall
N	Denotes a quantity on the north side of the grid point under consideration
P	Denotes the grid point under consideration
o	Quantity related to oxygen
S	Denotes a quantity on the south side of the gridpoint under consideration
v	Quantity evaluated at the vaporization point of the fuel
W	Denotes a quantity on the west side of the grid point under consideration
w	Quantity evaluated at the fuel wall
∞	Quantity evaluated far from the wall in the one-dimensional problem
1,2	Refers to state 1 or state 2, respectively

Superscripts

o	Refers to a quantity evaluated at the old timestep

Other

$\overline{T}$	Dimensional variable
T	Non-dimensional variable

Ignition and Flame Propagation Studies Over a Flat Fuel Surface

Bryan T. Amos

ABSTRACT

Numerical studies are performed which show the evolution of the combustion process over a flat fuel surface subjected to an external source of radiation. Ignition is caused either by the high temperature of the fuel surface or by radiation absorption by the fuel vapor. The surface is assumed to be either in a zero gravity, initially stagnant air environment or in a stagnation point flow field. Regardless of the source of ignition considered or the type of the flow field, the same sequence of events is predicted. This sequence of events begins with a pre-ignition, radiation dominated phase in which fuel and air mix above the fuel surface. After ignition occurs, there is a period of weak chemical reaction, which is followed by a period of stronger reaction in which a premixed flame front develops. Before dying out the premixed flame front separates the fuel from the oxygen and leaves behind a diffusion flame.

The combustion and radiation processes are shown to have a large effect on the flow field in the stagnation point flow cases. For the case in which ignition is caused by gas phase absorption, the radiation required to cause ignition is so high that an opposed jet flow is created. In the case in which ignition is caused by the hot fuel surface, the radiation is

lower and the boundary layer remains almost intact. For both types of ignition the premixed flame fronts produced heat fast enough that the expanding gas is able to drive the incoming flow back from the fuel surface. After the premixed flame front dies out leaving the diffusion flame the incoming flow again dominates and a boundary layer reappears.

A. C. Fernandez-Pello
Chairman, Thesis Committee

1. Introduction

The combustion processes which occur over a vaporizing fuel surface have often been studied in the past. These studies have usually concentrated on the ignition aspect of the problem or upon the nature of the steady state diffusion flame which may exist over the surface. For instance, references (1-9) have analyzed the ignition process for a fuel surface in a one dimensional geometry, while references (10-12) have analyzed the ignition process when the fuel surface is subjected to a stagnation point flow. References (12-17) have analyzed steady state diffusion flames in stagnation point flows while references (18-24) have studied these flames experimentally. No studies were found which tried to analyze the processes which occur after ignition and before the steady state diffusion flame is obtained.

While it is important to understand the ignition process and the structure and character of the steady state diffusion flame, it seems equally important to understand the processes which occur between the ignition point and before the steady state is reached. To study these processes requires that the entire combustion problem, from a quiesant initial condition to the diffusion flame, be considered. The purpose of this thesis is to solve and present the results of two problems in which the entire combustion problem over a flat fuel surface is analyzed. These problems will not only consider the ignition process, but will also identify regimes which occur in the post-ignition events,

and show how these regimes are related to one another. By studying these regimes, the sequence of events leading to the development of the steady state diffusion flame can be determined.

The problems are shown schematically in Figs. (1.1) and (1.2), respectively. The first problem considers a fuel surface initially in cold ambient air. At time, t=0, radiation is applied to the surface causing it to vaporize and mixing fuel vapor with air. The fuel-air mixture is then ignited in one of two different ways: i)the fuel vapor absorbs a fraction of the incoming radiation so that the mixture becomes hot enough to ignite, or ii) the vaporization temperature of the fuel vapor is high enough to cause ignition. Once ignition occurs, the chemical reaction becomes strong and premixed flame fronts will develop and propagate. The premixed flame fronts eventually burn themselves out leaving behind a diffusion flame. The post-ignition events are generally the same, regardless of the method of ignition used. However, the specific events which occur are highly dependent upon the method of ignition and also upon the parameters of the problem.

The second problem again considers a vaporizing fuel surface. In this case, however, the stagnant ambient air is replaced by a two dimensional stagnation point flow. This flow is generated by imposing a velocity perpendicular to the wall at a distance, L_b. Radiation is again applied to the fuel surface causing it to vaporize and the resulting fuel vapor mixes with

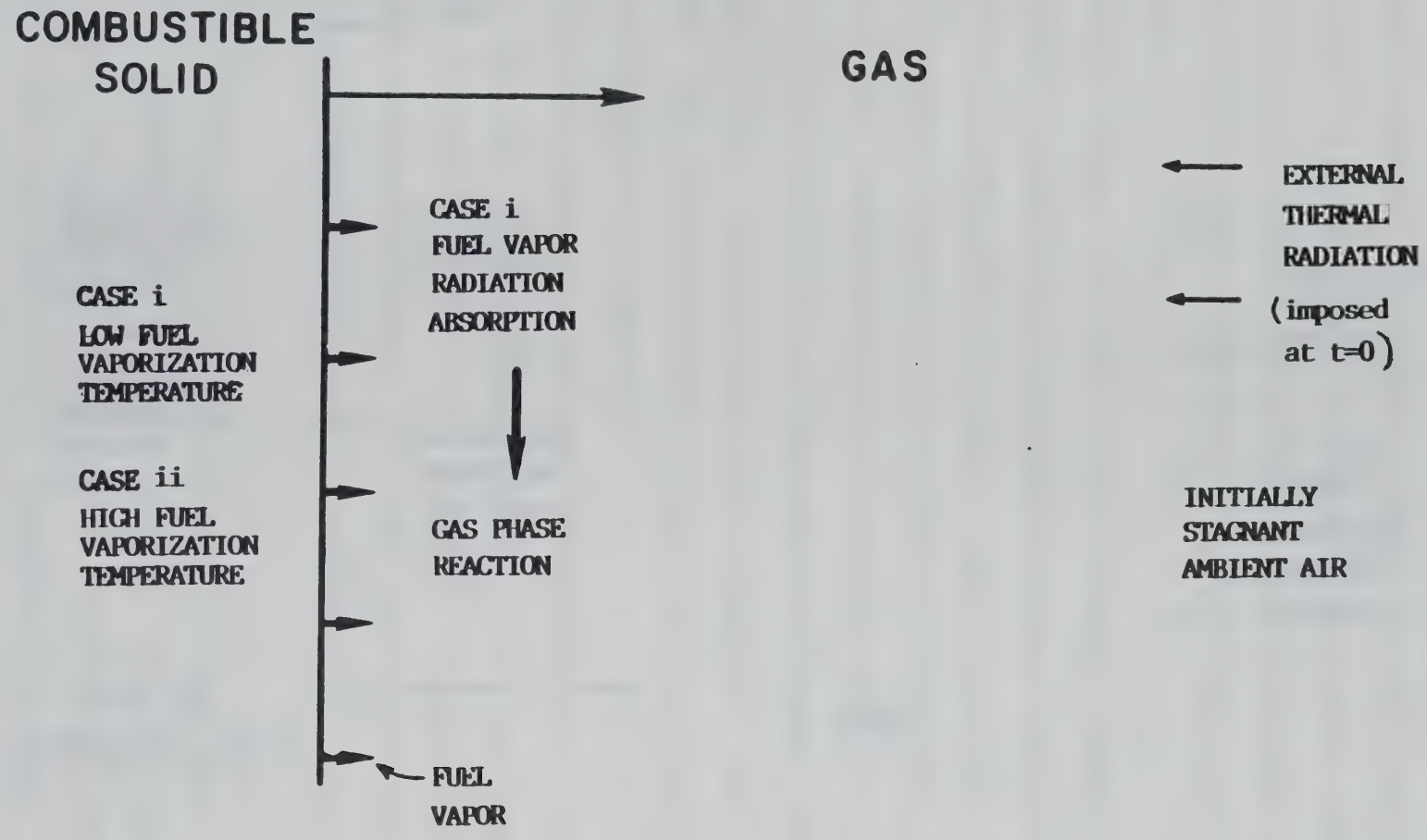

Figure 1.1 Schematic Diagram Illustrating the One Dimensional Problem

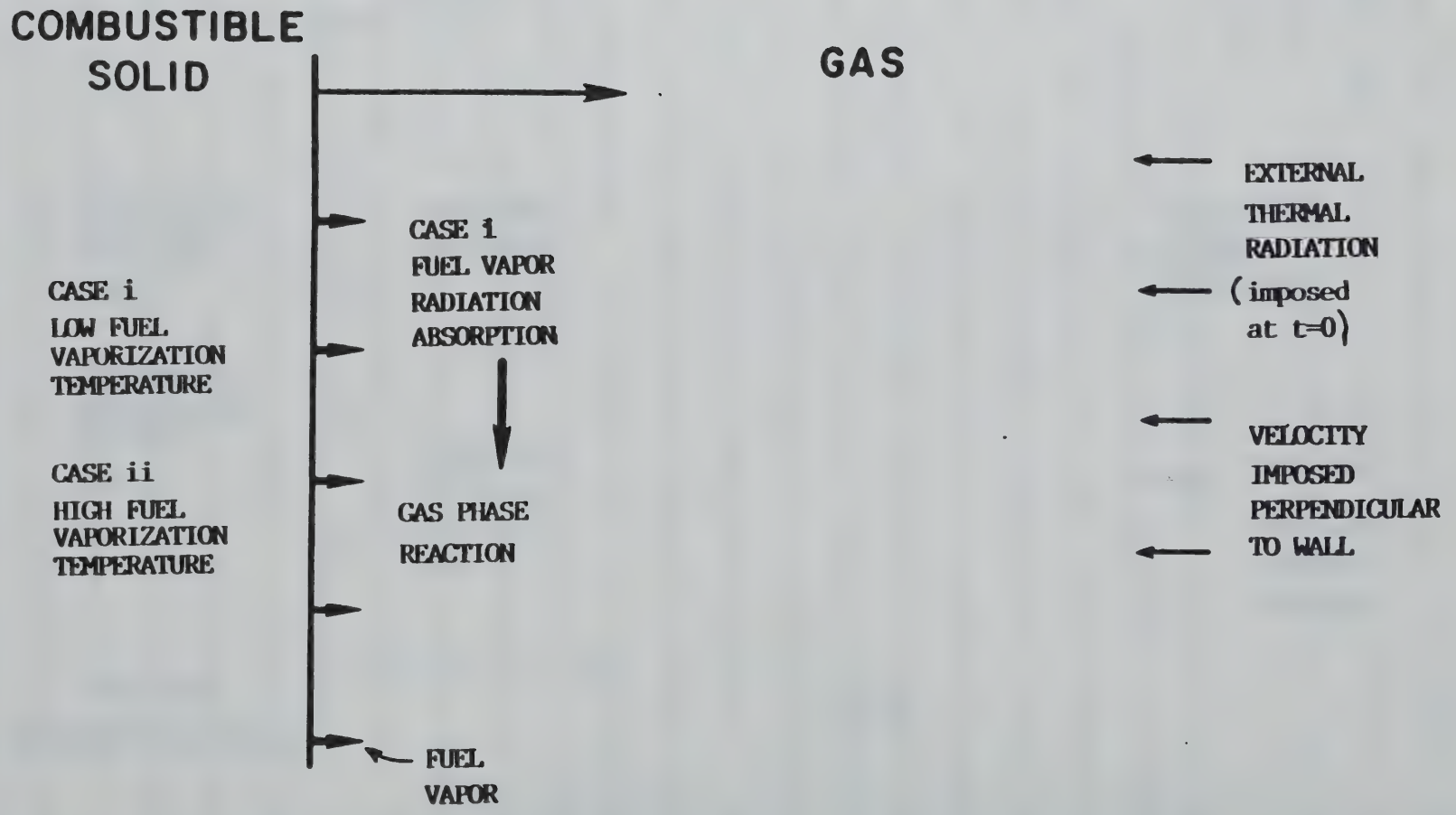

Figure 1.2 Schematic Diagram Illustrating the Stagnation Point Flow Problem

air. The same two methods of ignition are considered, with the post ignition events being generally similiar to those described above with the development of premixed flame fronts and a diffusion flame. However, the addition of a two dimensional flow field will be shown to significantly complicate the entire set of events.

These problems will be solved by first making appropriate assumptions to simplify the conservation equations along with their initial and boundary conditions. Then the equations are solved numerically according to the scheme discussed in the next chapter. The solution for the first and second problems will consist of temperature and mass fraction profiles showing their evolution from a quiescent state until a diffusion flame is obtained. The solution to the second problem will also show the evolution of the velocity profiles.

While the cases where ignition is caused by the hot fuel surface has been analyzed extensively,[1-9] the cases where ignition is caused by the gas phase absorption of radiation has only been studied experimentally.[12-18] Hence, several parametric studies on ignition by gas phase absorption will also be presented.

The solution to the above problems is difficult from a numerical standpoint because of the numerous time and length scales which are involved.[33] Williams(32) has shown that the premixed flame fronts which exist in the post-ignition phase of the problem, will have an large outer region which is dominated

by convection and diffusion and a much smaller inner region which is dominated by the chemical reaction and diffusion. Linan(15) has shown that the same regions exist for diffusion flames in which finite rate chemical kinetics are considered. These analyses were both performed under steady state assumptions. In the transient cases considered here, there are also disparate time scales which correspond to each of these regions. Hence, before proceeding with the presentation of the problems and their results, it is useful to first discuss the numerical techniques that must be employed.

2. Numerical Methods

2.1 Introduction

The problems which are addressed here tend to be computationally difficult because of the multiple time and length scales which are involved. As an example of these scales consider a premixed flame front which is moving in a stagnation point flow field. A velocity of say, .5 m/sec is imposed perpendicularly to the wall at 5 cm. A convective time scale for the overall flow may be taken as L_b/v_b or .10 sec. A diffusive time scale may be defined as

$$t_c = L_b^2 C_p / \lambda \qquad (2.1)$$

and is on the order of 60 seconds for air. Because of the premixed flame front there is also a thin region of rapid chemical reaction which has associated with it very small time and length scales. From reference (32), these length and time scales are

$$L_c = \left(\frac{(\rho D)_\infty T_\infty^2}{B Y_{O,\infty} e^{-\beta}} \right) \qquad (2.2)$$

and

$$t_c = \left(\frac{\rho_\infty T_\infty^2}{B Y_{O,\infty} e^{-\beta}} \right) \qquad (2.3)$$

respectively. For the fuels considered in this thesis, which are typical of hydrocarbon fuels, the length scale is on the order of 10^{-5} meters and the time scale is on the order of 10^{-6} seconds.

If the premixed flame is replaced by a diffusion flame with finite rate kinetics there is again a small region where a

chemical reaction takes place. While the reaction is not as rapid as in the premixed flame case because of the scarcity of reactants in the reaction zone, it is still much faster than the large-scale convective and diffusive processes. Thus, the diffusion flame is also computationally difficult to handle.

2.2 Review of Numerical Procedures

In the past at least three different methods have been used to solve problems with premixed flame fronts. These methods will be discussed in the order of the level of their sophistication. Generally, the more sophisticated a method is, the lower the computational time requirements. However, this sophistication also carries with it a loss of accuracy and detail.

The first and simplest method is a straight forward application of the finite difference scheme.[33] This method has the advantage of being the most accurate and will give a large amount of detailed information about the flame. The drawback of this method is that it has great difficulty in efficiently handling the multiple scales in the problem. For example the timestep in this method must be based upon the smallest time scale which is often the chemical time. Since the overall diffusion and convection processes must also be modeled over relatively long times, the method requires an extraordinarily large number of timesteps. Also the initial grid size must be based on the smallest length scale in the problem. Since this scale is the premixed flame length scale the initial grid will need to be very fine even though initially very little will be

happening in the problem. Thus, the computer program will often spend a large amount of time calculating values that may change little. Overall, this method will be quite expensive.

The second method which provides a solution to the initial grid size problem is the movable grid method described in references (34-35). In this method grid points are moved around based upon the temperature gradients with points being added in the regions of large temperature gradients and points being deleted in regions of small temperature gradients. The method has some of the advantages of the straight forward finite difference method such as being able to calculate the details of the flame fronts while saving computational time because the overall number of grid points is reduced. However, it is still restricted to using small timesteps and thus is computationally expensive, although less so than the first method. It is slightly less accurate than the first method producing a flame speed that may have an error of up to three percent.[34] Another drawback is that the programming required to adapt the grid to two spatial dimensions is quite complex with a corresponding increase in computational time. Since the problems considered here are all reducible to one spatial dimension and because of the advantages of obtaining large amounts of detailed information about the flames, this is the method of choice. It is discussed in more detail in the next section.

A third method which deserves mention is the flame discontinuity method developed by Chorin. In this method,

which is the most sophisticated method, the premixed flame front is treated as a discontinuity which is tracked through a coarse grid using a large timestep based upon flame speed. Because of the coarse grid and large timesteps, the computational savings over the first two methods are great. However, the details of the flame front are not calculated and a problem arises if the flame were to enter a very lean or very rich region where it will die out. In this case the flame front slowly changes from an approximate discontinuity to a front with finite gradients and the code must be 'fixed' to handle this situation. Nonetheless this is presently the only practical method available for transient problems which have more than one spatial dimension.

The last two methods discussed have been developed specifically to model premixed flame fronts. Neither of these methods are of use when modeling a diffusion flame with finite rate kinetics. To model a diffusion flame still requires a straight forward application of the finite difference method. Fortunately, the timestep and the gridsize are much larger in the diffusion flame than for the premixed flame fronts, and the program does not become excessively expensive.

2.3 Description of Movable Grid

As mentioned above, the algorithm used to adjust the movable grid involves examining the temperature profile and noting where the differences in temperature at two adjacent grid points either exceeds some maximum value or is less than some minimum value. If the difference exceeds the maximum value then a grid point is

inserted exactly between the two original grid points. If the difference is less than a minimum value then an additional comparison is made to the next adjacent point and if this temperature difference is also small, then the point in between is deleted.

In order to be physically realistic, as many quantities as possible must be conserved when adding or deleting a grid point. The method used here conserves mass, energy, and chemical species, but not momentum. To conserve momentum requires a new solution at the old timestep to determine pressures and this added complexity and computational expense defeats the purpose of the movable grid. When a grid point is added, it is added exactly in the middle of the two original points. Hence it can be shown that the values of the density, temperature, and species which satisfy the conservation laws at the new point are simply the averages of the values at the adjacent points. When a point is removed, it may not lie exactly in between its two neighboring points and thus conservation laws may not be satisfied by leaving the values unchanged at the neighboring points. Instead the quantities associated with the removed grid point must be carefully divided up between the neighboring points.

Another consideration that is important when using a movable grid is that the initial grid size must be fine enough to model the leading edge of a premixed flame front. Since the temperature differences in the leading edge of the flame front

are not large the movable grid may not supply enough points to model this region accurately. The consequence of not supplying enough initial points to model the leading edge is a premixed flame speed which varies erratically.

Finally, it is important that the programmer have an physical understanding of the problem so that the movable grid algorithm is applied only in areas where a premixed flame exists or will exist. As an example consider a problem in which there is a boundary layer which does not contain a flame. A fine grid is needed to correctly model velocity gradients in the boundary layer. However, since the boundary layer does not contain a flame it is unlikely that the boundary layer will contain large temperature gradients. If a movable grid is applied in this region, it will coarsen the grid and cause the boundary layer to be modeled inaccurately. To obtain the proper physical understanding may require that the programmer make several trial computer runs to determine the exact locations where the premixed flames will exists.

2.4 Description of Numerical Method

The numerical method chosen to solve the problem is presented in detail by Patankar. In the method discretization equations are derived using conservation principles. Using temperature as an example a typical discretization equationn is of the form

$$b_P \overline{T}_P = b_E \overline{T}_E + b_W \overline{T}_W + b_N \overline{T}_N + b_S \overline{T}_S + C \qquad (2.4)$$

where

$$b_i = \frac{\lambda \delta_x}{c_p \delta_y}\left[\left[0,\left(1-0.1|Pec_i|\right)^5\right]\right] + \left[\left[-(\bar{\rho}\bar{V})\delta_x, 0\right]\right] \qquad (2.5)$$

$$i = E, W, N, S,$$

$$Pec_i = \frac{(\bar{\rho}_i \bar{V}_i) c_p \delta_y}{\bar{\lambda}} \qquad i = E, W, N, S, \qquad (2.6)$$

$$b_p = b_E + b_W + b_N + b_S + b_p^0, \qquad (2.7)$$

$$b_p^0 = \frac{\rho_p^0 \delta_x \delta_y}{\Delta t}, \qquad (2.8)$$

and

$$C = \frac{Q \bar{Y}_0 \bar{Y}_F e^{-\bar{E}/R\bar{T}_p^0} \delta_x \delta_y}{c_p (\bar{T}_p^0)^2} + \Delta i \delta x \qquad (2.9)$$

The brackets indicate that the maximum of the two quantities contained within is to be taken. It can immediately be seen that the method is implicit in all terms except the chemical reaction rate which is handled explicitly in temperature. The reaction rate is written explicitly in temperature because it is highly non-linear and convergence is nearly impossible if it is written implicitly. Because of the scheme's overall implicitness the method should be highly stable. The coefficients between adjacent grid points are calculated based on a numerical Peclet number which, in turn, is based on the local grid size and the

local values of velocity, density, and thermal properties. If the numerical Peclet number is small, then diffusion dominates locally and a diffusion type of coefficient is used between the points. If the numerical Peclet number is large, then convection dominates locally and a convective type of coefficient is used. For intermediate values of the numerical Peclet number a combination of the diffusion and convection coefficients is used.

Equations similiar to Eqs. (2.4-2.9) can be written for fuel and oxygen species, and the x and y direction velocity by using the conservation of species equations and the conservation of momentum equations. Then, using the additional equation of the conservation of mass and appropriate boundary and initial conditions, a solution to the problem at a new timestep may be found by iteration. Timesteps can then be taken from the initial condition until a steady state solution is reached.

The major criticism of the above method is false diffusion which, as the name implies, is diffusion which is predicted to occur because of a numerical weakness in the solution algorithm rather than because of the physical situation. As discussed in reference (37), false diffusion only occurs when the direction of the fluid flow is not parallel to the gradients in temperature and species. Since in the one dimensional problems considered in chapter three, the velocity is always parallel to the gradients in temperature and species, false diffusion is not a consideration. However, for the stagnation point flow problems considered in chapter four, the velocity is often at an angle to

the temperature and species gradients and false diffusion is a consideration.

A second criterion for false diffusion to occur is that the numerical Peclet number be large where there are large gradients in temperature and species. One of the advantages of the movable grid is that it concentrates points in areas of large temperature and species gradients. Since the numerical Peclet number is based on grid size, the Peclet number is small in areas where there are steep gradients. Thus, the movable grid has the advantage of greatly minimizing or eliminating false diffusion from the stagnation point problem, and the numerical method presented should perform quite well for all problems considered here.

3.0 One Dimensional Problem

3.1 Introduction

The problem considered here is schematically shown in Fig. (3.1). A planar combustible solid wall is initially in a still, zero gravity air environment. The wall is at the vaporization temperature of the solid fuel and the surrounding air is at an ambient temperature which is less than the vaporization temperature. At time t=0, the wall is subjected to a radiant heat flux of constant intensity which the wall absorbs at its surface causing fuel to be vaporized. The fuel vapor mixes with the ambient air and one of three things may occur: a)the fuel may be reactive enough at the vaporization temperature of the fuel to ignite, b)the fuel is not reactive enough at its vaporization temperature to ignite, however it may absorb incoming radiation and become hot enough to ignite, or c)the fuel-air mixture does not ignite. Obviously the fuel may be hot enough to ignite at its vaporization temperature and it may also absorb radiation so that there is the possibility of a combined ignition mechanism. After ignition occurs the chemical reaction is self-sustaining and the radiation is turned off. The reaction eventually produces a premixed flame followed by a diffusion flame.

Many assumptions are made which are used to reduced the governing equations which describe the problem to solvable form. As mentioned above it is assumed that all processes are at zero gravity and since the only flow at a boundary is a uniform

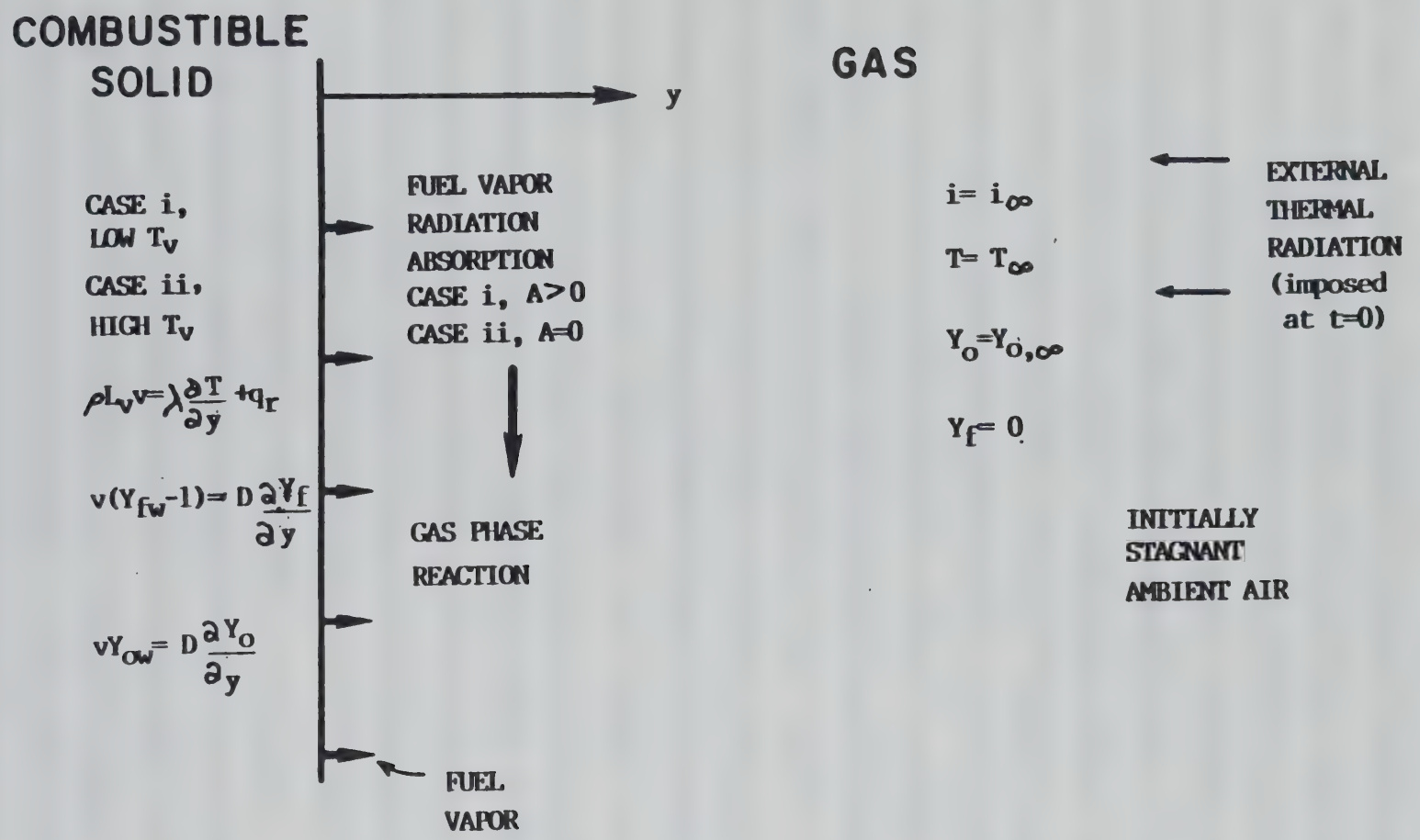

Figure 3.1 Detailed Schematic Diagram Illustrating the One Dimensional Problem

injection of fuel at the wall all processes should remain one dimensional. Since the analysis is concerned with gas phase processes the solid is assumed to remain uniformly at the vaporization temperature and is not considered except at its interface with the gas. The gas phase combustion is assumed to be a one step chemical reaction whose rate can be described by an Arrhenius expression. The gases are treated as ideal with a Lewis number of unity, a constant Prandtl number, constant specific heats, and a thermal conductivity that is given as an exponential function of temperature. It is assumed that the pressure remains approximately constant.

Also the radiation is assumed to be directed perpendicularly to the wall. Both the gas phase and the solid surface can absorb the incoming radiation but do not emit their own radiation and the gas does not scatter. The gas phase absorption process is assumed to be independent of temperature, but directly proportional to the fuel concentration and to the intensity, with the constant of proportionality being defined as the absorption coefficient. Finally, the fuel wall is assumed to be black and thus to absorb all incident radiation.

The ignition criterion that will be used in this analysis is that the chemical reaction has become self - sustaining. Using this definition the ignition point can be determined by an iterative process. At a given time the radiation is turned off and a timestep run. If the chemical reaction is strong enough to cause the temperature to continue to rise, then ignition has

occurred. If the temperature falls, then ignition has not occurred and the timestep is rerun with the radiation turned back on. The process is repeated until ignition point is reached.

For this ignition criterion the chemical reaction is still weak when the radiation is turned off. Hence, there will be period of slow chemical reaction just after ignition and before the reaction becomes strong. A weakness of this criterion is that the length of time that the weak chemical reaction lasts is highly dependent on when the laser is turned off. If the laser is turned off just at the ignition point, then the chemical reaction will just balance convective and diffusive losses and the weak chemical reaction period will last for a very long time. If the laser is left on slightly beyond the ignition point, then the chemical reaction will be stronger than the diffusive losses and the weak chemical reaction period will be much shorter.

A second criterion that is often used is to define the ignition time as the time when the chemical reaction becomes quite strong. Unlike the first criterion, this criterion is not defined precisely and it is this lack of precision which can lead to inconsistent results. A further discussion of the ignition criteria will be made in the results section.

In the following sections, the dimensional governing equations will be introduced and then non-dimensionalized. Then two limiting cases will be solved and the results presented. The first case corresponds to a gas with a high absorption coefficient and a low vaporization temperature. Ignition in this

case will be due to radiation absorption in the gas phase and will involve the vaporization of a considerable amount of fuel before ignition occurs. The fuel will ignite far away from the fuel surface. The second case involves a fuel with zero absorption coefficient and a high vaporization temperature. In this case ignition occurs because of the hot surface and the point of ignition is near the wall with little fuel vaporization taking place before ignition. Also, because there has been little theoretical work done on ignition by gas phase absorption, results of a parametric study are presented which show how ignition time and distance from the wall at which ignition occur vary as a function of the absorption coefficient and the intensity.

3.2 Analysis

3.2.1 Governing Equations

The equations that describe the problem are the transient one dimensional conservation equations with their associated boundary and initial conditions. With the assumptions listed above these equations become,

Continuity:

$$\frac{\partial \bar{\rho}}{\partial \bar{t}} + \frac{\partial}{\partial \bar{y}} (\bar{\rho} \bar{V}) = 0 \qquad (3.1)$$

Energy:

$$\bar{\rho} \frac{\partial \bar{T}}{\partial \bar{t}} + \bar{\rho} \bar{V} \frac{\partial \bar{T}}{\partial \bar{y}} = \frac{\partial}{\partial \bar{y}} \left(\frac{\bar{\lambda}}{c_p} \frac{\partial \bar{T}}{\partial \bar{y}} \right) + \frac{1}{c_p} \frac{d \bar{L}}{d \bar{y}} + \frac{Q}{c_p} \bar{W} \qquad (3.2)$$

Fuel conservation:

$$\bar{\rho}\frac{\partial \bar{Y}_F}{\partial \bar{t}} + \bar{\rho}\bar{V}\frac{\partial \bar{Y}_F}{\partial \bar{y}} = \frac{\partial}{\partial \bar{y}}\left(\overline{\rho D}\frac{\partial \bar{Y}_F}{\partial \bar{y}}\right) - \bar{w} \tag{3.3}$$

Oxygen Conservation:

$$\bar{\rho}\frac{\partial \bar{Y}_O}{\partial \bar{t}} + \bar{\rho}\bar{V}\frac{\partial \bar{Y}_O}{\partial \bar{y}} = \frac{\partial}{\partial \bar{y}}\left(\overline{\rho D}\frac{\partial \bar{Y}_O}{\partial \bar{y}}\right) - \frac{m\omega_O \nu_O}{m\omega_F \nu_F}\bar{w} \tag{3.4}$$

Y-momentum conservation:

$$\bar{\rho}\frac{\partial \bar{V}}{\partial \bar{t}} + \bar{\rho}\bar{V}\frac{\partial \bar{V}}{\partial \bar{y}} = -\frac{\partial \bar{P}}{\partial \bar{y}} \tag{3.5}$$

where the chemical reaction rate, $\bar{w}$, is given by

$$\bar{w} = B\bar{Y}_O\bar{Y}_F\bar{T}^{-2}\exp\left(-\frac{E}{R_u\bar{T}}\right), \tag{3.6}$$

for the one step chemical reaction of the form

$$\nu_F F + \nu_O O \longrightarrow \nu_P P. \tag{3.7}$$

The $d\bar{i}/d\bar{x}$ term in the energy equation represents a heat source term due to the absorption of radiation in the fuel vapor. This radiation absorption is assumed to be of the form

$$\frac{d\bar{i}}{d\bar{y}} = \bar{\rho}a_\lambda\bar{Y}_F\bar{i} \tag{3.8}$$

where a_λ is the absorption coefficient and $\bar{i}$ is the radiation intensity which is a function of $\bar{y}$. The y-momentum equation is not necessary for the solution of this problem because of the one-dimensionality and the assumption that the pressure remains approximately constant. It is used, however, as a check of the constant pressure assumption to insure that the pressure does not

vary significantly from the ambient pressure during periods of rapid chemical reaction. The last equation that is necessary is the equation of state which reduces to

$$\frac{\bar{p}_1 \bar{T}_1}{m\omega_1} = \frac{\bar{p}_2 \bar{T}_2}{m\omega_2} \tag{3.9}$$

The initial and boundary conditions that specify the problem are: At time $\bar{t}=0$,

$$\bar{V}(0,y) = 0, \tag{3.10}$$

$$\bar{T}(0,\bar{y}) = T_\infty \tag{3.11}$$

$$\bar{Y}_F(0,\bar{y}) = 0 \tag{3.12}$$

$$\bar{Y}_O(0,\bar{y}) = Y_{O,\infty} \tag{3.13}$$

At the solid/gas interface, $\bar{y}=0$, the temperature is the vaporization temperature of the fuel

$$\bar{T}(\bar{t},0) = T_v \tag{3.14}$$

An energy balance at the wall gives the mass flux at the wall,

$$\bar{\rho}\,\bar{V} L_v = \bar{\lambda}\,\frac{\partial \bar{T}}{\partial \bar{y}} + \bar{L} \tag{3.15}$$

which is then used in the fuel and oxygen conservation equation boundary conditions,

$$\bar{\rho}\bar{v}\bar{Y}_{F_T} = (\bar{\rho}\bar{v}\bar{Y}_F) - \left(\overline{\rho D}\,\frac{\partial \bar{Y}_F}{\partial \bar{y}}\right) \tag{3.16}$$

$$\bar{\rho}\bar{v}\bar{Y}_O = \overline{\rho D}\,\frac{\partial \bar{Y}_O}{\partial \bar{y}} \tag{3.17}$$

Far away from the wall conditions should always approach the ambient and thus the boundary conditions as $\bar{y}$ approaches infinity are,

$$\bar{T} = T_\infty, \tag{3.18}$$

$$\bar{Y}_O = Y_{O,\infty}, \tag{3.19}$$

$$\bar{Y}_F = 0, \tag{3.20}$$

$$\bar{i} = i_\infty \tag{3.21}$$

Finally, the power generated above the surface per unit area of surface is

$$\overline{\dot{P}''_F} = \int_0^\infty B\bar{Y}_O\bar{Y}_F\,\bar{T}^{-2}e^{-E/R_u\bar{T}}\,dy \tag{3.22}$$

It can easily be seen by setting the time derivatives to zero in Eqs. (3.3-3.5) and by applying the boundary conditions, Eqs. (3.14-3.21), that no steady state solution exists. This will have an effect upon the final solution and will be discussed more in the results.

3.2.2 Non-Dimensionalization

The non-dimensionalization is not a straight forward process for this problem because of a lack of characteristic length and time scales in the boundary and initial conditions and because of the many different physical regimes that are present. A characteristic quantity which may fit one regime quite well may have no significance in another physical regime. Hence, some compromises are necessary in choosing the characteristic quantities. The following non-dimensional quantities are used in this problem:

Time,

$$t = \frac{\bar{t}}{\left(\frac{\rho_\infty T_\infty^2}{A Y_{o,\infty} e^{-\beta}} \right)} , \tag{3.23}$$

where β is a non-dimensional activation energy given by

$$\beta = E / R_u T_f , \tag{3.24}$$

and T_f is given by

$$T_f = (1+\alpha) T_\infty , \tag{3.25}$$

where

$$\alpha = \frac{Q Y_{o,\infty} \nu_F MW_F}{c_p T_\infty \nu_o MW_o} , \tag{3.26}$$

Length,

$$y = \frac{\bar{y}}{\left(\frac{(\rho D)_\infty T_\infty^2}{A Y_{o,\infty} e^{-\beta}} \right)^{1/2}} \tag{3.27}$$

Velocity,

$$V = \frac{\bar{V}}{\left(\frac{(\rho D)_\infty A Y_{o,\infty}}{\rho_\infty^2 T_\infty^2} e^{-\beta} \right)^{1/2}} \tag{3.28}$$

Oxygen mass fraction,

$$Y_O = \frac{\bar{Y}_O}{Y_{O,\infty}} \tag{3.29}$$

Fuel mass fraction,

$$Y_F = \frac{(\bar{Y}_F \nu_O m\omega_O)}{(Y_{O,\infty} \nu_F m\omega_F)} \tag{3.30}$$

Temperature,

$$T = \frac{c_p \nu_O m\omega_O}{Q \nu_F m\omega_F Y_{O,\infty}} (\bar{T} - T_\infty) \tag{3.31}$$

Intensity,

$$i = \frac{\bar{i}}{i_\infty} \tag{3.32}$$

Density,

$$\rho = \bar{\rho}/\rho_\infty \tag{3.33}$$

Thermal conductivity,

$$\lambda = \bar{\lambda}/\lambda_\infty \tag{3.34}$$

Viscosity,

$$\mu = \bar{\mu}/\mu_\infty \tag{3.35}$$

and Pressure,

$$P = \frac{\bar{p}}{(\rho_\infty V_c^2)} \tag{3.36}$$

The characteristic time in Eq. (3.24) is the chemical time and for most hydrocarbon fuels this is quite small. The characteristic velocity is on the order of the premixed flame

velocity, while the characteristic length is the thickness of a premixed flame front. Hence, these characteristic quantities apply best to a reaction zone in a premixed flame and really do not apply to other parts of the flow field outside the flame or to regimes that do not contain premixed flames.

The characteristic fuel mass fraction is the mass fraction of fuel that would be required to burn the oxygen at infinity if the fuel and oxygen were stoichiometrically mixed. This variable is thus a measure of the richness or the leanness of the mixture. The characteristic temperature is the temperature rise that would occur if a stoichiometric mixture were burned with the oxygen being at its concentration at infinity. Other quantities are self explanatory.

If these quantities are introduced into the dimensional conservation equations, and into their boundary and initial conditions, Eqs. (3.1-3.22), then the following equations result:

Continuity,

$$\frac{\partial \rho}{\partial t} + \frac{\partial}{\partial y}(\rho V) = 0, \tag{3.37}$$

Energy,

$$\rho \frac{\partial T}{\partial t} + \rho V \frac{\partial T}{\partial y} = \frac{\partial}{\partial y}\left(\lambda \frac{\partial T}{\partial y}\right) + I_1 \frac{dJ_1}{dy} + \frac{Y_F Y_O}{(Ta+1)^2} e^{\left[\frac{-\beta(1-T)}{\frac{1}{2}+T}\right]}, \tag{3.38}$$

Fuel conservation

$$\rho \frac{\partial Y_F}{\partial t} + \rho V \frac{\partial Y_F}{\partial y} = \frac{\partial}{\partial y}\left(\rho D \frac{\partial Y_F}{\partial y}\right) + \frac{Y_F Y_O}{(Ta+1)^2} e^{\left[-\frac{\beta(1-T)}{\frac{1}{2}+T}\right]} \tag{3.39}$$

Oxygen conservation,

$$\rho \frac{\partial Y_o}{\partial t} + \rho V \frac{\partial Y_o}{\partial y} = \frac{\partial}{\partial y}\left(\rho D \frac{\partial Y_o}{\partial y}\right) + \frac{Y_F Y_o}{(Ta+1)^2} e^{\left[-\frac{\beta(1-T)}{\frac{1}{a}+T}\right]} \quad (3.40)$$

Conservation of y-momentum

$$\rho \frac{\partial V}{\partial t} + \rho V \frac{\partial V}{\partial y} = -\frac{\partial P}{\partial y} \quad (3.41)$$

The radiation absorption term becomes,

$$\frac{di}{dy} = A \rho Y_F i \quad (3.42)$$

The equation of state is

$$\left(\frac{\nu_F}{\nu_o} Y_{F,1} + Y_{O,1}\right) \rho_1 \left(T_1 + \frac{1}{a}\right) = \left(\frac{\nu_F}{\nu_o} Y_{F,2} + Y_{O,2}\right) \rho_2 \left(T_2 + \frac{1}{a}\right) \quad (3.43)$$

The transformed initial conditions at time, t=0, are

$$V = 0 \quad (3.44)$$

$$T = 0 \quad (3.45)$$

$$Y_o = 1 \quad (3.46)$$

$$Y_F = 0 \quad (3.47)$$

The boundary condition at the solid gas interface, y=0, are for temperature,

$$T = T_w = \frac{1}{a T_\infty}\left(T_v - T_\infty\right) \quad (3.48)$$

For the mass flux,

$$\rho V = \left(\frac{c_p \alpha T_\infty}{L_v}\right) \frac{dT}{dy} + \left(\frac{c_p \alpha T_\infty}{L_v}\right)\left(\frac{i_o}{\rho_\infty c_p \alpha T_\infty V_c}\right) i \qquad (3.49)$$

For the conservation of fuel and oxygen equations,

$$\frac{\nu_o MW_o Y_{FT}}{\nu_F MW_F Y_{O,\infty}} \rho V = \rho V Y_F - \rho D \frac{\partial Y_F}{\partial y}, \qquad (3.50)$$

$$\rho V Y_o = \rho D \frac{\partial Y_o}{\partial y}. \qquad (3.51)$$

At the outer boundary where $y \to \infty$, the transformed conditions become,

$$T = 0 \qquad (3.52)$$

$$Y_o = 1 \qquad (3.53)$$

$$Y_F = 0 \qquad (3.54)$$

$$i = 1 \qquad (3.55)$$

Finally, a non-dimensional power per unit area of fuel surface may be defined as

$$P_F = \frac{\overline{PF}}{c_p T_\infty \rho_\infty V_c \alpha D_a} = \int_0^\infty \frac{Y_o Y_F e^{\left[-\frac{\alpha(1-T)}{\frac{1}{\alpha}+T}\right]} dy}{(\alpha T + 1)} \qquad (3.56)$$

Including the Lewis number which has already been assumed to be one there are nine non-dimensional groups which appear in

Eqs. (3.36-3.55). These groups are defined and summarized in Table 3.1.

3.3 Results

3.3.1 Results of the Ignition and Flame Propagation Study with Ignition Caused by Gas Phase Absorption

The results of two cases run with different absorption coefficients are presented in this section. The first case is run with an absorption coefficient of $A=4.78\times10^{-6}$ and the second case is run with $A=4.78\times10^{-4}$. While there is little data available on the absorption coefficients of hydrocarbon fuel vapors, a previous study has suggested that the total absorption coefficient for the hydrocarbon fuel, polymethylmethacrylate(PMMA) is 1.5×10^{-6}.[38-39] If a laser which has a wavelength in the absorption band of the fuel is used to irradiate the surface then the 4.78×10^{-6} case is quite realistic. The absorption coefficient of 4.78×10^{-4} is probably too high, but there are enough interesting physical differences between the two cases to justify its presentation.

The other data used in this calculation are shown in dimensional form in Table 3.2 and are shown in non-dimensional form in Table 3.3. The properties correspond approximately to those of PMMA[40] with the exception of the absorption coefficient discussed above and the constants in the Arrhenius chemical reaction rate. There is presently no single set of constants available which would accurately model the chemical reaction

Table 3.1: Summary of non-dimensional groups appearing in the one dimensional equations

Symbol	Non-dimensional group	Description
A	$\left(\frac{\rho_\infty a_\lambda Y_{O,\infty} \nu_F m\omega_F Y_C}{\nu_O m\omega_O}\right)$	Non-dimensional absorption coefficient
H	$\left(\frac{c_p \alpha T_\infty}{L_v}\right)$	Non-dimensional ratio of heat of combustion to heat of vaporization
I	$\left(\frac{i_\infty}{\rho_\infty c_p \alpha T_\infty V_C}\right)$	Non-dimensional intensity
Le	$\left(\frac{(\rho D)_\infty c_p}{\lambda_\infty}\right)$	Lewis number
S	$\left(\frac{\nu_O m\omega_O Y_F \tau}{Y_{O,\infty} \nu_F m\omega_F}\right)$	Non-dimensional fuel-oxygen ratio
T_w	$\left[\frac{1}{\alpha T_\infty}(T_v - T_\infty)\right]$	Non-dimensional wall temperature
α	$\left(\frac{Q Y_{O,\infty} \nu_F m\omega_F}{c_p T_\infty \nu_O m\omega_O}\right)$	Non-dimensional heat of combustion
β	$\left(\frac{E}{R_u (1+\alpha) T_\infty}\right)$	Non-dimensional activation energy
—	$\left(\frac{\nu_F}{\nu_O}\right)$	Moles of fuel required per mole of oxygen

Table 3.2: Values of the dimensional parameters used in the one dimensional problem

Symbol	Case with ignition and flame propagation caused by gas phase absorption	Case with ignition and flame propagation caused a hot fuel surface
a_λ	10 m^2/kg, 1000 m^2/kg	0. m^2/kg
B	$1.6*10^{15}$ kg*°K^2/(m^3*sec)	$1.6*10^{15}$ kg*°K^2/(m^3*sec)
c_p	1220. joules/(kg*°K)	1220. joules/(kg*°K)
E	$1.8*10^8$ joules/(kgmole)	$1.8*10^8$ joules/(kgmole)
i	20. watts/cm^2	1.3 watts/cm^2
L_v	$1.59*10^6$ joules/kg	$1.59*10^6$ joules/kg
MW_f	100 kg/mole	100 kg/mole
MW_o	32 kg/mole	32 kg/mole
Q	$2.6*10^7$ joules/kg	$2.0*10^7$ joules/kg
R_μ	8315 joules/(kgmole*°K)	8315 joules/(kgmole*°K)
T_∞	298°K	298°K
T_w	663°K	1326°K
Y_{FT}	1.	1.
$Y_{o,\infty}$	0.23	0.23
λ_∞	$2.97*10^{-2}$ watts/(m*°K)	$2.97*10^{-2}$ watts/(m*°K)
ρ_∞	1.17 kg/m^3	1.17 kg/m^3
ν_F	1	1
ν_o	6	6

Table 3.3: Values of the non-dimensional parameters used in the one dimensional problem

Symbol	Case with ignition and flame propagation caused by gas phase absorption	Case with ignition and flame propagation caused by a hot fuel surface
A	$4.78*10^{-4}$, $4.78*10^{-6}$	0.
H	1.96	1.51
I	$9.04*10^{-3}$	$2.05*10^{-3}$
Le	1.0	1.0
S	8.35	8.35
T	0.143	0.523
α	8.57	6.59
β	7.59	9.57
ν_F/ν_o	0.16	0.16

rate of PMMA in all of the combustion regimes.[41] The particular set of constants used here were picked to give premixed flame speeds on the order of 1.0 m/sec. This flame speed is of the correct order of magnitude for hydrocarbon fuels and thus the chemical reaction model is realistic, if not exact.[42]

The initial evolution of the temperature profiles and mass fraction profiles are shown in Figs. (3.2) and (3.3), respectively, for the absorption coefficient of 4.78×10^{-6}. As can be seen from the figures, the application of the radiation causes the fuel to be vaporized rapidly enough to push the air back away from the wall and to create a fuel-air interface. Diffusion takes place across the interface mixing fuel with air, and the fuel vapor absorbs a fraction of the incoming radiation so that the gases become hot. Eventually, ignition occurs in a very rich part of the mixing region at a time of 6.30×10^{5} and at a location where the non-dimensional oxygen mass fraction is 0.07. After ignition the radiation is removed and a relatively long time period of weak chemical reaction follows. The weak reaction eventually gains strength leading to the development of a premixed flame front which propagates away from the wall. A premixed flame front propagating towards the wall does not develop for the simple reason that there is very little oxygen present between the point of ignition and the wall.

The power output as given by Eq. (3.56) is plotted in Fig. (3.4) for this time period. Because ignition occurred where there was very little oxygen, the temperature in the

ignition region is limited and the chemical power produced remains small. Hence, the power does not really begin to show a sharp rise until after a premixed flame front has developed. If the second criterion for ignition, which is that ignition has not occurred until the power begins to increase rapidly, were applied in this problem then a premixed flame will have developed and begun to propagate before ignition has been formally declared to have occurred.

The initial evolution of the temperature and mass fraction profiles for an absorption coefficient of 4.78×10^{-4} is shown in Fig. (3.5), and Fig. (3.6), respectively. Several differences occur between the two cases. The first difference is that the heating is more rapid leading to the faster time of ignition of 3.89×10^{4} . This fast heating combined with the high absorption coefficient which causes the fuel to absorb a significant fraction of the incoming radiation, limits the amount of fuel that vaporizes before ignition and the oxygen never gets pushed back away from the wall as in the previous case. Ignition again occurs in a rich region but the non-dimensional oxygen mass fraction is much higher and has the value of 0.50. Thus, temperatures in the ignition region will become much higher and the power which is shown in Fig. (3.7) for this case, shows a large, but extremely short-lived spike. This spike begins to dissappear just as the premixed flame fronts develop. Also because of the high oxygen content at the point of ignition two premixed flame fronts develop, a strong front travelling away

from the wall and a weaker front travelling towards the wall.

The sequence of events which occur after the premixed flame fronts become well developed are qualitatively similiar between the two cases, and it will be necessary to run only one of the two cases to completion. The case with an absorption coefficient of 4.78×10^{-4} will be chosen because it has several numerical advantages. These advantages arise because ignition occurred at a much earlier time. This fast ignition time allowed for only a small amount of fuel and oxygen to mix creating a relatively small premixed region. Also less fuel was vaporized and this will lead to the diffusion flame becoming weaker and dying out sooner. These two factors combine to produce a substantial savings in computational time over the low absorption coefficient case. Any expected differences between the two cases will be noted.

The temperature and mass fraction profiles over a longer time period are shown in the Figs. (3-8a) and (3.9a), respectively, for the high absorption coefficient. As can be seen from the profiles at time 6.36×10^{4}, three regions of chemical reaction now exist. The first region is the premixed flame front travelling away from the wall. It has moved from the rich region where it has left behind excess fuel, past through a stoichiometric point and entered a lean region where it is leaving behind excess oxygen. The temperature gradient in the flame front is becoming less steep and the premixed front is showing signs of dying out. Before it does, however, it has

served to separate the fuel and the oxygen and leave behind a diffusion flame at the stoichiometric point which is the second region of reaction. The maximum temperature in the problem occurs at the stoichiometric point soon after the premixed flame front passes through. The third area of chemical reaction occurs near the wall where the premixed flame front travelling towards the wall has reached the wall and been quenched. A residual amount of oxygen is left at the wall and is slowly diffusing into a hot fuel rich region where it is burned off. Since there was no flame front travelling towards the wall in the low absorption coefficient case this third region will not exist in that case.

The above explanation of how the diffusion flame develops is only approximate because it treats the flame front as a discontinuity and the diffusion flame as a flame sheet. In reality both the premixed flame and the diffusion flame have finite thicknesses and consequently, it is not clear exactly when the diffusion flame begins to exist nor is it clear how the diffusion flame affects the temperature profile. It is beyond the scope of this thesis to study these effects further, but it suggests an area of future research.

Finally, temperature and mass fraction profiles at much later times are shown in Figs. (3.8b) and (3.9b), respectively. The premixed flame front travelling away from the wall has now completely died out. The residual oxygen left at the wall has now been burned off. This leaves only the diffusion flame, which since there is no steady state solution in this problem, will

never reach an equilibrium position. Instead, it will continually burn out the oxygen and must move away from the wall searching for more. As it moves, its temperature is slowly dropping and it is continually being weakened. Eventually it is expected that the diffusion flame will die out.

The processes considered here are, from a qualitative standpoint, not unique. As will be seen in the next sections, the one-dimensional problem where ignition occurs because of high wall temperature will go through a similiar sequence of events as will the stagnation point problems which are considered in the next chapter.

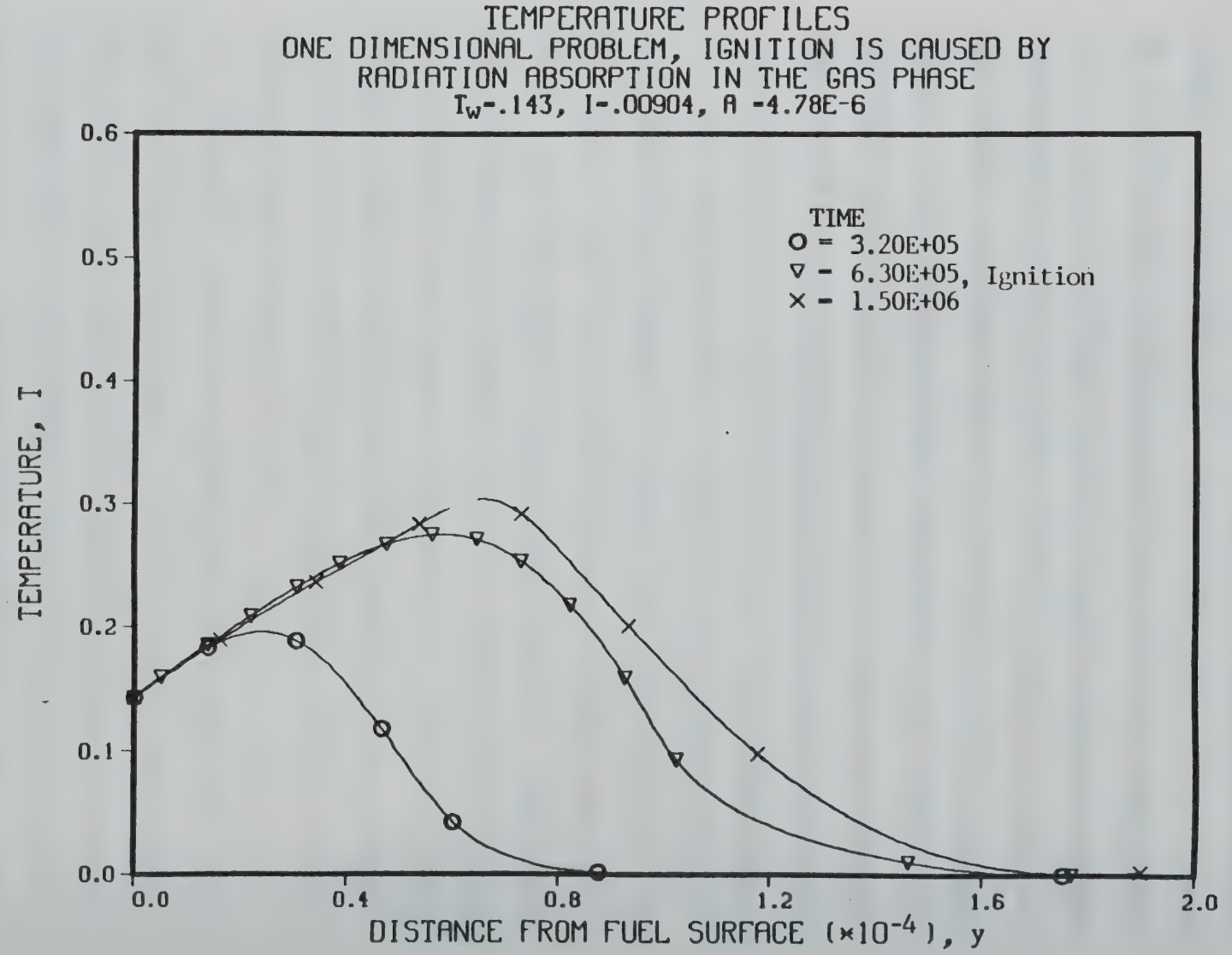
TEMPERATURE PROFILES
ONE DIMENSIONAL PROBLEM, IGNITION IS CAUSED BY
RADIATION ABSORPTION IN THE GAS PHASE
T_w-.143, I-.00904, A -4.78E-6
TIME
O = 3.20E+05
▽ - 6.30E+05, Ignition
× - 1.50E+06
TEMPERATURE, I
0.0
0.1
0.2
0.3
0.4
0.5
0.6
0.0
0.4
0.8
1.2
1.6
2.0
DISTANCE FROM FUEL SURFACE (×10^{-4}), y

Figure 3.2a

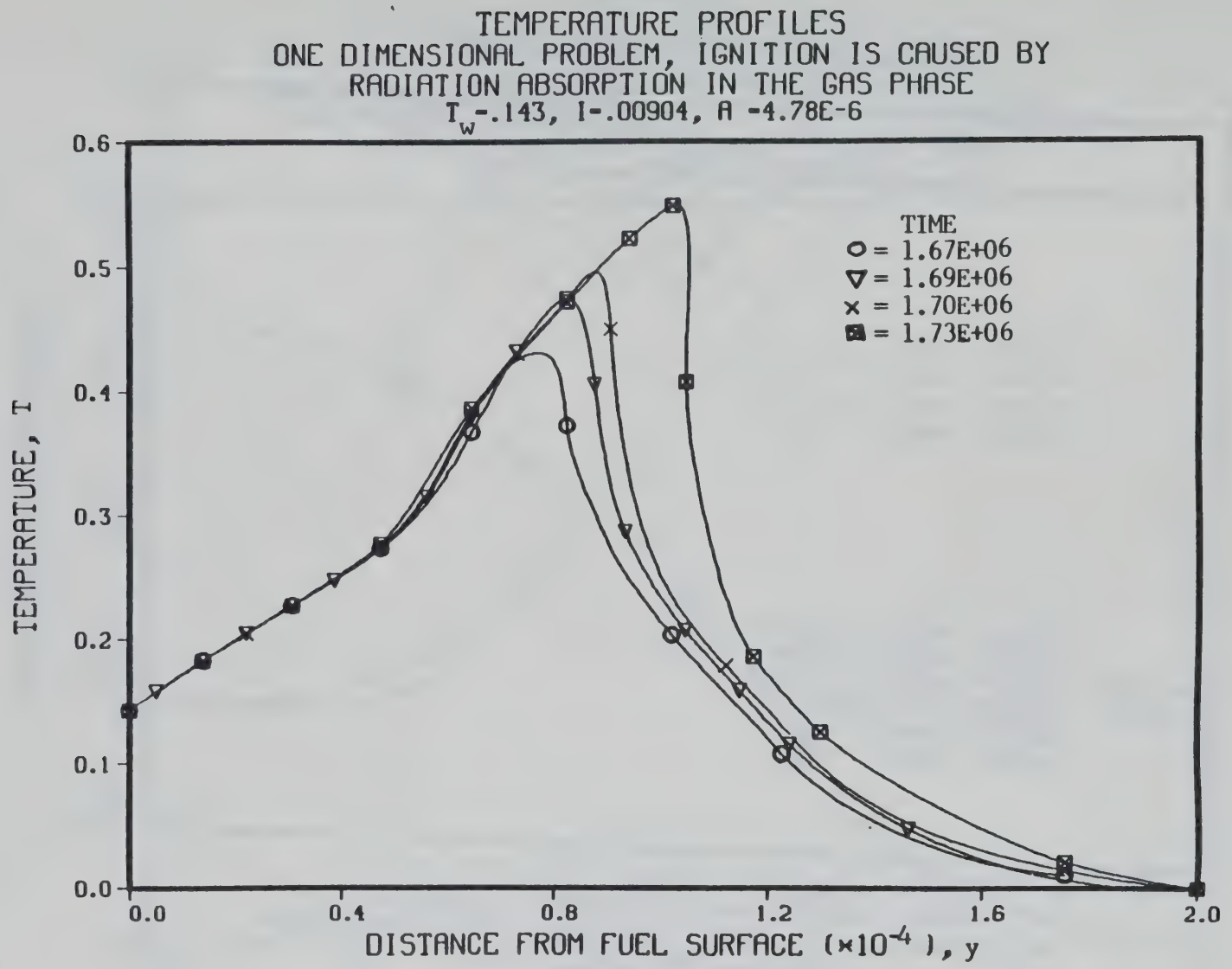
TEMPERATURE PROFILES
ONE DIMENSIONAL PROBLEM, IGNITION IS CAUSED BY
RADIATION ABSORPTION IN THE GAS PHASE
T_w -.143, I-.00904, A -4.78E-6
TIME
= 1.67E+06
= 1.69E+06
= 1.70E+06
= 1.73E+06
TEMPERATURE, T
0.0
0.1
0.2
0.3
0.4
0.5
0.6
0.0
0.4
0.8
1.2
1.6
2.0
DISTANCE FROM FUEL SURFACE (×10^{-4}), y

Figure 3.2b

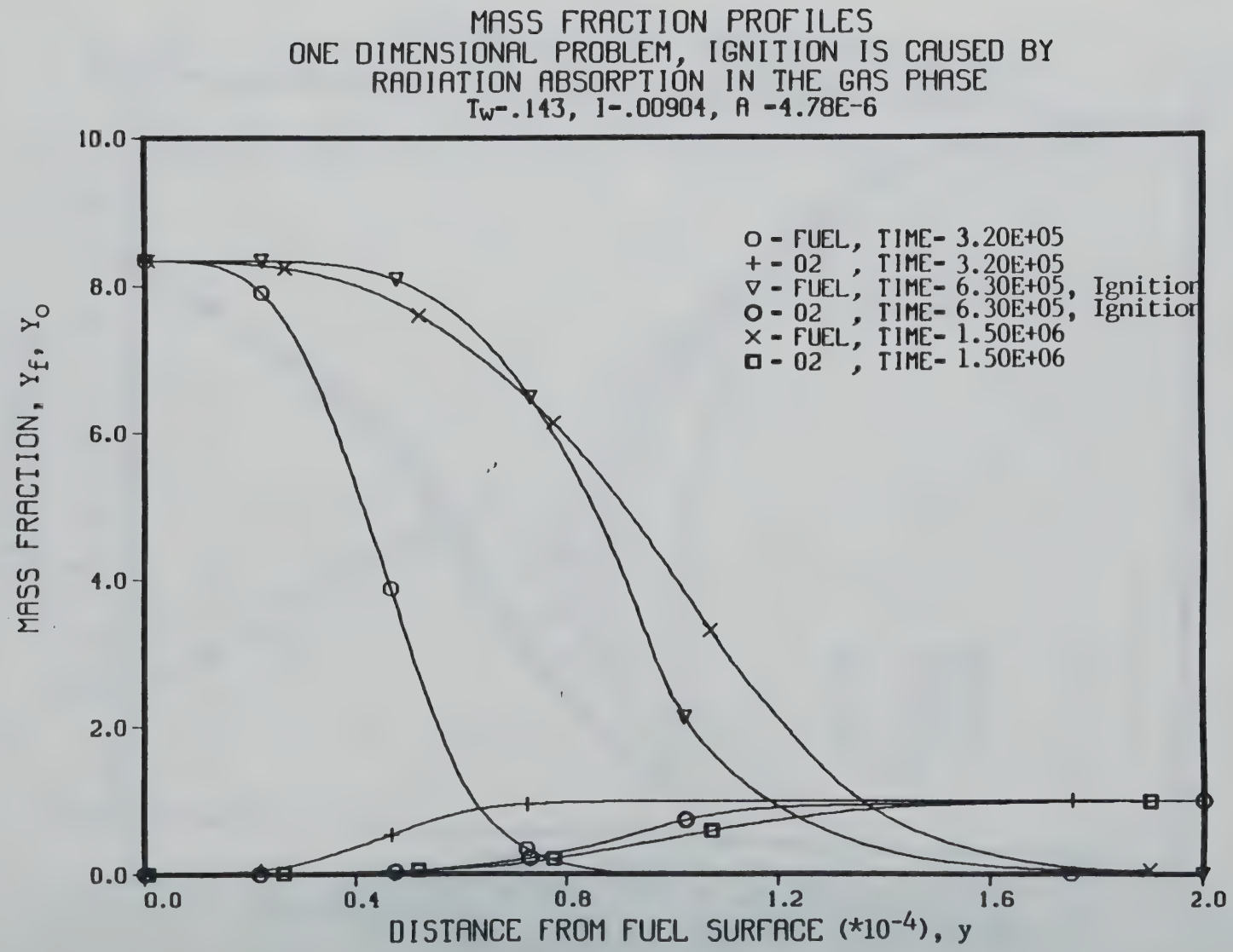
MASS FRACTION PROFILES
ONE DIMENSIONAL PROBLEM, IGNITION IS CAUSED BY
RADIATION ABSORPTION IN THE GAS PHASE
Tw=-.143, I-.00904, A -4.78E-6
O - FUEL, TIME- 3.20E+05
+ - 02 , TIME- 3.20E+05
▽ - FUEL, TIME- 6.30E+05, Ignition
O - 02 , TIME- 6.30E+05, Ignition
× - FUEL, TIME- 1.50E+06
□ - 02 , TIME- 1.50E+06
MASS FRACTION, Y_f, Y_o
10.0
8.0
6.0
4.0
2.0
0.0
0.0
0.4
0.8
1.2
1.6
2.0
DISTANCE FROM FUEL SURFACE (*10^{-4}), y

Figure 3.3a

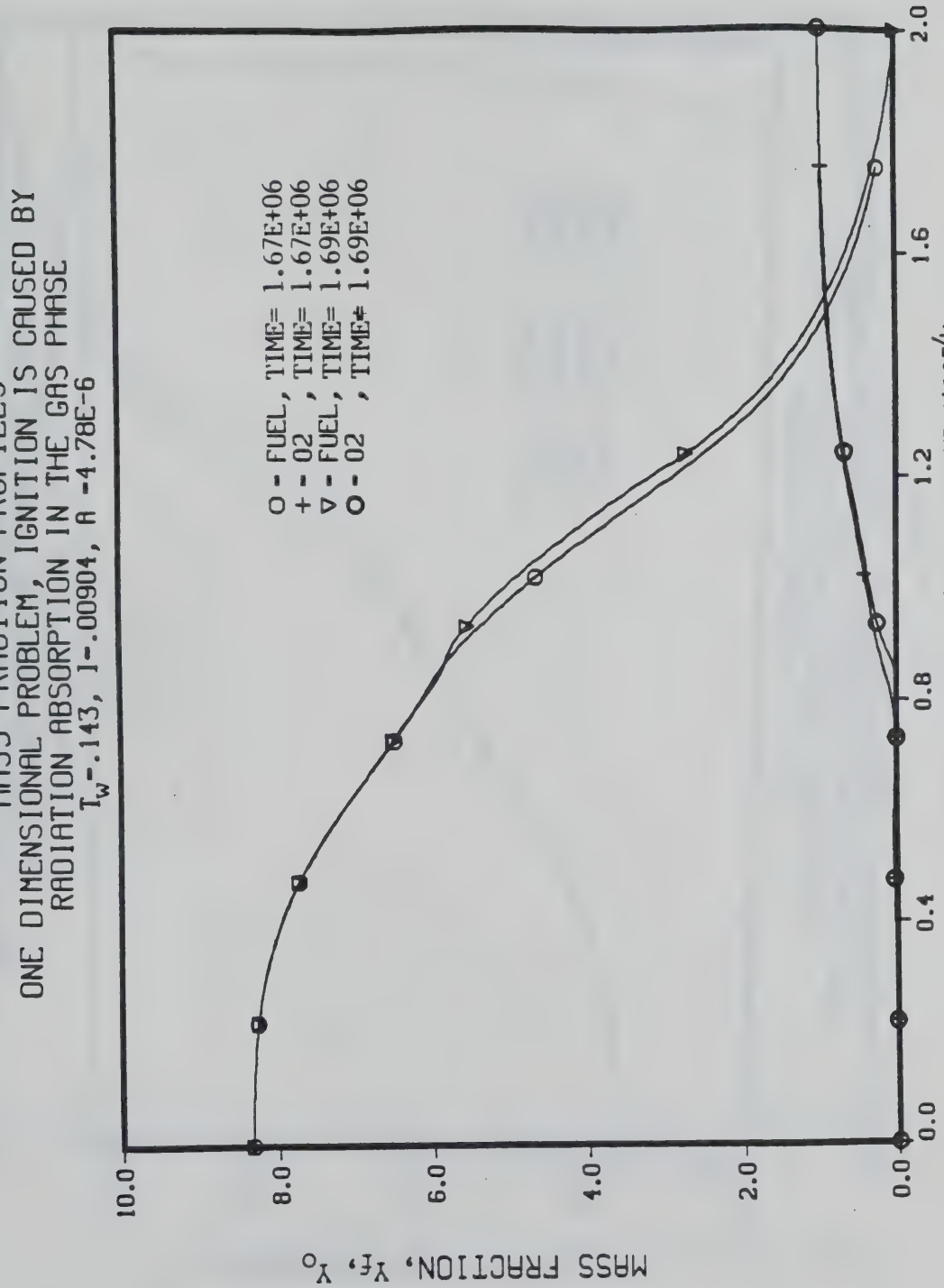
MASS FRACTION PROFILES
ONE DIMENSIONAL PROBLEM, IGNITION IS CAUSED BY
RADIATION ABSORPTION IN THE GAS PHASE
T_w=.143, l=.00904, A =4.78E-6
O - FUEL, TIME= 1.67E+06
+ - O2 , TIME= 1.67E+06
∇ - FUEL, TIME= 1.69E+06
O - O2 , TIME= 1.69E+06
MASS FRACTION, Y_F, Y_O
DISTANCE FROM FUEL SURFACE (*10^{-4}), y
0.0
2.0
4.0
6.0
8.0
10.0
0.0
0.4
0.8
1.2
1.6
2.0

Figure 3.3b

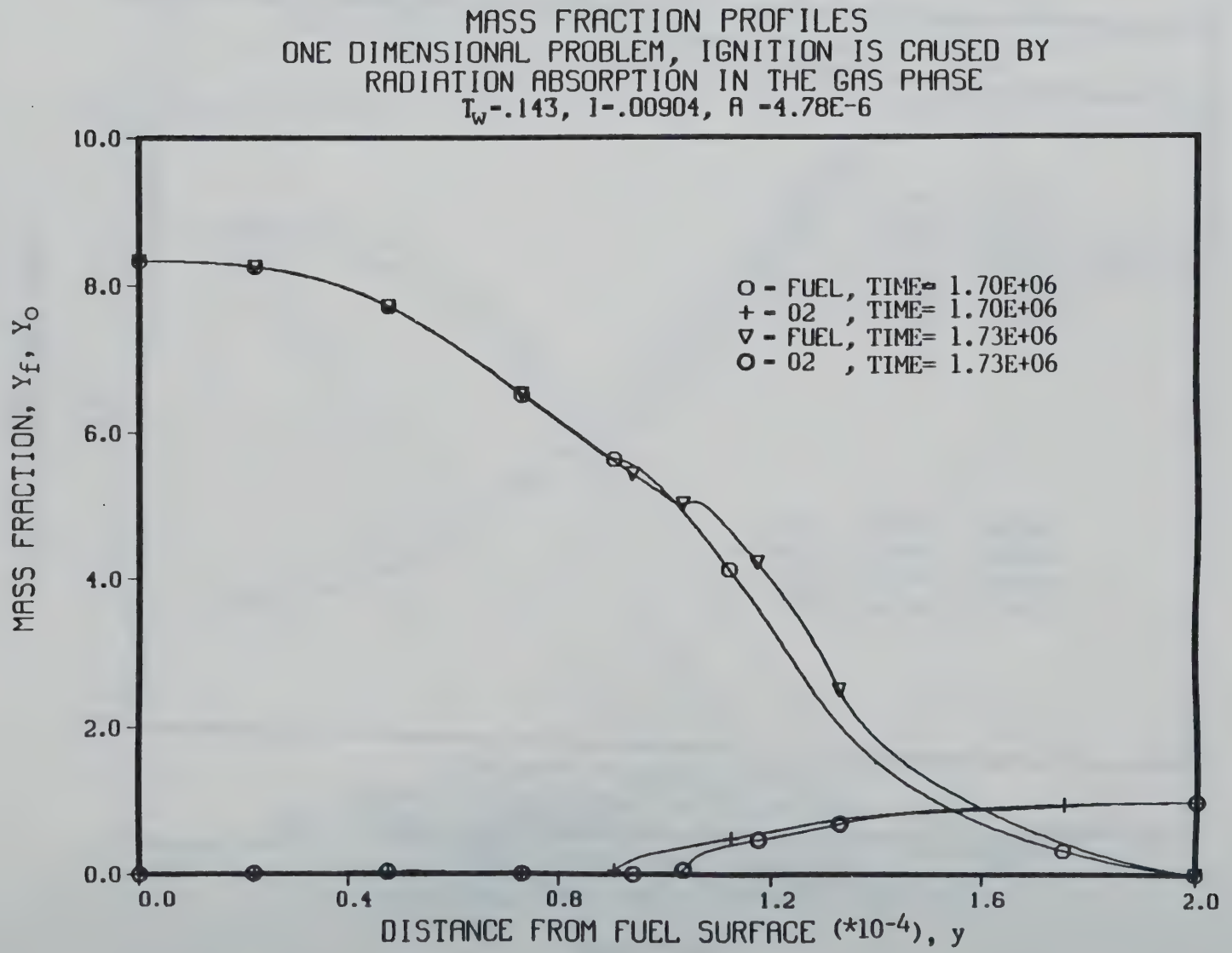
MASS FRACTION PROFILES
ONE DIMENSIONAL PROBLEM, IGNITION IS CAUSED BY
RADIATION ABSORPTION IN THE GAS PHASE
T_w-.143, l-.00904, A -4.78E-6
O - FUEL, TIME= 1.70E+06
+ - 02 , TIME= 1.70E+06
▽ - FUEL, TIME= 1.73E+06
O - 02 , TIME= 1.73E+06
MASS FRACTION, Y_f, Y_O
10.0
8.0
6.0
4.0
2.0
0.0
0.0
0.4
0.8
1.2
1.6
2.0
DISTANCE FROM FUEL SURFACE (*10^{-4}), y

Figure 3.3c

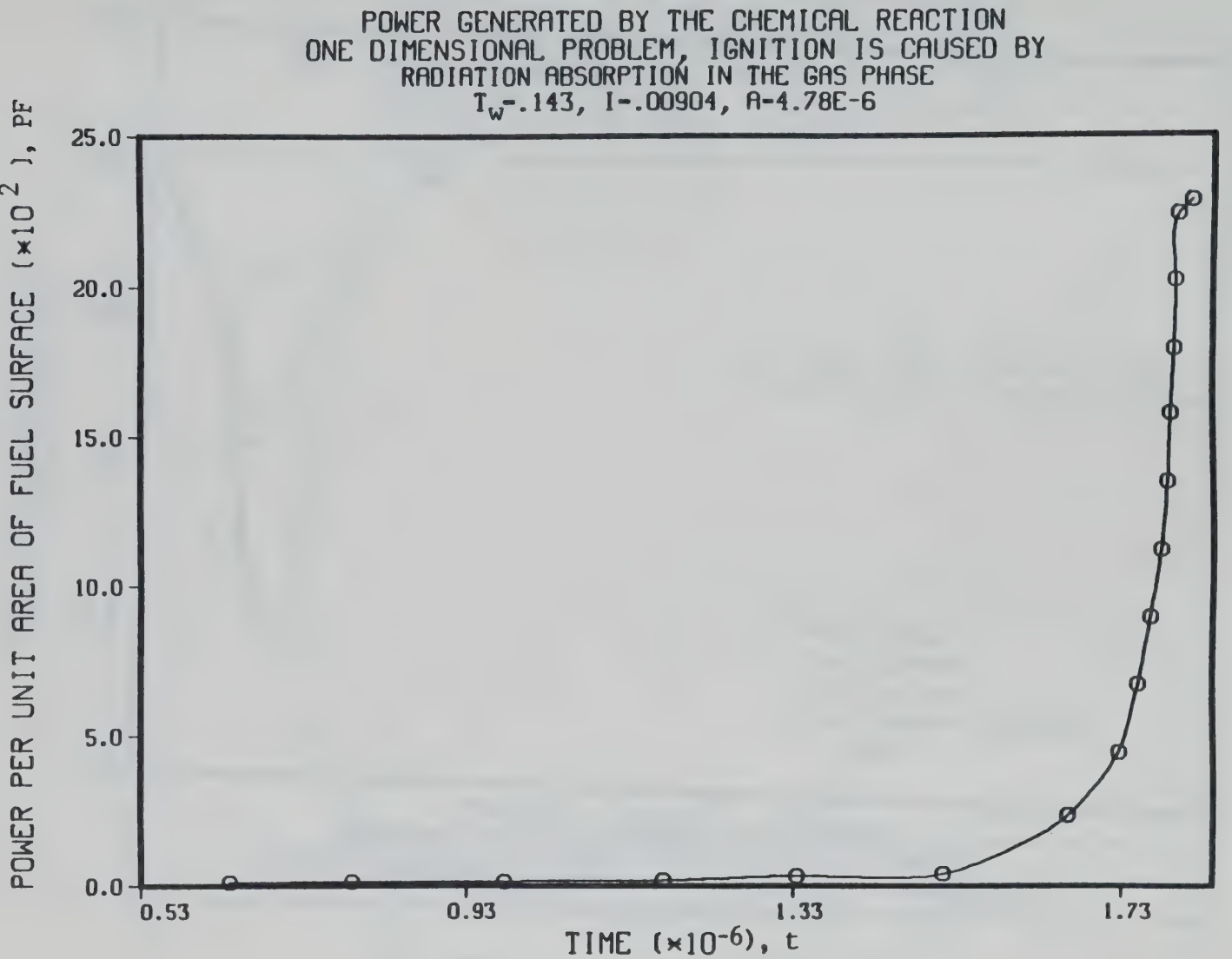
POWER GENERATED BY THE CHEMICAL REACTION
ONE DIMENSIONAL PROBLEM, IGNITION IS CAUSED BY
RADIATION ABSORPTION IN THE GAS PHASE
T_w-.143, I-.00904, A-4.78E-6
POWER PER UNIT AREA OF FUEL SURFACE (×10^2), PF
25.0
20.0
15.0
10.0
5.0
0.0
0.53
0.93
1.33
1.73
TIME (×10^{-6}), t

Figure 3.4

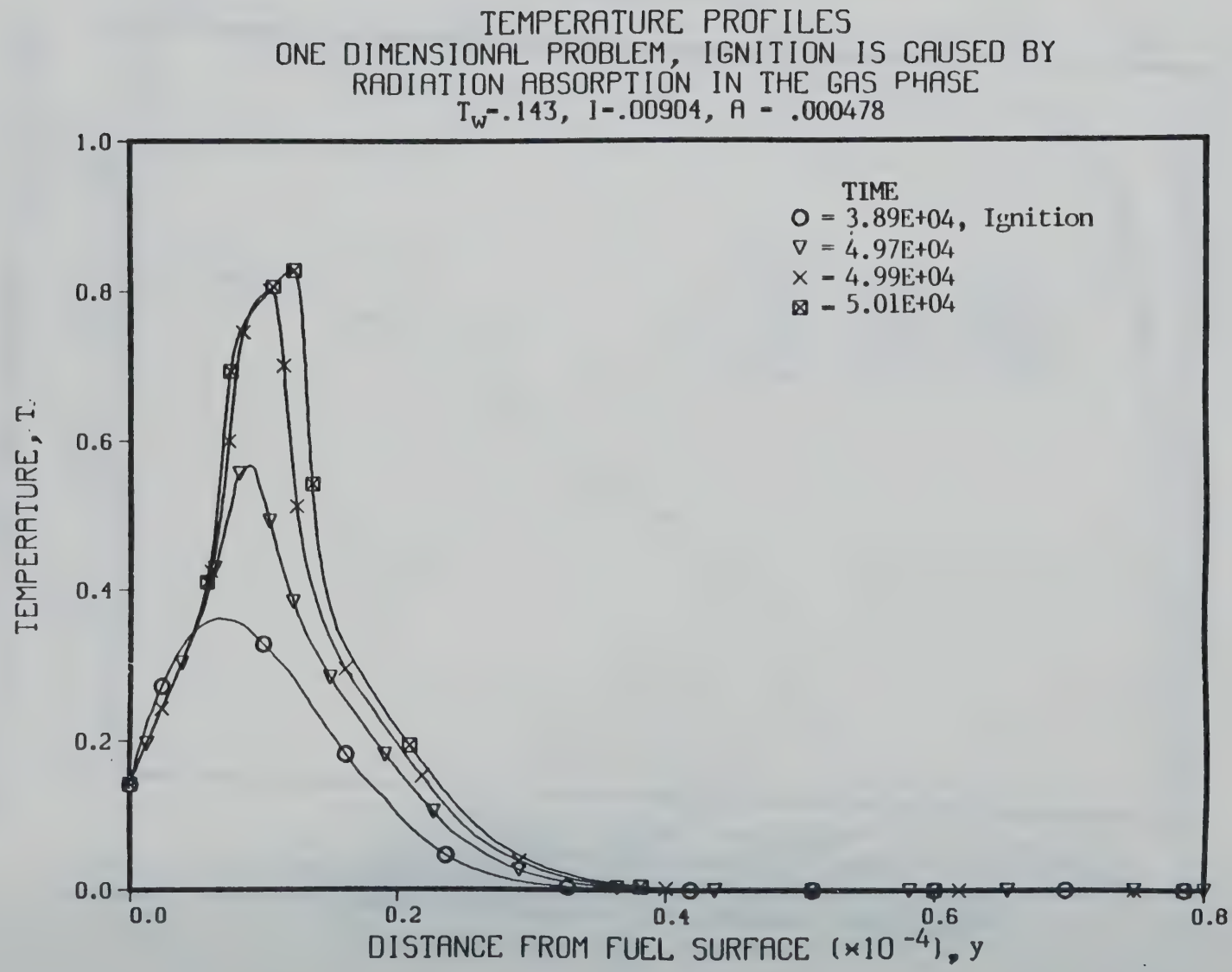
TEMPERATURE PROFILES
ONE DIMENSIONAL PROBLEM, IGNITION IS CAUSED BY
RADIATION ABSORPTION IN THE GAS PHASE
T_w-.143, l-.00904, A - .000478
TIME
O = 3.89E+04, Ignition
▽ = 4.97E+04
× - 4.99E+04
⊠ - 5.01E+04
TEMPERATURE, T
1.0
0.8
0.6
0.4
0.2
0.0
0.0
0.2
0.4
0.6
0.8
DISTANCE FROM FUEL SURFACE (×10 $^{-4}$), y

Figure 3.5

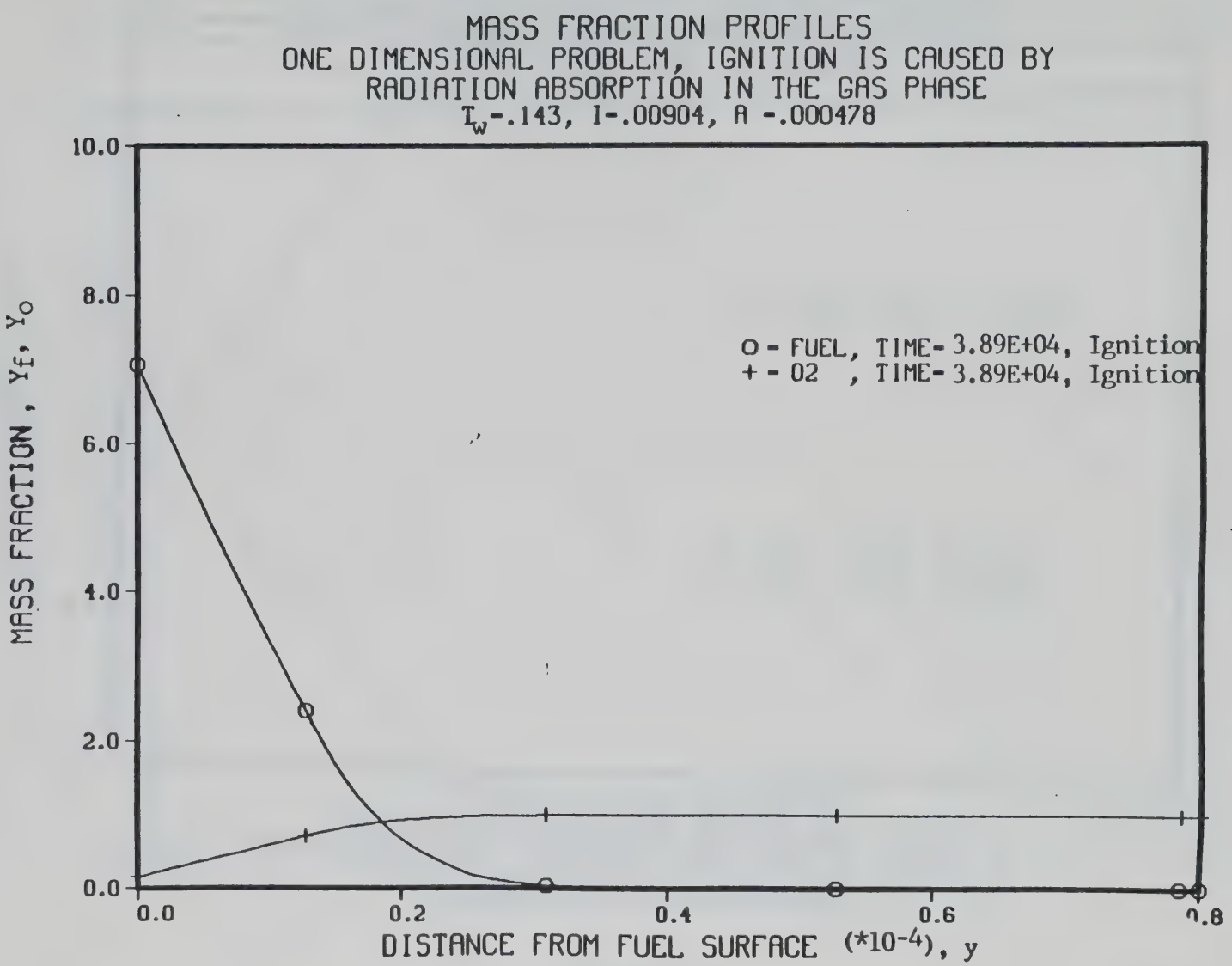
MASS FRACTION PROFILES
ONE DIMENSIONAL PROBLEM, IGNITION IS CAUSED BY
RADIATION ABSORPTION IN THE GAS PHASE
T_w=.143, I=.00904, A =.000478
MASS FRACTION , Y_F, Y_O
10.0
8.0
6.0
4.0
2.0
0.0
0.0
0.2
0.4
0.6
0.8
DISTANCE FROM FUEL SURFACE (*10-4), y
O - FUEL, TIME- 3.89E+04, Ignition
+ - 02 , TIME- 3.89E+04, Ignition

Figure 3.6a

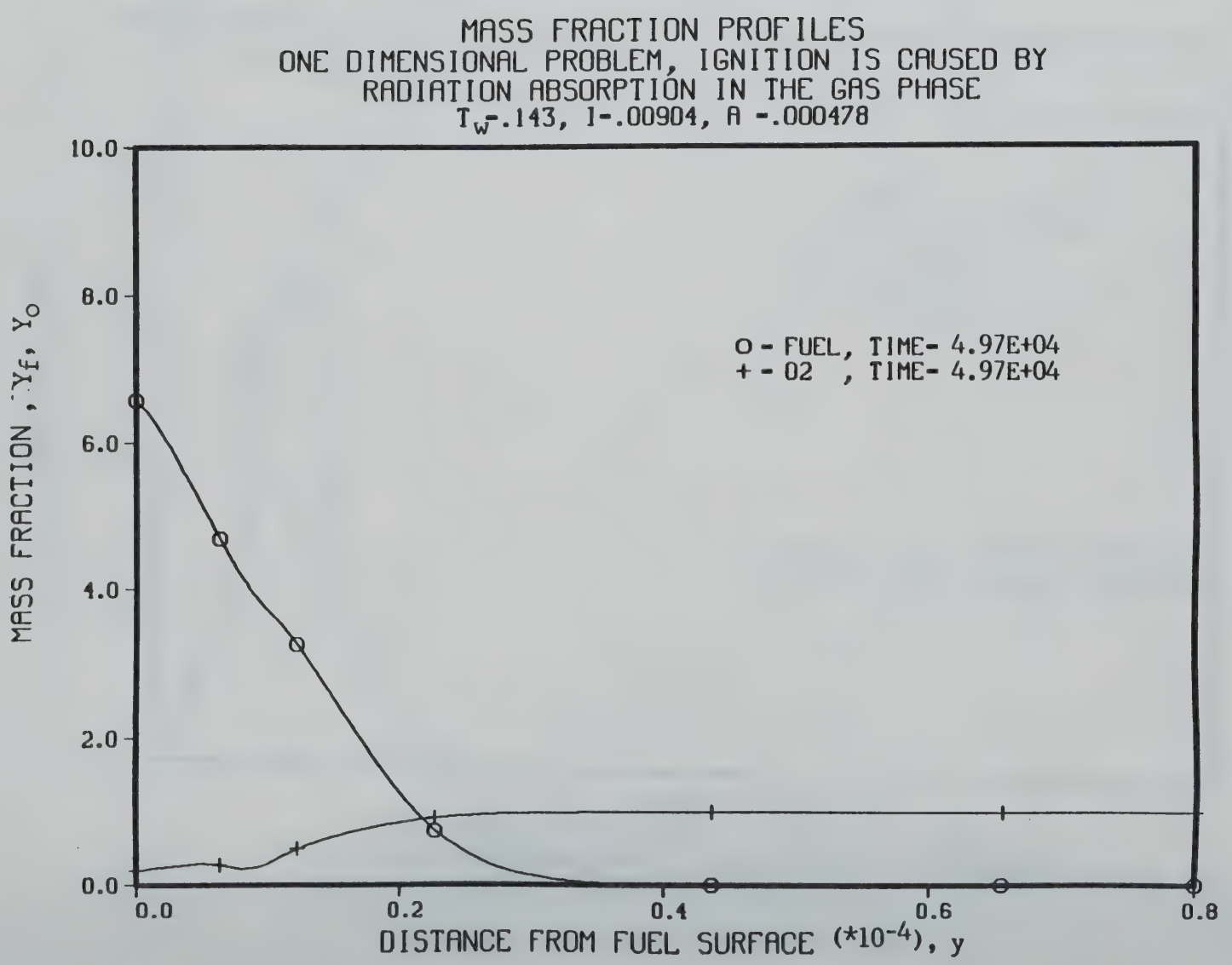
MASS FRACTION PROFILES
ONE DIMENSIONAL PROBLEM, IGNITION IS CAUSED BY
RADIATION ABSORPTION IN THE GAS PHASE
T_w=.143, I=.00904, A =.000478
O - FUEL, TIME- 4.97E+04
+ - O2 , TIME- 4.97E+04
MASS FRACTION , Y_f, Y_o
10.0
8.0
6.0
4.0
2.0
0.0
0.0
0.2
0.4
0.6
0.8
DISTANCE FROM FUEL SURFACE (*10^{-4}), y

Figure 3.6b

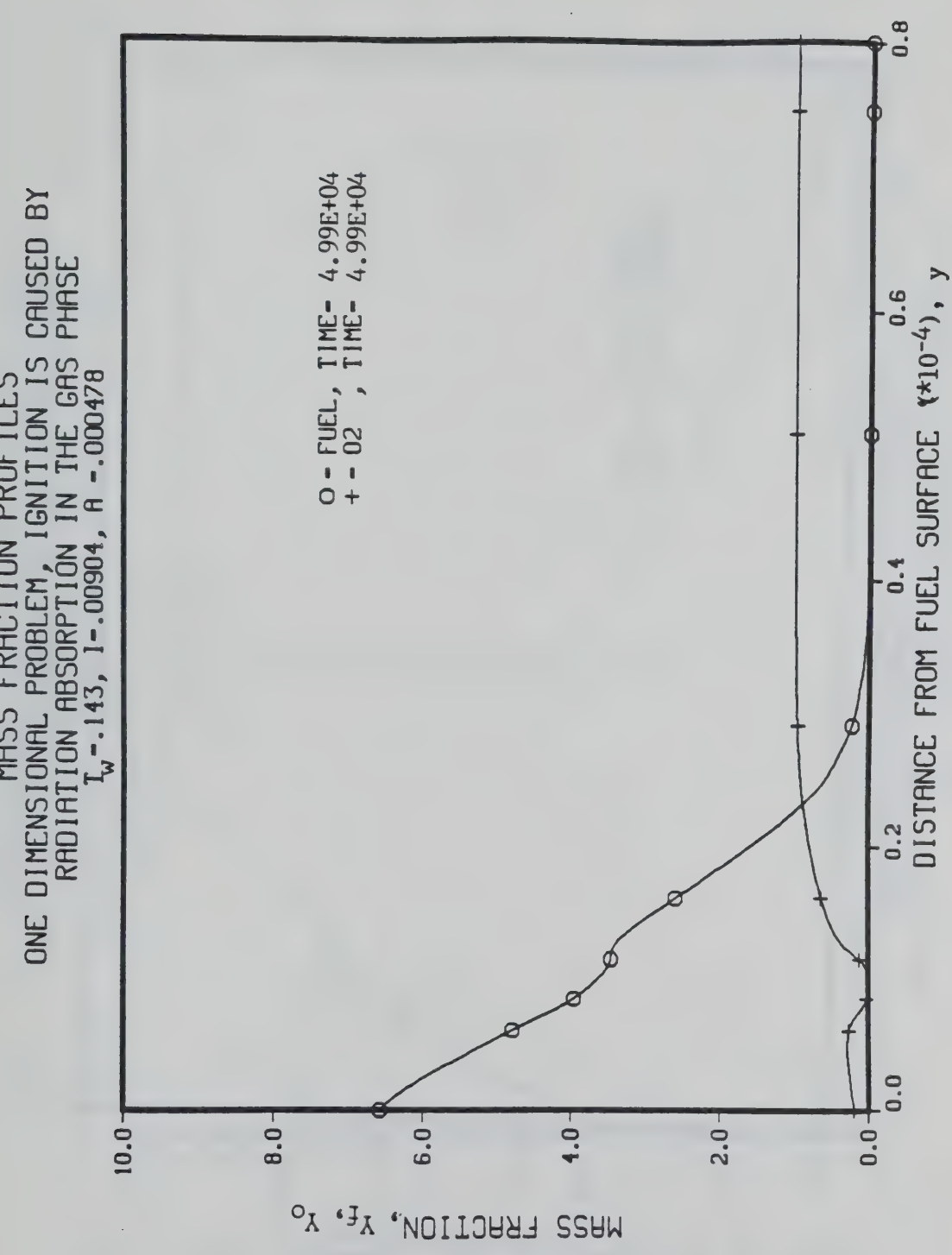
MASS FRACTION PROFILES
ONE DIMENSIONAL PROBLEM, IGNITION IS CAUSED BY
RADIATION ABSORPTION IN THE GAS PHASE
I_w=.143, I=.00904, A =.000478
O = FUEL, TIME= 4.99E+04
+ = O2 , TIME= 4.99E+04
MASS FRACTION, Y_F, Y_O
10.0
8.0
6.0
4.0
2.0
0.0
0.0
0.2
0.4
0.6
0.8
DISTANCE FROM FUEL SURFACE (*10^{-4}), y

Figure 3.6c

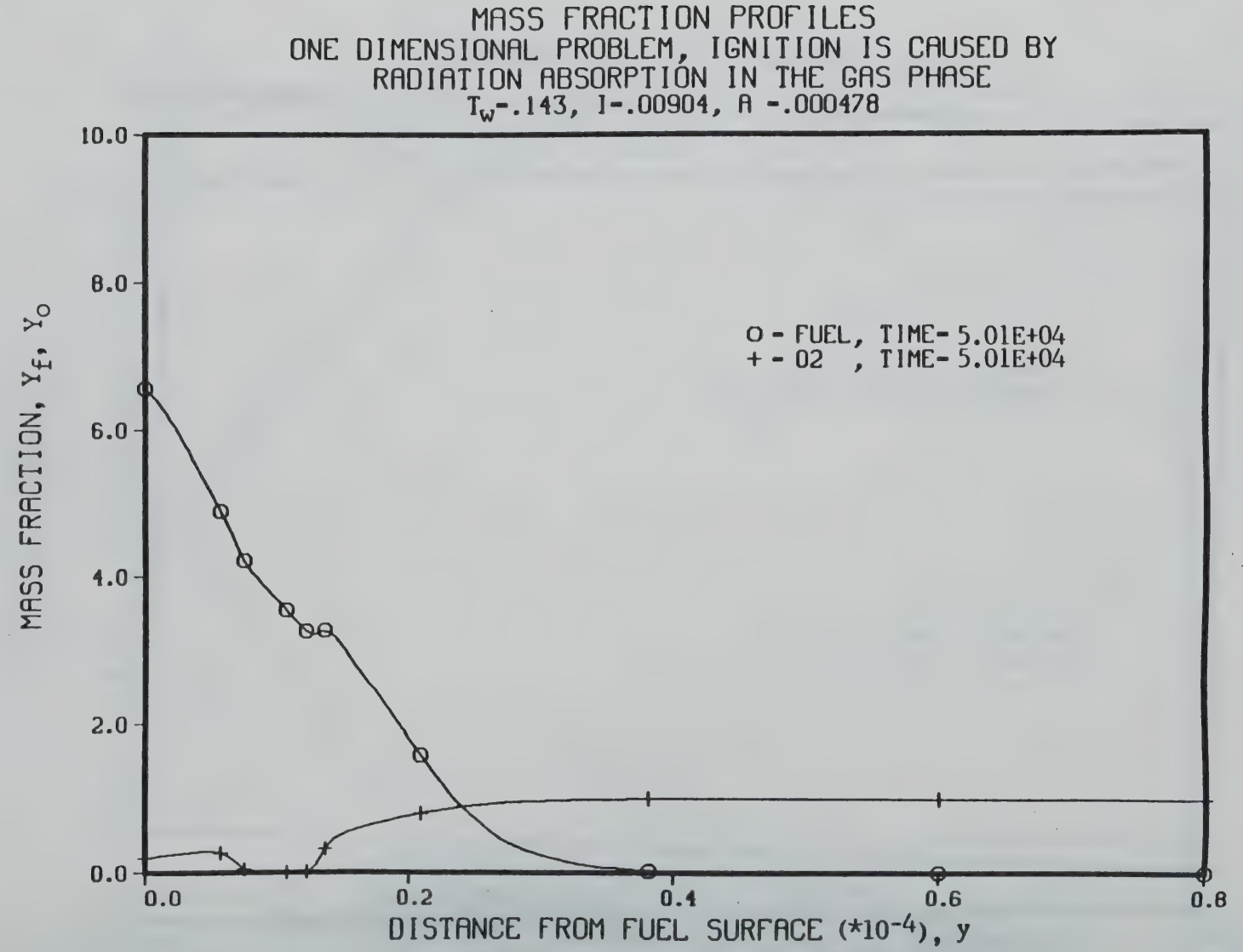
MASS FRACTION PROFILES
ONE DIMENSIONAL PROBLEM, IGNITION IS CAUSED BY
RADIATION ABSORPTION IN THE GAS PHASE
T_w-.143, I-.00904, A -.000478
O - FUEL, TIME- 5.01E+04
+ - O2 , TIME- 5.01E+04
MASS FRACTION, Y_f, Y_o
10.0
8.0
6.0
4.0
2.0
0.0
0.0
0.2
0.4
0.6
0.8
DISTANCE FROM FUEL SURFACE (*10^{-4}), y

Figure 3.6d

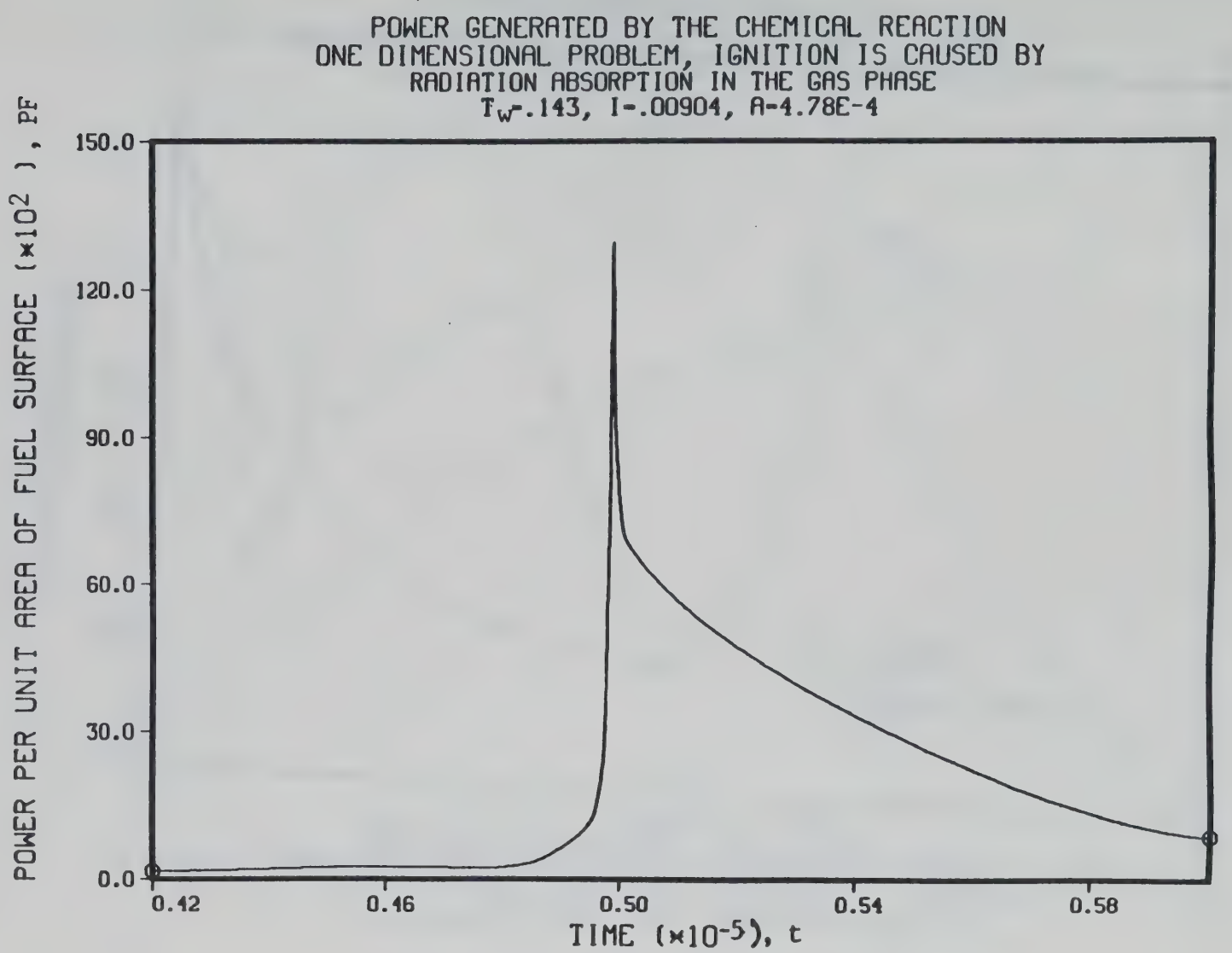
POWER GENERATED BY THE CHEMICAL REACTION
ONE DIMENSIONAL PROBLEM, IGNITION IS CAUSED BY
RADIATION ABSORPTION IN THE GAS PHASE
T_w=.143, I=.00904, A=4.78E-4
POWER PER UNIT AREA OF FUEL SURFACE (×10²), PF
150.0
120.0
90.0
60.0
30.0
0.0
0.42
0.46
0.50
0.54
0.58
TIME (×10⁻⁵), t

Figure 3.7

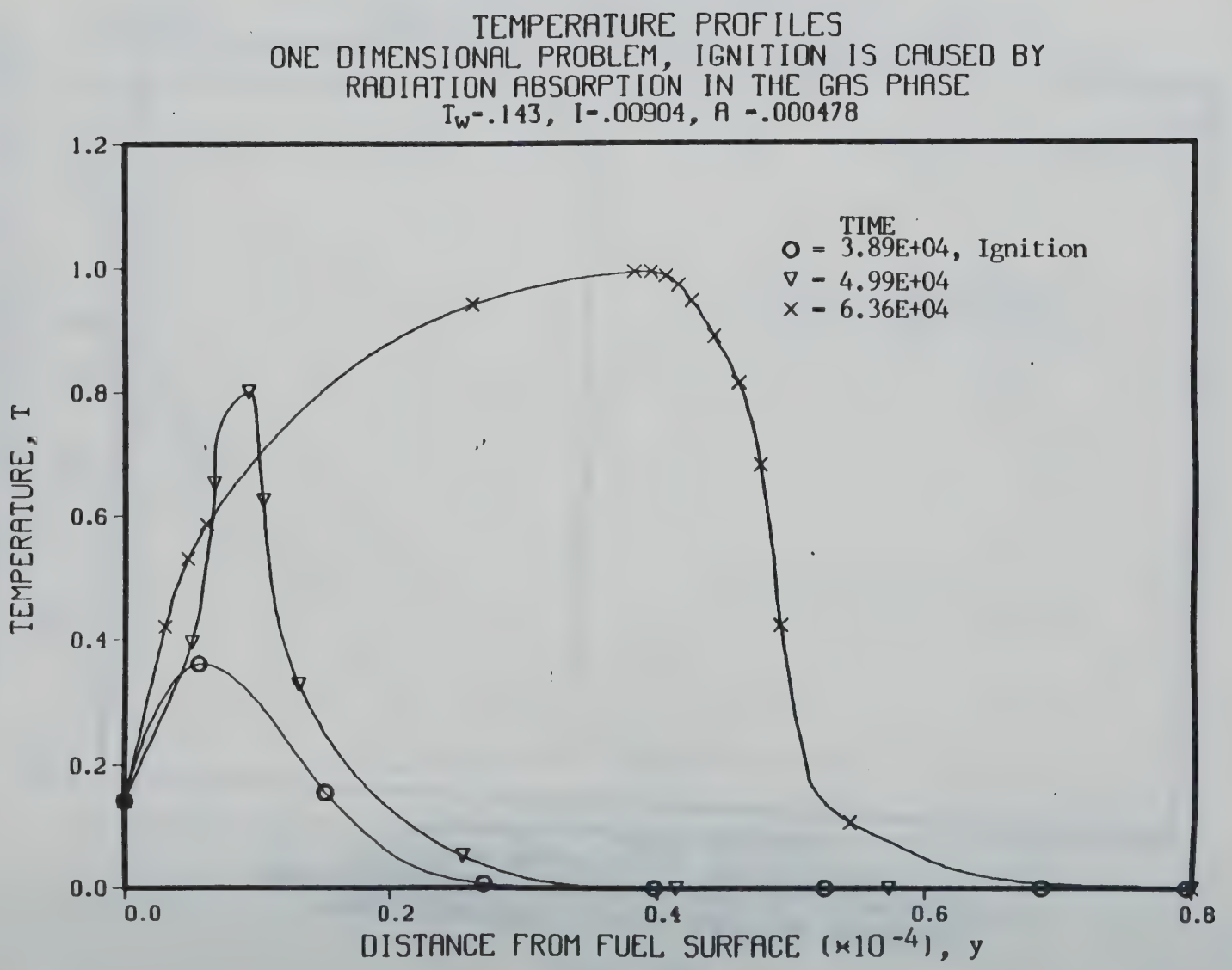
TEMPERATURE PROFILES
ONE DIMENSIONAL PROBLEM, IGNITION IS CAUSED BY
RADIATION ABSORPTION IN THE GAS PHASE
T_w-.143, I-.00904, A -.000478
TIME
O = 3.89E+04, Ignition
▽ - 4.99E+04
× - 6.36E+04
TEMPERATURE, T
1.2
1.0
0.8
0.6
0.4
0.2
0.0
0.0
0.2
0.4
0.6
0.8
DISTANCE FROM FUEL SURFACE (×10^{-4}), y

Figure 3.8a

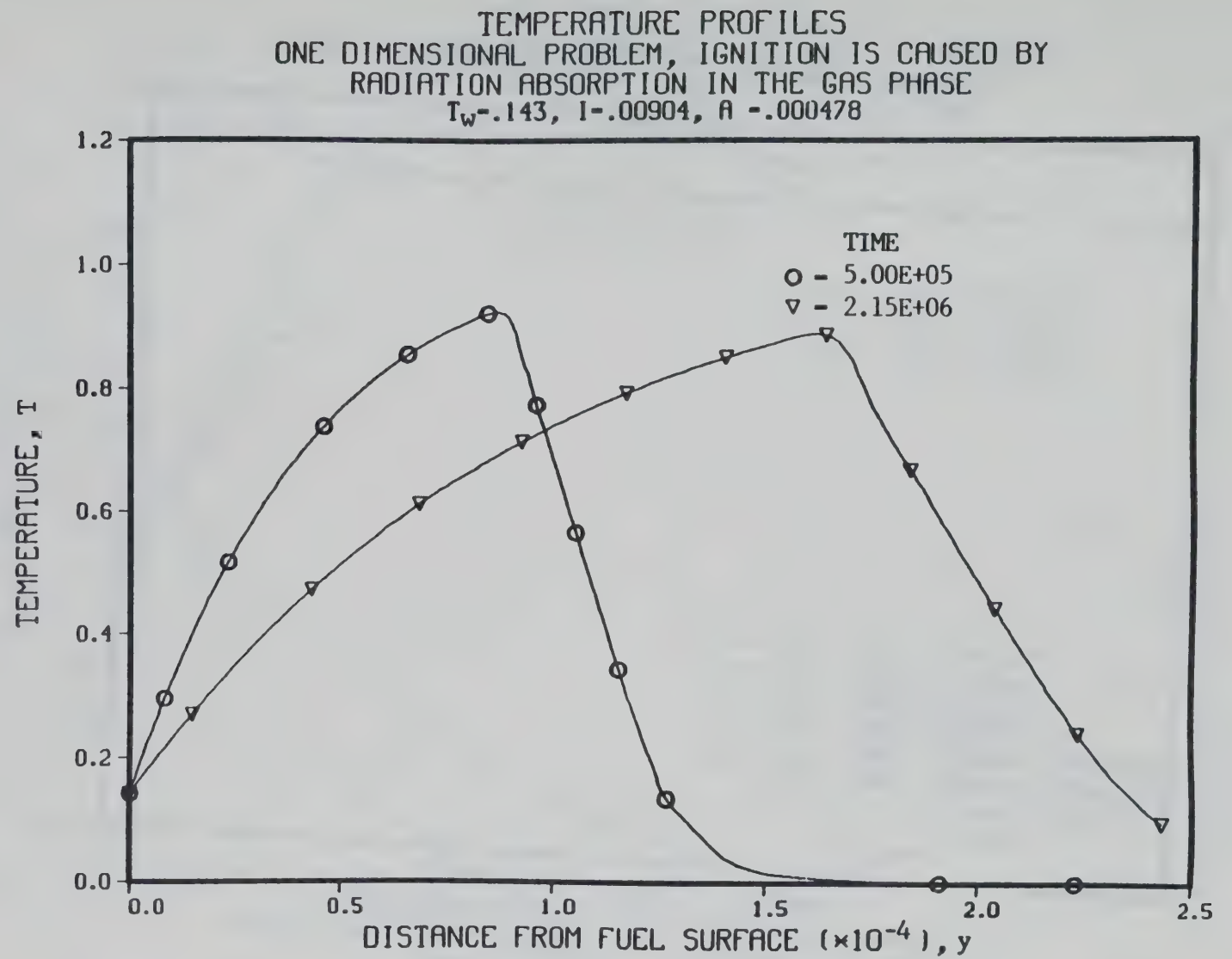
TEMPERATURE PROFILES
ONE DIMENSIONAL PROBLEM, IGNITION IS CAUSED BY
RADIATION ABSORPTION IN THE GAS PHASE
T_w-.143, I-.00904, A -.000478
TIME
O - 5.00E+05
▽ - 2.15E+06
TEMPERATURE, T
1.2
1.0
0.8
0.6
0.4
0.2
0.0
0.0
0.5
1.0
1.5
2.0
2.5
DISTANCE FROM FUEL SURFACE (×10^{-4}), y

Figure 3.8b

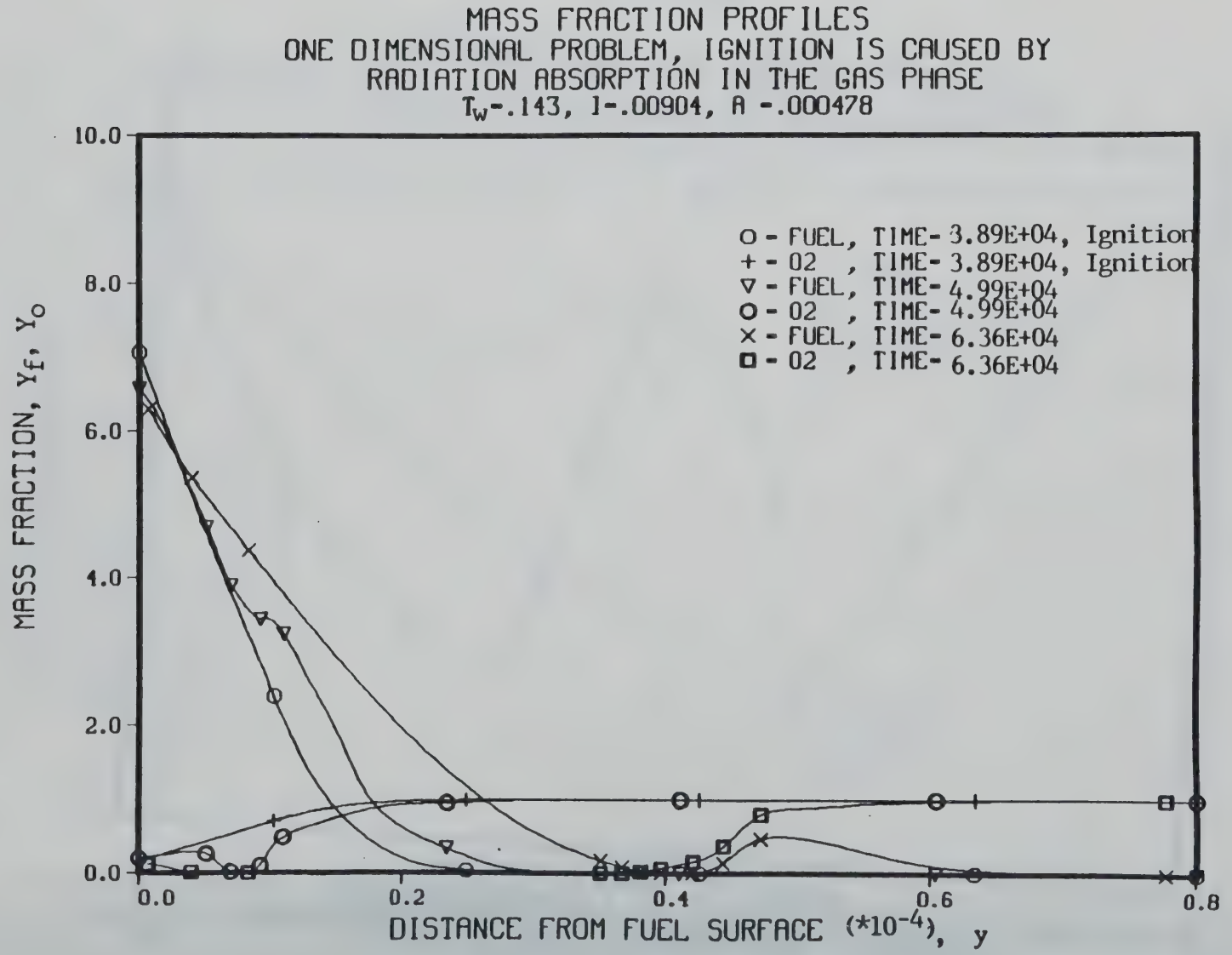
MASS FRACTION PROFILES
ONE DIMENSIONAL PROBLEM, IGNITION IS CAUSED BY
RADIATION ABSORPTION IN THE GAS PHASE
T_w-.143, 1-.00904, A -.000478
O - FUEL, TIME- 3.89E+04, Ignition
+ - 02 , TIME- 3.89E+04, Ignition
▽ - FUEL, TIME- 4.99E+04
O - 02 , TIME- 4.99E+04
× - FUEL, TIME- 6.36E+04
□ - 02 , TIME- 6.36E+04
MASS FRACTION, Y_f, Y_o
10.0
8.0
6.0
4.0
2.0
0.0
0.0
0.2
0.4
0.6
0.8
DISTANCE FROM FUEL SURFACE ($*10^{-4}$), y

Figure 3.9a

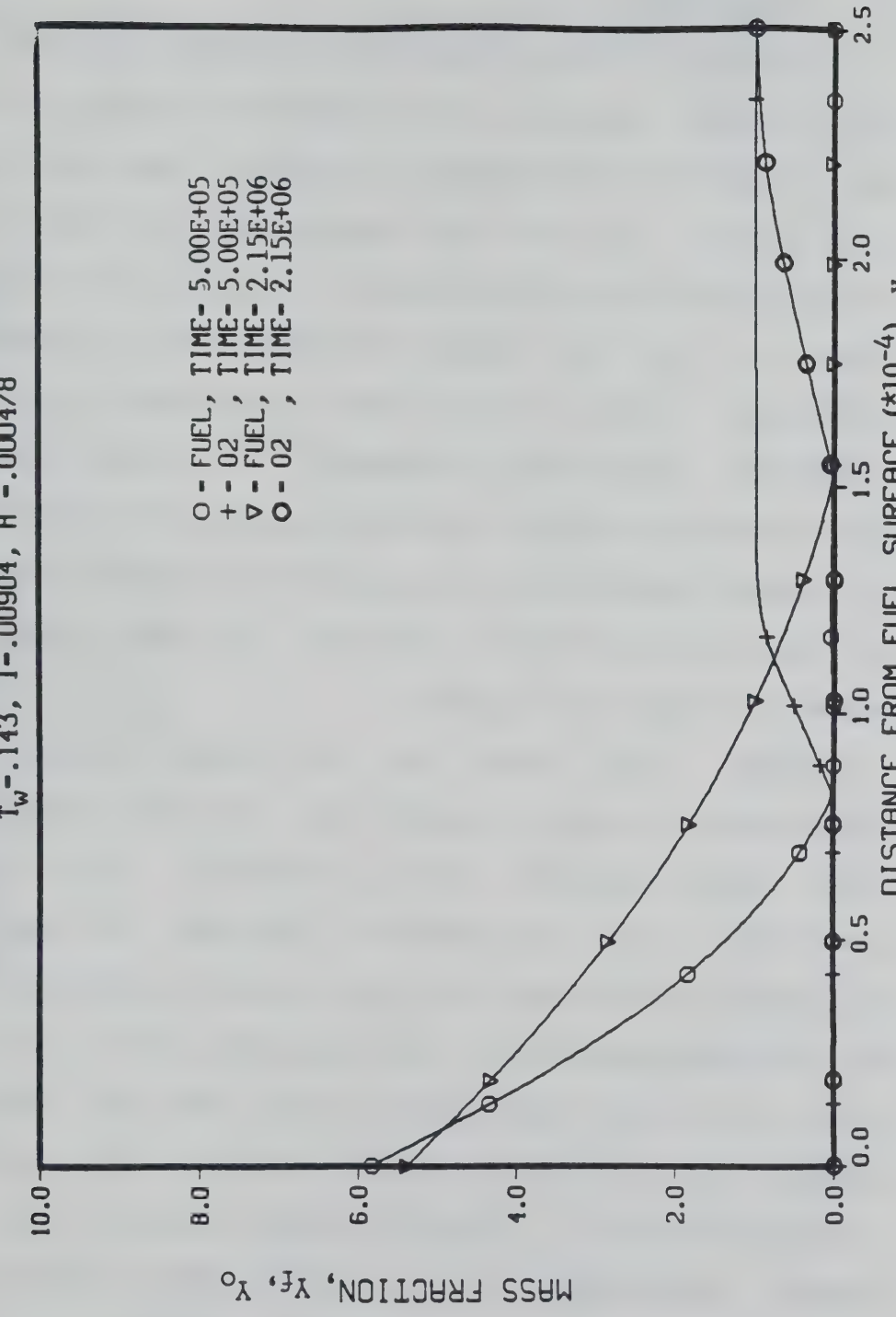
MASS FRACTION PROFILES
ONE DIMENSIONAL PROBLEM, IGNITION IS CAUSED BY
RADIATION ABSORPTION IN THE GAS PHASE
T_w=.143, I=.00904, A =.000478
O - FUEL, TIME- 5.00E+05
+ - O2 , TIME- 5.00E+05
∇ - FUEL, TIME- 2.15E+06
O - O2 , TIME- 2.15E+06
MASS FRACTION, Y_F, Y_O
DISTANCE FROM FUEL SURFACE (*10^{-4}), y
0.0
2.0
4.0
6.0
8.0
10.0
0.0
0.5
1.0
1.5
2.0
2.5

Figure 3.9b

3.3.2 Results of the Parametric Study on Ignition Caused by Gas Phase Absorption

A parametric study was performed to determine the effect of the absorption coefficient and the radiation intensity on the time to ignition and the location of ignition. These results are shown in Figs. (3.10) and (3.11) respectively. From Fig. (3.10) it can be seen that the ignition delay is approximately inversely related to both the radiation intensity and the absorption coefficient. These results agree qualitatively with the experimental observations of Kashiwagi[25-29] and Mutoh,[31] and can be explained by noting that the radiant heating of the fuel vapor is directly proportional to the product of the intensity and to the absorption coefficient. Obviously, the faster the gas is heated the sooner it will ignite.

Figure (3.11) shows that the ignition distance is approximately inversely related to the absorption coefficient while being independent of the intensity. The inverse relationship with the absorption coefficient can again be explained by the fact that the radiant heating is proportional to the absorption coefficient. The independence of the distance from the wall at which ignition occurs from the radiation intensity can be best explained by noting that the injection velocity of the fuel, if the fuel vapor is optically thin, is directly proportional to the intensity while the time to ignition, as noted above is inversely proportional to the intensity. Since the distance that a particle will travel away

from the wall before igniting is the product of the velocity and the time to ignition the intensity will cancel out and the ignition distance should be independent of intensity.

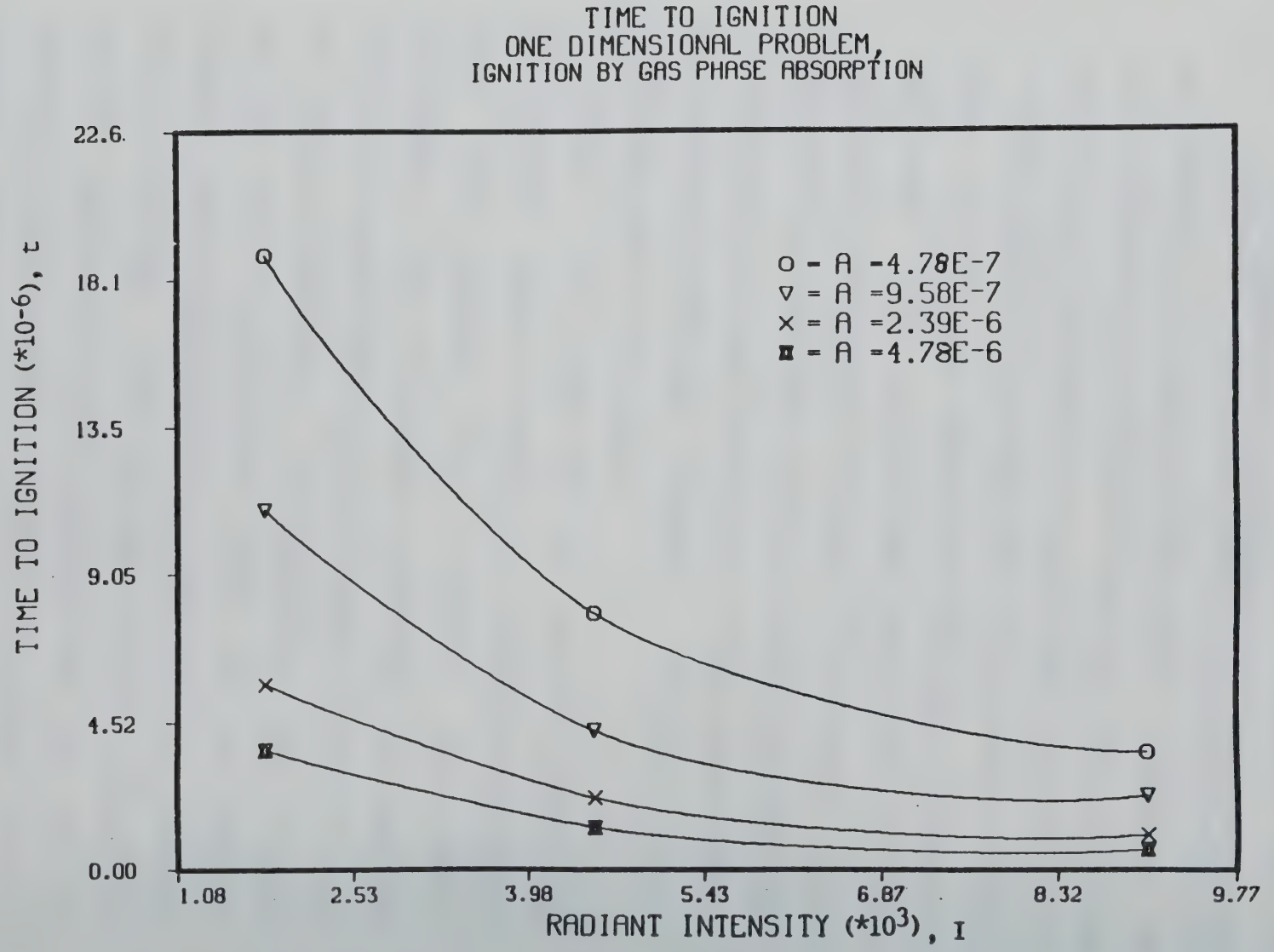
TIME TO IGNITION
ONE DIMENSIONAL PROBLEM,
IGNITION BY GAS PHASE ABSORPTION
22.6
18.1
13.5
9.05
4.52
0.00
TIME TO IGNITION (*10-6), t
o - A -4.78E-7
▽ = A =9.58E-7
× = A =2.39E-6
■ = A =4.78E-6
1.08
2.53
3.98
5.43
6.87
8.32
9.77
RADIANT INTENSITY (*10^3), I

Figure 3.10

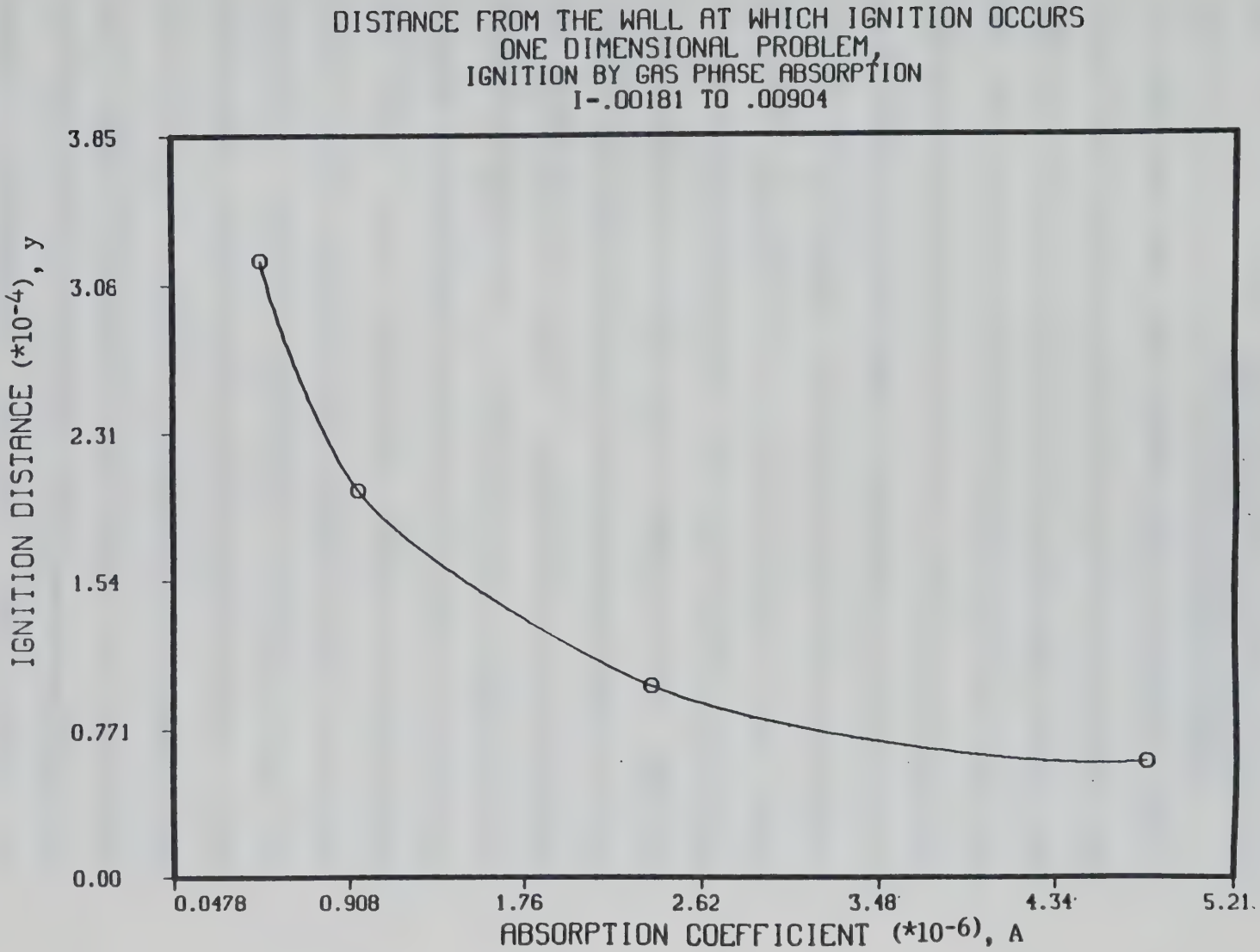
DISTANCE FROM THE WALL AT WHICH IGNITION OCCURS
ONE DIMENSIONAL PROBLEM,
IGNITION BY GAS PHASE ABSORPTION
I-.00181 TO .00904
IGNITION DISTANCE (*10-4), y
3.85
3.06
2.31
1.54
0.771
0.00
0.0478
0.908
1.76
2.62
3.48
4.34
5.21
ABSORPTION COEFFICIENT (*10-6), A

Figure 3.11

3.3.3 Results of the Ignition and Flame Propagation Study with Ignition Caused by a Hot Fuel Surface

The parameters which define this case are shown in dimensional form in Table (3.2) and in non-dimensional form in Table (3.3). The differences between this case and the previous case are that the absorption coefficient is set to zero, the vaporization temperature of the fuel and thus the temperature of the fuel wall is increased, the intensity of the radiation is decreased and the heat of combustion is decreased. The first two changes are obvious because they are necessary to change the source of ignition from gas phase absorption to ignition by the hot wall. The reduction in the intensity of radiation is possible because the function of the radiation is now simply to vaporize the fuel, rather than to vaporize the fuel and to heat the fuel vapor to a high temperature. The radiation intensity used here of 1.3 watts/cm^2 is about the same intensity that would be found in a house fire.[43] Hence, this form of ignition will occur naturally and a special high powered laser is not required. The final parameter that is changed is the heat of combustion which is reduced by approximately twenty percent. The reason for this reduction is numerical. Because the vaporization temperature of the fuel is increased there will be a corresponding increase in the temperatures that were obtained in the premixed flame if the heat of combustion is remained unchanged. The chemical reaction will be very fast at these high

temperatures and very small timesteps would be required. The lower heat of combustion avoids the high temperatures and thus keeps the reaction rate within reasonable bounds.

The evolution of the temperature profiles and mass fraction profiles are shown in Figs. (3.12) and (3.13), respectively. Since the intensity of radiation in this case is relatively low, only a small amount of fuel is vaporized before ignition takes place and the fuel and the air mix in a region very close to the wall. The point of ignition is then very close to the wall as shown in Fig. (3.12a). The ignition process is analyzed in detail by Kindelan.[4]

After ignition occurs, the post-ignition events are somewhat similiar to the events in the gas phase absorption cases. Ignition occurs in a rich region where there is still a high concentration of oxygen. A period of weak chemical reaction follows the ignition event, and as the reaction becomes stronger a spike develops in the power curve similiar to that shown in Fig. (3.7). After the power spike dies down a premixed flame appears which propagates away from the wall. It begins propagating in the rich region, passes through the stoichiometric point and enters the lean region where it dies out. A diffusion flame is left behind at the stoichiometric point which propagates away from the wall. Again, it is expected that the diffusion flame will weaken and die out when it gets far enough away from the wall.

While events in general are similiar to the gas phase

absorption cases there are several differences. The most obvious difference is that events occur much closer to the wall. Another is that very little fuel is vaporized before ignition takes place. Hence, the premixed flame front does not travel nearly as far and dies out close to the wall. Also, unlike the gas phase absorption case, a great deal of fuel is vaporized after ignition because of the development of the premixed flame front takes place right next to the wall creating steep gradients in temperature at the wall surface. However, the total amount of fuel vaporized is still less than that vaporized in the gas phase absorption cases. Because there is less fuel vaporized the diffusion flame should weaken sooner and die out closer to the wall than in the previous case. This weakening is exacerbated by the lower heat of combustion which reduces the temperature of the diffusion flame.

This completes the discussion of the one dimensional problem. The next chapter will discuss the stagnation point flow problem.

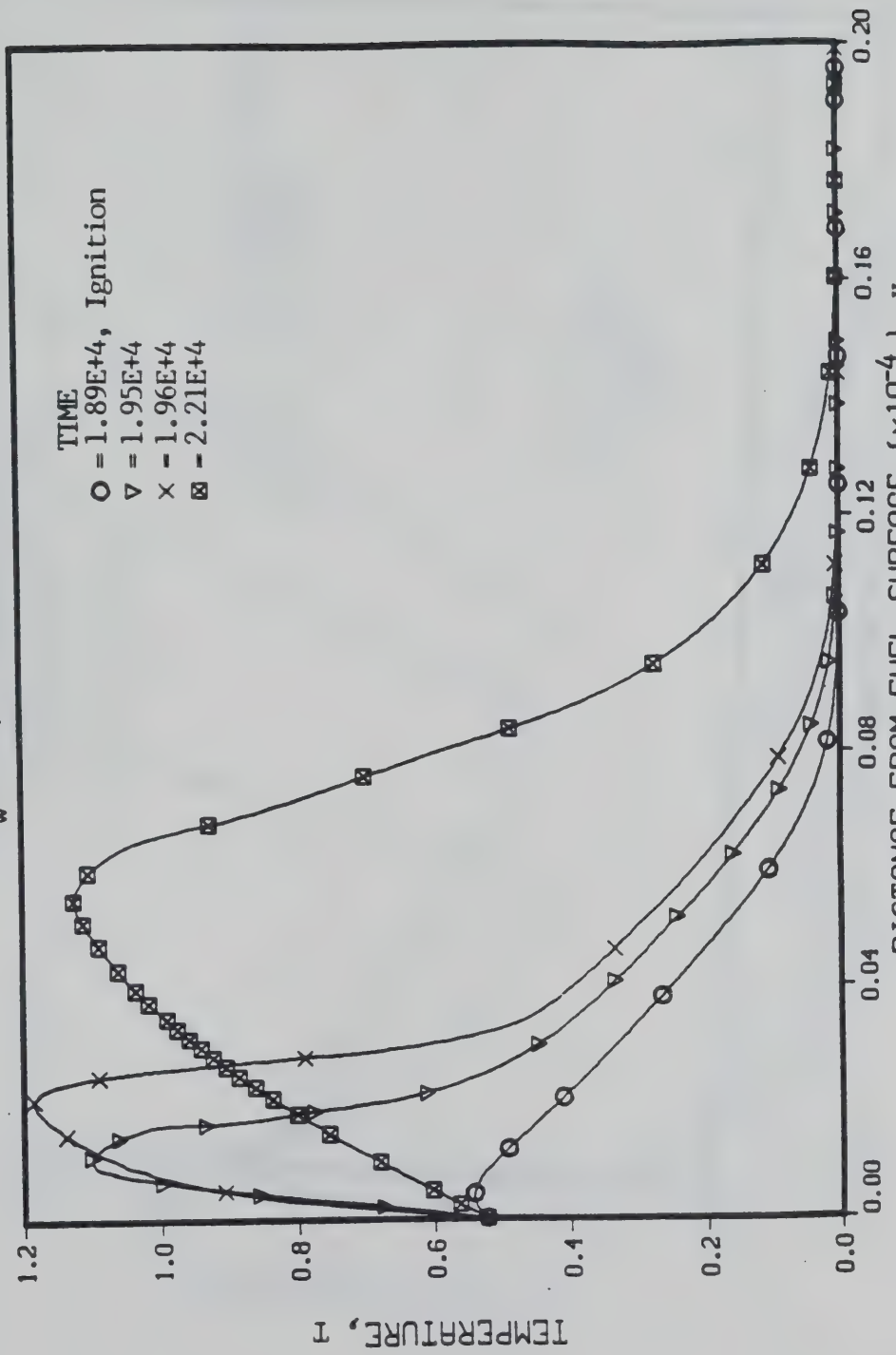
TEMPERATURE PROFILES
ONE DIMENSIONAL PROBLEM, IGNITION IS CAUSED BY
A HIGH TEMPERATURE FUEL SURFACE
T_w=.523, 1-.00205, A -0.
TIME
O = 1.89E+4, Ignition
∇ = 1.95E+4
× = 1.96E+4
⊠ = 2.21E+4
TEMPERATURE, T
DISTANCE FROM FUEL SURFACE (×10^{-4}), y
0.0
0.2
0.4
0.6
0.8
1.0
1.2
0.00
0.04
0.08
0.12
0.16
0.20

Figure 3.12a

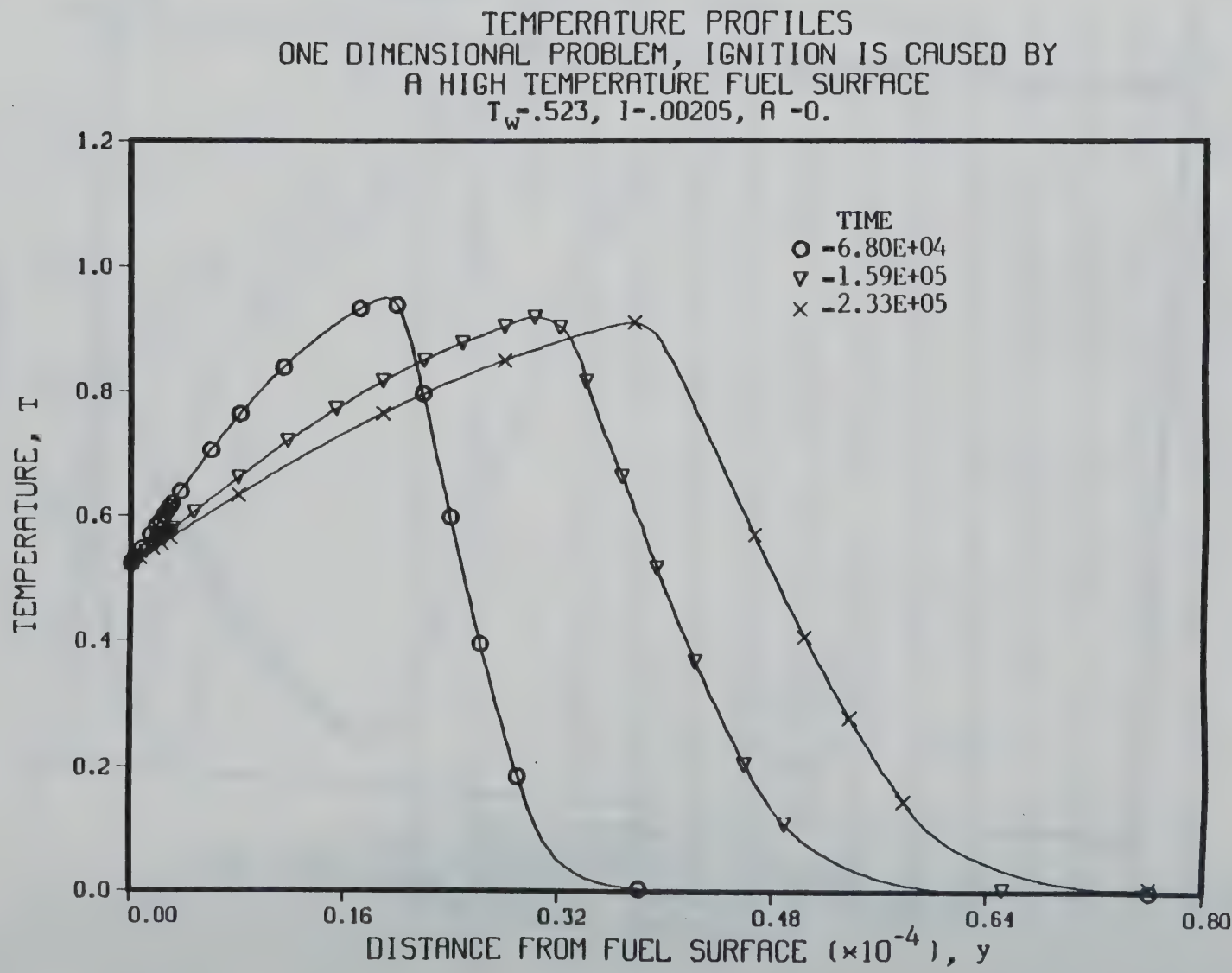
TEMPERATURE PROFILES
ONE DIMENSIONAL PROBLEM, IGNITION IS CAUSED BY
A HIGH TEMPERATURE FUEL SURFACE
T_w=.523, I=.00205, A =0.
TIME
O =6.80E+04
▽ =1.59E+05
× =2.33E+05
TEMPERATURE, T
1.2
1.0
0.8
0.6
0.4
0.2
0.0
0.00
0.16
0.32
0.48
0.64
0.80
DISTANCE FROM FUEL SURFACE (×10^{-4}), y

Figure 3.12b

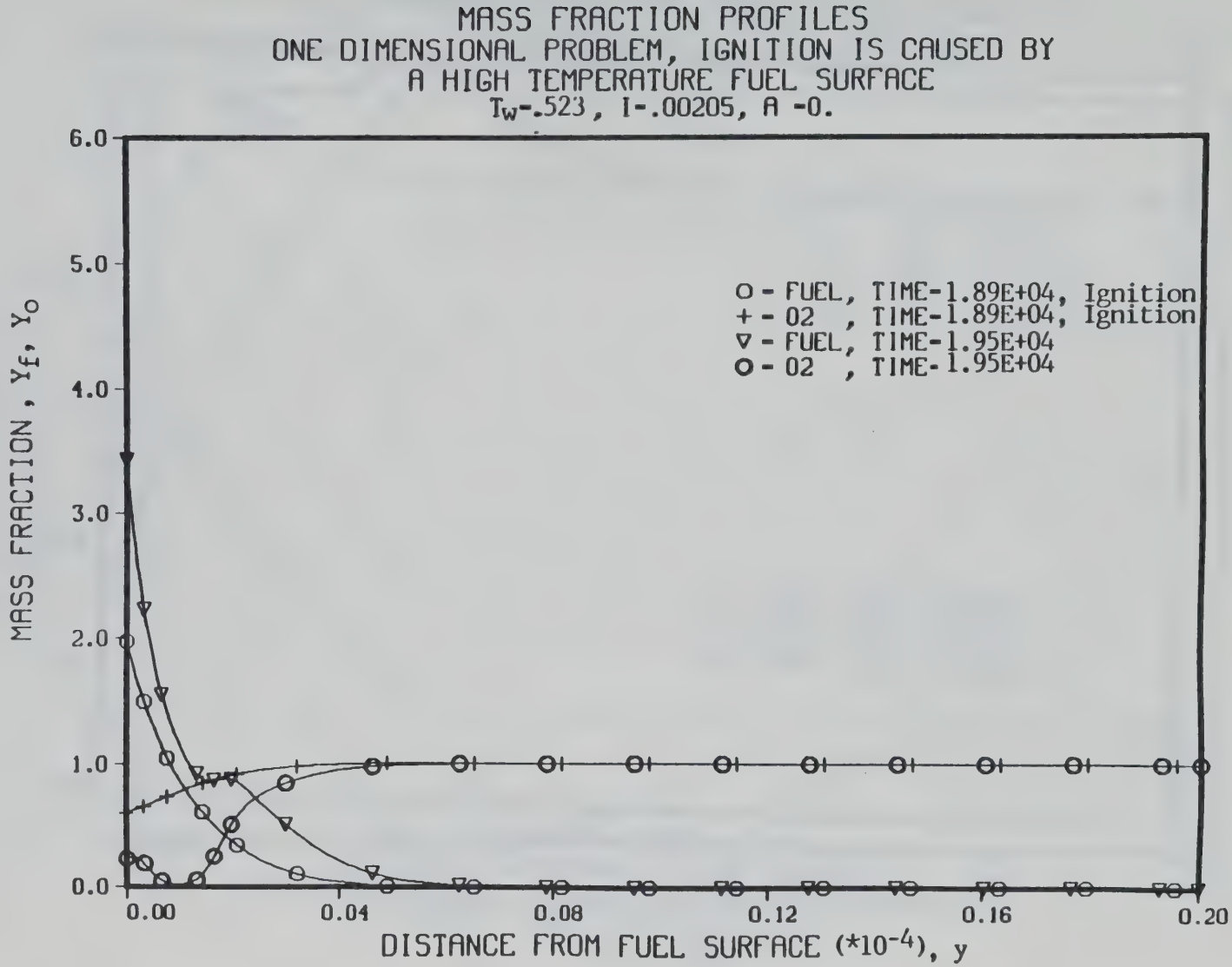
MASS FRACTION PROFILES
ONE DIMENSIONAL PROBLEM, IGNITION IS CAUSED BY
A HIGH TEMPERATURE FUEL SURFACE
Tw-.523, I-.00205, A -0.
O - FUEL, TIME-1.89E+04, Ignition
+ - 02 , TIME-1.89E+04, Ignition
∇ - FUEL, TIME-1.95E+04
O - 02 , TIME-1.95E+04
MASS FRACTION, Yf, Yo
6.0
5.0
4.0
3.0
2.0
1.0
0.0
0.00
0.04
0.08
0.12
0.16
0.20
DISTANCE FROM FUEL SURFACE (*10-4), y

Figure 3.13a

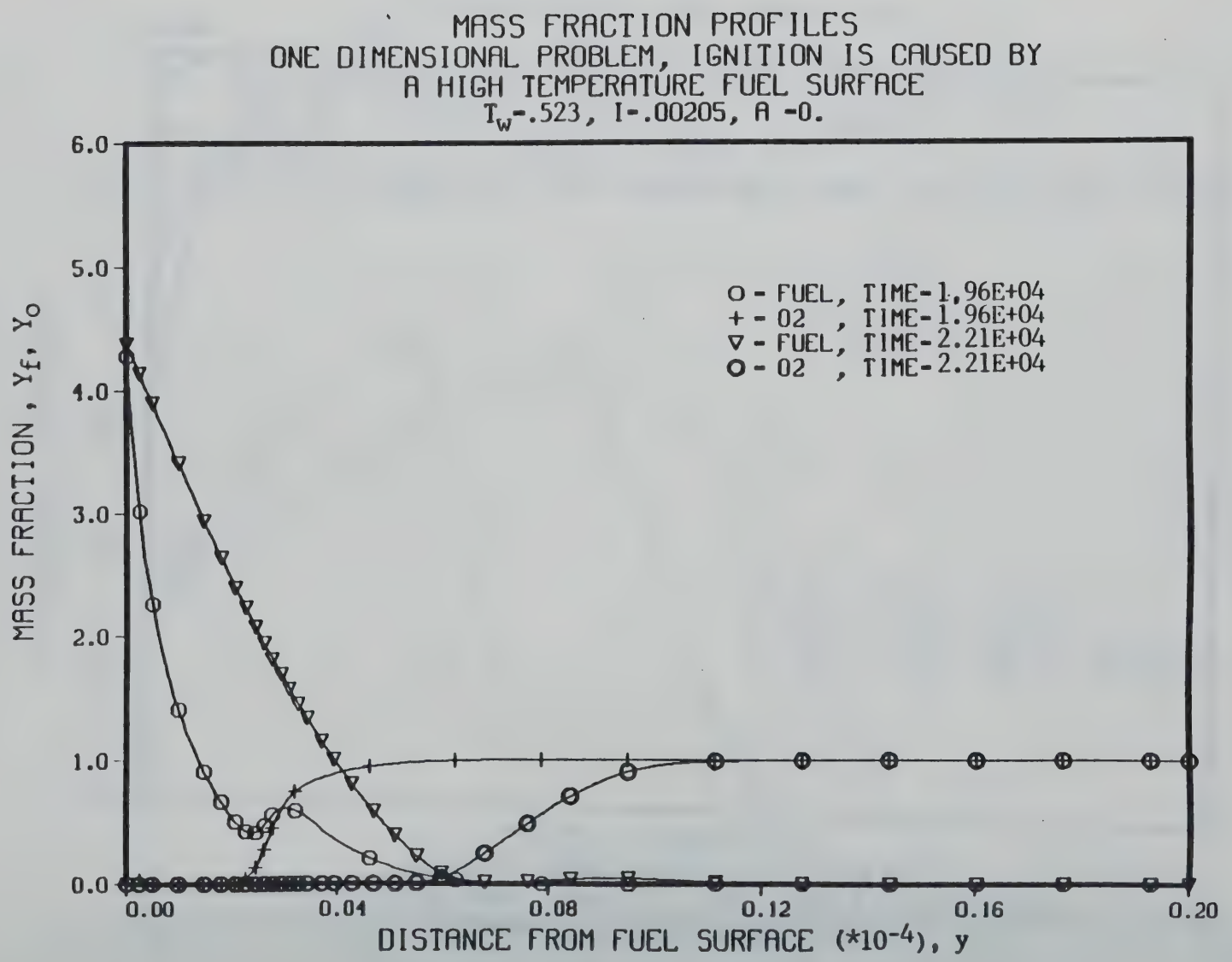
MASS FRACTION PROFILES
ONE DIMENSIONAL PROBLEM, IGNITION IS CAUSED BY
A HIGH TEMPERATURE FUEL SURFACE
T_w-.523, I-.00205, A -0.
O - FUEL, TIME-1.96E+04
+ - 02 , TIME-1.96E+04
▽ - FUEL, TIME-2.21E+04
O - 02 , TIME-2.21E+04
MASS FRACTION , Y_F, Y_O
6.0
5.0
4.0
3.0
2.0
1.0
0.0
0.00
0.04
0.08
0.12
0.16
0.20
DISTANCE FROM FUEL SURFACE (*10^{-4}), y

Figure 3.13b

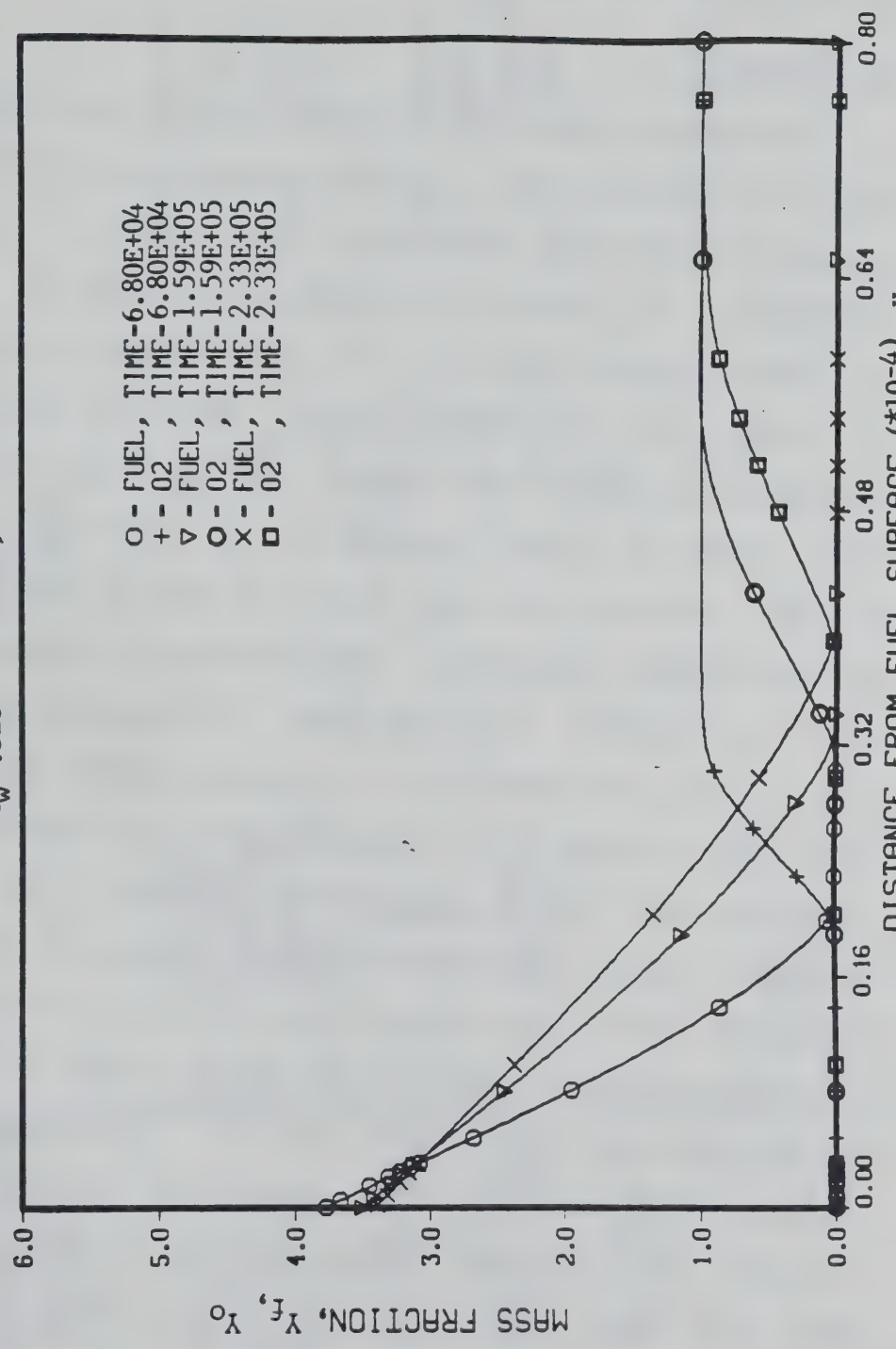
MASS FRACTION PROFILES
ONE DIMENSIONAL PROBLEM, IGNITION IS CAUSED BY
A HIGH TEMPERATURE FUEL SURFACE
T_w=.523 I=.00205, A =0.
O - FUEL, TIME-6.80E+04
+ - O2 , TIME-6.80E+04
∇ - FUEL, TIME-1.59E+05
O - O2 , TIME-1.59E+05
× - FUEL, TIME-2.33E+05
□ - O2 , TIME-2.33E+05
MASS FRACTION, Y_F, Y_O
DISTANCE FROM FUEL SURFACE (*10^{-4}), y
0.0
1.0
2.0
3.0
4.0
5.0
6.0
0.00
0.16
0.32
0.48
0.64
0.80

Figure 3.13c

4.0 Stagnation Point Problem

4.1 Introduction

The stagnation point flow problem is shown schematically in Fig. (4.1). The problem has similiar characteristics to the one dimensional problem with the exception that a velocity is imposed perpendicular to the wall at a certain distance from the wall, L_b. There is again a combustible fuel surface which is subjected to radiant heat flux at time, t=0.0. The solid begins to vaporize mixing the fuel with the air, and, here again, one of three things may occur depending on the conditions of the problem: a)ignition may occur because the fuel is reactive at the vaporization temperature, b)ignition may occur because of radiation absorption in the gas phase, or c)ignition may not occur. Also, the possibility of a combined ignition mechanism exists where the fuel is hot enough to ignite at its vaporization temperature and the fuel vapor absorbs radiation. One major difference between the stagnation point flow case and the one dimensional case is that a steady state solution can be obtained for vaporization without ignition. The results of Fig. (3.10) for the one-dimensional case tended to show that, given enough time, ignition would eventually occur even for low values of the intensity. For a given set of input parameters in the stagnation point flow case, however, there will be a definite minimum radiant intensity required to cause ignition. Also, if ignition does occur in the stagnation point flow case, a steady state diffusion flame solution can be obtained rather than the flame

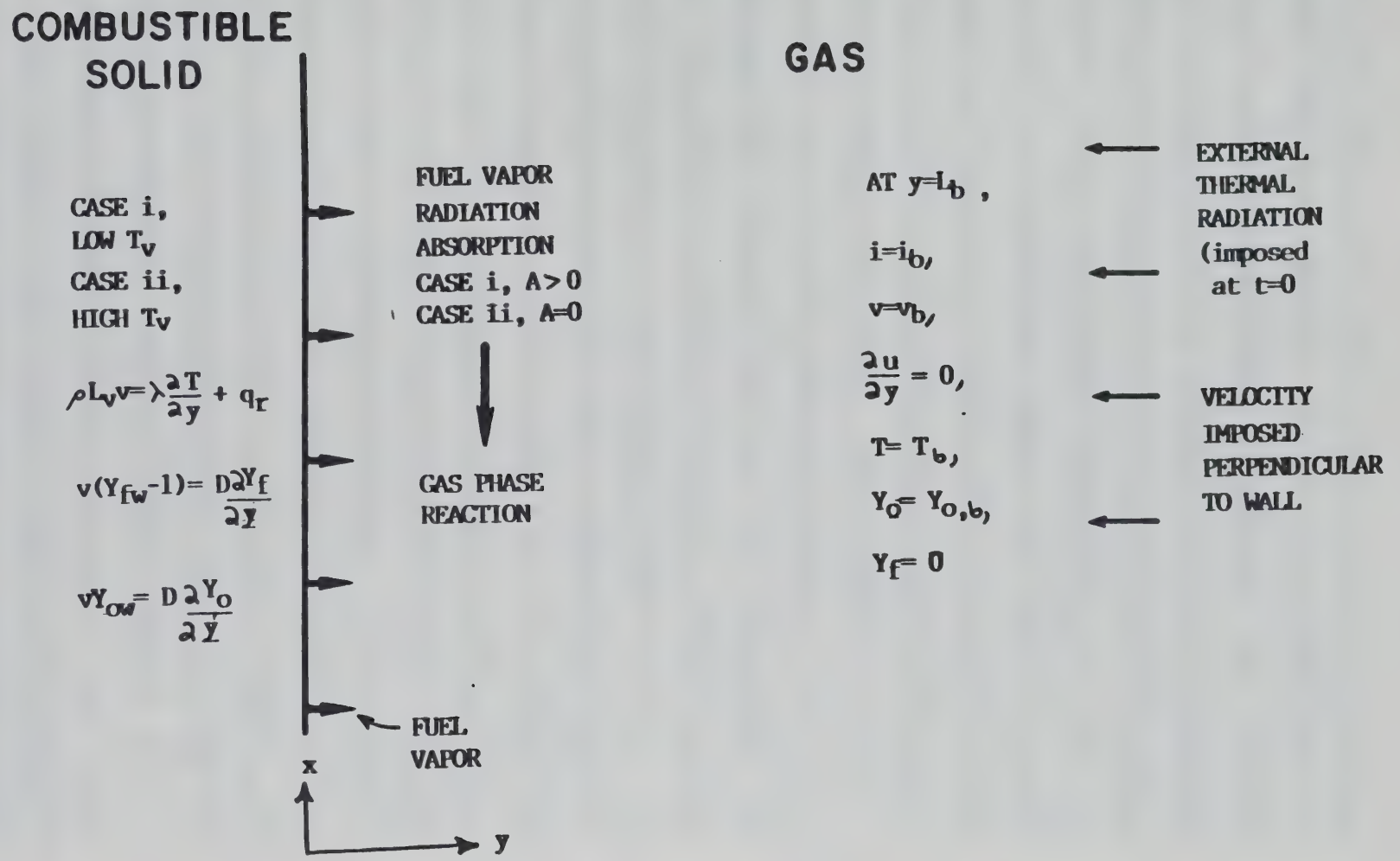

Figure 4.1 Detailed Schematic Diagram
Illustrating the Stagnation Point Flow Problem

continuously moving away from the wall and eventually dying out.

The assumptions made in the one dimensional problem concerning the thermodynamic properties of the gases and the radiation and radiation properties will also be made here. Also remaining the same is the zero gravity assumption, the assumption that the pressure remains approximately constant, and the assumption that the chemical reaction rate is a one step reaction described by an Arrhenius expression. The ignition criterion used in the previous problem will also be used here.

In the solution of the steady state stagnation point flow problem with a uniformly evaporating surface, it is assumed that the temperature, the fuel mass fraction, the oxygen mass fraction and the y-direction velocities are functions of y only and not of x. This assumption will be extended to the present transient analysis where it will be assumed that these quantities are functions of y and t only and not of x. No restrictions are placed upon the x-direction velocity or upon the pressure. However, as will be shown in the analysis section, the above assumptions will restrict the x dependence of the x-direction velocity and the x dependence of the pressure to a specific form. This restriction will have a significant effect upon some of the results and will be discussed more in that section.

As mentioned above, in order to generate the stagnation point flow a y-direction velocity is imposed a given distance from the wall and remains constant for all values of time. This boundary condition is different from the standard boundary

condition which is applied in a steady state stagnation point flow. The standard boundary condition is that the x-direction velocity approaches the potential flow value as y approaches infinity while the y-direction velocity is not specified and is determined such that overall conservation of mass is satisfied.[44] The pressure gradient in the x-direction is then that of the potential flow solution. While the standard boundary condition works well in the steady state, problems develop when a transient case is to be solved. As an example if a flame is developing near the wall, then the density of the gas is decreasing with time and fluid must be moved away from the wall. Since the x-direction pressure gradient is specified, the x-direction velocities can change only in a limited fashion. The mass must be removed by increasing the y-direction velocities and the result is that the y-direction velocity at the outer boundary is an increasing and undetermined function of time. Hence, a solution calculated using the standard boundary condition would be very difficult to verify experimentally. It would be easier to experimentally verify the condition used here where the y-direction velocity is imposed at the outer boundary. This condition complicates the problem somewhat since the x-direction pressure gradient must now be allowed to vary in order to conserve mass on an overall basis.

An additional disadvantage of imposing the y-direction velocity at the outer boundary is that the relationship between the stagnation point problem and the one-dimensional problem is

lost. If the standard stagnation point boundary condition was applied then the one dimensional problem would be a limiting case of the stagnation point problem when the pressure gradient in the x-direction is set equal to zero. With the present boundary condition there appears to be a very limited relationship between the two problems.

Following a development which parallels the one dimensional problem, the dimensional equation will be presented next, followed by a presentation of the non-dimensional parameters and equations. Then the results of a study where ignition is caused by gas phase absorption will be presented along with a parametric study of ignition by gas phase absorption. Finally the results of a case where ignition is caused by a hot fuel surface will be presented.

4.2 Analysis

4.2.1 Governing Equations

Under the assumptions listed above the conservation of momentum equation in the y-direction, the conservation of energy equation, and the mass fraction conservation equations become,

Y-momentum:

$$\bar{\rho}\frac{\partial \bar{v}}{\partial \bar{t}} + \bar{\rho}\bar{v}\frac{\partial \bar{v}}{\partial \bar{y}} = \frac{\partial}{\partial \bar{y}}\left(\bar{\mu}\frac{\partial \bar{v}}{\partial \bar{y}}\right) - \frac{\partial \bar{p}}{\partial \bar{y}} \qquad (4.1)$$

Energy:

$$\bar{\rho}\frac{\partial \bar{T}}{\partial \bar{t}} + \bar{\rho}\bar{v}\frac{\partial \bar{T}}{\partial \bar{y}} = \frac{\partial}{\partial \bar{y}}\left(\frac{\bar{\lambda}}{c_p}\frac{\partial \bar{T}}{\partial \bar{y}}\right) + \frac{1}{c_p}\frac{d\bar{J}}{d\bar{y}} + \frac{Q}{c_p}\bar{w} \qquad (4.2)$$

Fuel conservation:

$$\bar{\rho}\frac{\partial \bar{Y}_F}{\partial \bar{t}} + \bar{\rho}\bar{V}\frac{\partial \bar{Y}_F}{\partial \bar{y}} = \frac{\partial}{\partial \bar{y}}\left(\overline{\rho D}\frac{\partial \bar{Y}_F}{\partial \bar{y}}\right) - \overline{W} \tag{4.3}$$

Oxygen Conservation:

$$\bar{\rho}\frac{\partial \bar{Y}_O}{\partial \bar{t}} + \bar{\rho}\bar{V}\frac{\partial \bar{Y}_O}{\partial \bar{y}} = \frac{\partial}{\partial \bar{y}}\left(\overline{\rho D}\frac{\partial \bar{Y}_O}{\partial \bar{y}}\right) - \frac{m\omega_O \nu_O}{m\omega_F \nu_F}\overline{W} \tag{4.4}$$

where the chemical reaction rate, $\bar{w}$, is given by

$$\overline{W} = B\bar{Y}_O\bar{Y}_F\bar{T}^{-2}\exp\left(\frac{-\bar{E}}{R_u\bar{T}}\right) \tag{4.5}$$

for the one step chemical reaction of the form

$$\nu_F F + \nu_O O \longrightarrow \nu_P P. \tag{4.6}$$

The $d\bar{i}/d\bar{y}$ term is given as

$$\frac{d\bar{i}}{d\bar{y}} = \bar{\rho}a_\lambda\bar{Y}_F\bar{i} \tag{4.7}$$

By plugging $\bar{v}$ and $\bar{\rho}$ into the conservation of mass equation, it can be shown that u must be restricted to the following form

$$\bar{u} = \bar{x}\bar{F} = \frac{\left(\frac{\partial \bar{\rho}}{\partial \bar{t}} - \frac{\partial}{\partial \bar{y}}\left(\bar{\rho}\bar{V}\right)\right)\bar{x}}{\bar{\rho}} \tag{4.8}$$

Then the x-direction momentum equation can be written in the reduced form as

$$\bar{\rho}\frac{\partial \bar{F}}{\partial \bar{t}} + \bar{\rho}\bar{F}^2 + \bar{\rho}\bar{V}\frac{\partial \bar{F}}{\partial \bar{y}} = \frac{\partial}{\partial \bar{y}}\left(\bar{\mu}\frac{\partial \bar{F}}{\partial y}\right) - \frac{\partial \bar{P}}{\partial x} \tag{4.9}$$

Since the terms in the momentum equations that do not contain the pressure gradient are functions of $\bar{y}$ and $\bar{t}$ only, it can be shown

that the pressure is restricted to the following form

$$\bar{P} = \frac{1}{2}\overline{P_x(t)}\,\bar{x} + \bar{P}_y(y,t) \tag{4.10}$$

This equation implies that the pressure gradient in the x-direction is uniform at given values of $\bar{x}$ and $\bar{t}$. The last equation that is needed is the equation of state,

$$\frac{\bar{\rho}_1 \bar{T}_1}{m\omega_1} = \frac{\bar{\rho}_2 \bar{T}_2}{m\omega_2} \tag{4.11}$$

The initial condition is that of a stagnation point flow with momentum and thermal boundary layers near the wall. The momentum boundary layer is caused by the no slip condition at the wall while the thermal boundary layer is caused by the difference in temperature between the ambient incoming flow and the fuel wall. The fuel mass fraction in the flow field is initially zero, while the oxygen mass fraction is $Y_{O,b}$.

At the solid/gas interface, $\bar{y}=0$, the boundary conditions are,

$$\bar{T} = T_v \tag{4.12}$$

$$\bar{F} = 0 \tag{4.12a}$$

$$\bar{\rho}\bar{V}L_v = \bar{\lambda}\frac{\partial \bar{T}}{\partial \bar{y}} + \bar{i} \tag{4.13}$$

$$\bar{\rho}\bar{V}\bar{Y}_{Fr} = \bar{\rho}\bar{V}\bar{Y}_F - \overline{\rho D}\frac{\partial Y_F}{\partial y} \tag{4.14}$$

$$\bar{\rho}\bar{V}\bar{Y}_O = \overline{\rho D}\frac{\partial \bar{Y}_O}{\partial \bar{y}} \tag{4.15}$$

At the outer boundary, $y=L_b$, the following conditions are

imposed,

$$\bar{V} = V_b \tag{4.16}$$

$$\frac{\partial \bar{u}}{\partial \bar{y}} = 0 \longrightarrow \frac{\partial \bar{F}}{\partial \bar{y}} = 0 \tag{4.17}$$

$$\bar{T} = T_b \tag{4.18}$$

$$\bar{Y}_o = Y_{o,b} \tag{4.19}$$

$$\bar{Y}_F = 0 \tag{4.20}$$

$$\bar{\iota} = \iota_b \tag{4.21}$$

The solution of Eqs. (4.1-4.21) is obtained by employing the following iterative technique:

1) An initial guess is made of the functions $P_x(t)$, in Eq. (4.10), and initial values are assumed for $\bar{v}$, $\bar{T}$, $\bar{Y}_F$, $\bar{Y}_o$.

2) Using this guess the x-direction momentum equation is solved to find $\bar{F}$ and $\bar{u}$.

3) Conservation of mass is applied to each grid point to find $\bar{v}$.

4) Conservation of momentum in the y-direction is applied to find the pressure gradient in the

y-direction.

5)Conservation of energy and species are solved to find the temperature and mass fraction fields.

6)Overall conservation of mass is then used to adjust the guess for $P_x(t)$ and the process is repeated until convergence is obtained.

4.2.2 Non-Dimensionalization

As in the one dimensional problem, several different physical regimes will be present and, again, a characteristic quantity may fit one regime but not to the other regimes. Hence, some compromise is necessary when picking the characteristic quantities. The following non-dimensional quantities are used in this problem:

Time,

$$t = \frac{\bar{t} V_b}{L_b} \tag{4.22}$$

Velocity,

$$V = \frac{\bar{V}}{\left(\frac{V_b \mu_b}{\rho_b L_b}\right)^{1/2}} \tag{4.23}$$

Length,

$$\eta = \frac{\bar{y}}{\left(\frac{\mu_b L_b}{\rho_b V_b}\right)^{1/2}} \tag{4.24}$$

Oxygen mass fraction,

$$Y_o = \frac{\bar{Y}_o}{Y_{o,b}} \tag{4.25}$$

Fuel mass fraction,

$$Y_F = \frac{Y_F \nu_o m\omega_o}{Y_{o,b} \nu_F m\omega_F} \tag{4.26}$$

Temperature,

$$T = \frac{c_p \nu_o m\omega_o (T - T_b)}{Q \nu_F m\omega_F Y_{o,b}} \tag{4.27}$$

Intensity,

$$i = \frac{\bar{i}}{i_b} \tag{4.28}$$

Density,

$$\rho = \frac{\bar{\rho}}{\rho_b} \tag{4.29}$$

Thermal conductivity,

$$\lambda = \bar{\lambda}/\lambda_b \tag{4.30}$$

Viscosity,

$$\mu = \bar{\mu}/\mu_b \tag{4.31}$$

and Pressure,

$$P = \frac{\bar{P}}{\rho_b V_c^2} \tag{4.32}$$

The characteristic time in Eq. (4.22) is the residence time for a fuel particle entering at the outer boundary. The

characteristic length is a momentum boundary layer thickness, while the characteristic velocity is the velocity perpendicular to the wall that would be expected in the boundary layer. All other characteristic quantities are the same as in the one dimensional problem. This particular set of characteristic quantities apply best to the steady state stagnation point flow with a diffusion flame in the boundary layer.

If these quantities are introduced into the dimensional conservation equations, and into their corresponding boundary and initial conditions, Eqs. (4.1-4.21), then the following equations result:

Y-momentum,

$$\rho \frac{\partial V}{\partial t} + \rho V \frac{\partial V}{\partial x} = \frac{\partial}{\partial x}\left(\mu \frac{\partial V}{\partial x}\right) - \frac{\partial P_y(x,t)}{\partial x} \tag{4.33}$$

Energy,

$$\rho \frac{\partial T}{\partial t} + \rho V \frac{\partial T}{\partial x} = \frac{1}{Pr} \frac{\partial}{\partial x}\left(\lambda \frac{\partial T}{\partial x}\right) + I \frac{dI}{dx} + Da W \tag{4.34}$$

Fuel conservation,

$$\rho \frac{\partial Y_F}{\partial t} + \rho V \frac{\partial Y_F}{\partial x} = \frac{1}{Pr} \frac{\partial}{\partial x}\left(\rho D \frac{\partial Y_F}{\partial x}\right) + Da W \tag{4.35}$$

Oxygen conservation,

$$\rho \frac{\partial Y_O}{\partial t} + \rho V \frac{\partial Y_O}{\partial x} = \frac{1}{Pr} \frac{\partial}{\partial x}\left(\rho D \frac{\partial Y_O}{\partial x}\right) + Da W \tag{4.36}$$

with the reaction rate given by

$$w = \frac{Y_F Y_O}{(T\alpha+1)^2} \exp\left[\frac{-\beta(1-T)}{\frac{1}{\alpha}+T}\right] \tag{4.37}$$

The radiation absorption term becomes,

$$\frac{dI}{dy} = A\rho Y_F i \tag{4.38}$$

The continuity equation is,

$$F = \left(\frac{\partial \rho}{\partial t} - \frac{\partial}{\partial x}(\rho V)\right)/\rho \tag{4.39}$$

while the x-direction momentum equation is

$$\rho \frac{\partial F}{\partial t} + \rho F^2 + \rho V \frac{\partial F}{\partial x} = \frac{\partial}{\partial x}\left(\mu \frac{\partial F}{\partial x}\right) - P_x(t) \tag{4.40}$$

The equation of state is,

$$\left(\frac{\nu_F}{\nu_O} Y_{F,1} + Y_{O,1}\right)\rho_1\left(T_1 + \frac{1}{\alpha}\right) = \left(\frac{\nu_F}{\nu_O} Y_{F,2} + Y_{O,2}\right)\rho_2\left(T_2 + \frac{1}{\alpha}\right) \tag{4.41}$$

The boundary conditions at the solid-gas interface, $x=0$, are

$$T = T_w = \frac{1}{\alpha T_b}(T_v - T_b) \tag{4.42}$$

$$u = 0, \quad F = 0 \tag{4.43}$$

$$P_r \rho V = H\lambda \frac{\partial I}{\partial x} + HI P_r i \tag{4.44}$$

$$S\rho V = \rho V Y_F - \frac{\rho D}{P_r}\frac{\partial Y_F}{\partial x} \tag{4.45}$$

$$\rho V Y_o = \frac{\rho D}{P_r} \frac{\partial Y_F}{\partial \eta} \tag{4.46}$$

At the outer boundary where $\eta = \frac{L_b}{\left(\frac{\mu_b L_b}{\rho_b V_b}\right)^{1/2}}$ the transformed conditions become,

$$V = \left(\frac{\rho_b V_b L_b}{\mu_b} \right)^{1/2} \tag{4.47}$$

$$\frac{\partial F}{\partial y} = 0 \tag{4.48}$$

$$T = 0 \tag{4.49}$$

$$Y_o = 1 \tag{4.50}$$

$$Y_F = 0 \tag{4.51}$$

$$i = 1 \tag{4.52}$$

Including the Lewis number which has already been assumed to be one there are twelve non-dimensional groups which appear in Eqs. (4.33-4.52). These groups are defined and summarized in Table (4.1).

Table 4.1: Summary of non-dimensional groups appearing in the stagnation point flow equations

Symbol	Non-dimensional group	Description
A	$\frac{a_\lambda Y_{o,b} \nu_F MW_F}{\nu_o MW_o}\left[\frac{\rho_b u_b L_b}{V_b}\right]^{1/2}$	Non-dimensional absorption coefficient
Da	$\left(\frac{B L_b Y_{o,b} e^{-\beta}}{\rho_b V_b T_b^2}\right)$	Damkohler number
H	$\left(\frac{\alpha C_p T_b}{L_v}\right)$	Non-dimensional ratio of heat of combustion to heat of vaporization
I	$\left(\frac{i_b}{\alpha C_p T_b\left[\frac{V_b u_b \rho_b}{L_b}\right]^{1/2}}\right)$	Non-dimensional intensity
Le	$\left(\frac{(\rho D)_b C_p}{\lambda_b}\right)$	Lewis number
Pr	$\left(\frac{u_b C_p}{\lambda_b}\right)$	Prandtl number
Re	$\left(\frac{\rho_b V_b L_b}{u_b}\right)$	Reynolds number based on values at outer boundary
S	$\left(\frac{Y_{FT} \nu_o MW_o}{Y_{o,b} \nu_F MW_F}\right)$	Non-dimensional measure of the fuel richness
T_w	$\left[\frac{1}{\alpha T_b}(T_v - T_b)\right]$	Non-dimensional wall temperature
α	$\left(\frac{Q Y_{o,b} \nu_F MW_F}{C_p T_b \nu_o MW_o}\right)$	Non-dimensional heat of combustion
β	$\left[\frac{E}{R_u(1+\alpha)T_b}\right]$	Non-dimensional activation energy
—	$\left(\nu_F/\nu_o\right)$	Moles of fuel required per mole of oxygen

4.3 Results

4.3.1 Results of the Ignition and Flame Propagation Study with Ignition Caused by Gas Phase Absorption

The data used in this calculation are shown in dimensional form in Table (4.2) and in non-dimensional form in Table (4.3). Besides the imposition of a velocity directed perpendicular to the wall, the major difference between the constants shown in Table (4.2) and those shown in Table (3.2) for the one dimensional problem is an increase in the value of the intensity. The increase in intensity is required because of the convective cooling now present and the value of intensity used here is, in fact, the minimum intensity required to cause ignition. Since an intensity this high is mostly associated with lasers, a high powered laser is probably required to cause ignition in this case.

This problem can most easily be understood by dividing it into five different regimes according to how strong the chemical reaction is or whether or not radiation is being applied to the wall. The regimes are, in order of their appearance: a) an initial condition regime in which neither the radiation or chemistry plays a role, b) a pre-ignition regime in which radiation is applied to the wall, c) a post-ignition regime in which the chemical reaction is weak, d) a regime in which a pre-mixed flame front dominates, and e) an unsteady diffusion flame regime. These regimes are discussed in more detail next.

Table 4.2: Values of the dimensional parameters used in the stagnation point flow problem

Symbol	Case with ignition and flame propagation caused by gas phase absorption	Case with ignition and flame propagation caused by a hot fuel surface
a_λ	10. m^2/kg	0. m^2/kg
B	$1.6*10^{15}$ $kg*^oK^2/(m^3*sec)$	$1.6*10^{15}$ $kg*^oK^2/(m^3*sec)$
c_p	1220 joules/(kg*°K)	1220 joules/(kg*°K)
E	$1.8*10^8$ joules/(kgmole)	$1.8*10^8$ joules/(kgmole)
i	38. watts/cm^2	1.3 watts/cm^2
L_v	$1.59*10^6$ joules/kg	$1.59*10^6$ joules/kg
L_b	0.05 m	0.05 m
MW_f	100 kg/mole	100 kg/mole
MW_o	32 kg/mole	32 kg/mole
Q	$2.6*10^7$ joules/kg	$2.0*10^7$ joules/kg
R_μ	8315 joules/(kgmole*°K)	8315 joules/(kgmole*°K)
T_b	298°K	298°K
T_w	663°K	1326°K
V_b	0.5 m/sec	0.5 m/sec
Y_{FT}	1.	1.
$Y_{o,b}$	0.23	0.23
λ_b	$2.97*10^{-2}$ watts/(m*°K)	$2.97*10^{-2}$ watts/(m*°K)
ρ_b	1.17 kg/m^3	1.17 kg/m^3
μ_b	$1.85*10^{-5}$ kg/(m*sec)	$1.85*10^{-5}$ kg/(m*sec)
ν_F	1	1
ν_o	6	6

Table 4.3: Values of the non-dimensional parameters used in the stagnation point flow problem

Symbol	Case with ignition and flame propagation caused by gas phase absorption	Case with ignition and flame propagation caused by a hot fuel surface
A	$1.76*10^{-3}$	0.
Da	$1.81*10^{5}$	$2.47*10^{4}$
H	1.96	1.51
I	7.86	0.369
Le	1.0	1.0
Pr	0.76	0.76
Re	1580	1580
S	8.35	8.35
T_w	0.143	0.523
α	8.57	6.59
β	7.59	9.57
ν_F/ν_o	0.16	0.16

The first regime is the initial condition regime and is illustrated in Figs. (4.2a), and (4.4a) for time, t=0.0. As mentioned above there is no chemical reaction and the radiation has not been applied to the wall. Hence, these figures illustrate a steady state stagnation point flow. In the flow momentum and thermal boundary layers exist near the wall and an isothermal potential flow exists outside the boundary layers. No figures showing mass fraction profiles are presented since no fuel has been vaporized and the flow field consists entirely of air.

The second regime is a pre-ignition regime and corresponds to when the radiant heat flux is applied to the wall. It occurs for times greater than t= 0.0, and for times less than or equal to t=5.88 and is illustrated in Figs. (4.2a), (4.3a), and (4.4b). The radiant heat flux in this case is so strong and vaporization of fuel so rapid that the incoming air is pushed back from the wall and an opposing jet flow is created. Fuel composes the bottom jet while oxygen composes the top jet. At the interface between the opposing fuel and air jets a thin mixing region is created by the diffusion of fuel and oxygen. Additionally, during this period a fraction of the incoming radiant flux is absorbed eventually causing the air-fuel mixture to reach a temperature at which the mixture will ignite. Ignition is observed to occur in the rich region with a very low non-dimensional oxygen mass fraction of 0.08. Because of the low mass fraction, only one premixed flame front travelling away from

the wall will develop and the power curve will look qualitatively similiar to Fig. (3.4).

Once ignition occurs the radiant heat flux is removed and and the fuel jet collapses. This is the beginning of the third regime which begins after time, t = 5.88 and lasts roughly until t=6.00. It is illustrated in Figs. (4.2a), (4.3b) and (4.4c). The regime is characterized by a weak chemical reaction and the reappearance of a boundary layer type of flow. The boundary layer and a portion of the potential flow near the wall are now composed of fuel, while the portion of the potential flow far from the wall is composed of air. The incoming flow is slowly pushing the reaction zone and the fuel back towards the wall. However, before the flow can flush the system of the fuel the chemical reaction becomes strong and the fourth regime begins.

The fourth regime, which is characterized by a strong chemical reaction, begins at time, t=6.00, and lasts until approximately time ,t=6.50. It is illustrated in Figs. (4.2a), (4.2b), (4.3c), (4.3d), (4.4d) and (4.4e). During this regime a premixed flame front appears and begins propagating away from the wall. As in the one dimensional problems, the premixed flame begins propagating in a rich region, passes through the stoichiometric point and enters a lean region where it will die out. In the process it will leave behind the diffusion flame at the stoichiometric point. As can be seen by examining the Figs. (4.4d) and (4.4e) the chemical reaction in this regime has a large effect on the flow field. The chemical reaction becomes

so strong that the expanding gases produced are able to push the incoming air flow away from the reaction zone. This phenomenon is most clearly shown in Fig. (4.4d), where a dividing streamline exists between the incoming air flow and the flow of the hot combustion gases at a distance of 24 away from the wall. Because of this strong flow field the reaction zone is now able to push itself away from the wall somewhat.

A rather peculiar velocity field occurs near the end of this regime, and is illustrated by Fig. (4.4e). The figure shows a region of low x-direction velocities near the reaction zone. At the time shown in the figure the premixed flame is beginning to weaken so that less hot gas is produced by the flame. Since less hot gas is being produced the x-direction velocities must be reduced by the x-direction pressure gradient in order to conserve mass on an overall basis. Because of the assumption made that the y-direction velocity is a function of y and t only, the pressure gradient is of the form of Eq. (4.10) and is applied uniformly at constant values of x. The low density regions are affected the most, thus, giving the low x-direction velocities near the reaction zone.

Whether or not the flow field illustrated in Fig. (4.4e) is correct or not will depend upon whether or not the assumption that the y-direction velocity is a function of y and t only is valid in this regime. To determine if this assumption applies in this regime would require the solution of the problem with an unrestricted two-dimensional flow field. This solution is

beyond the scope of this thesis.

The fifth and final regime occurs when the premixed flame front begins to die out leaving the diffusion flame. This regime occurs from time, t=6.50, and lasts until the steady state diffusion flame is obtained. It is illustrated in Figs. (4.2b), (4.3f), and (4.4f). The regime is characterized by a relatively slow reaction, so that the incoming flow dominates and a boundary layer is reestablished near the wall. At the start of the regime the diffusion flame exists outside of the boundary layer. The flow slowly flushes out the excess fuel which exists behind the diffusion flame and pushes the flame back towards the wall. Eventually the flame gets close enough to the wall to stabilize itself and to reach a steady state. The value of the mass fraction of fuel at the wall eventually reaches that of the steady state diffusion flame solution where the flame is treated as a flame sheet.[45]

This completes the discussion of the stagnation point flow problem where ignition is caused by gas phase absorption. Next, results of a parametric study of ignition caused by gas phase absorption will be presented.

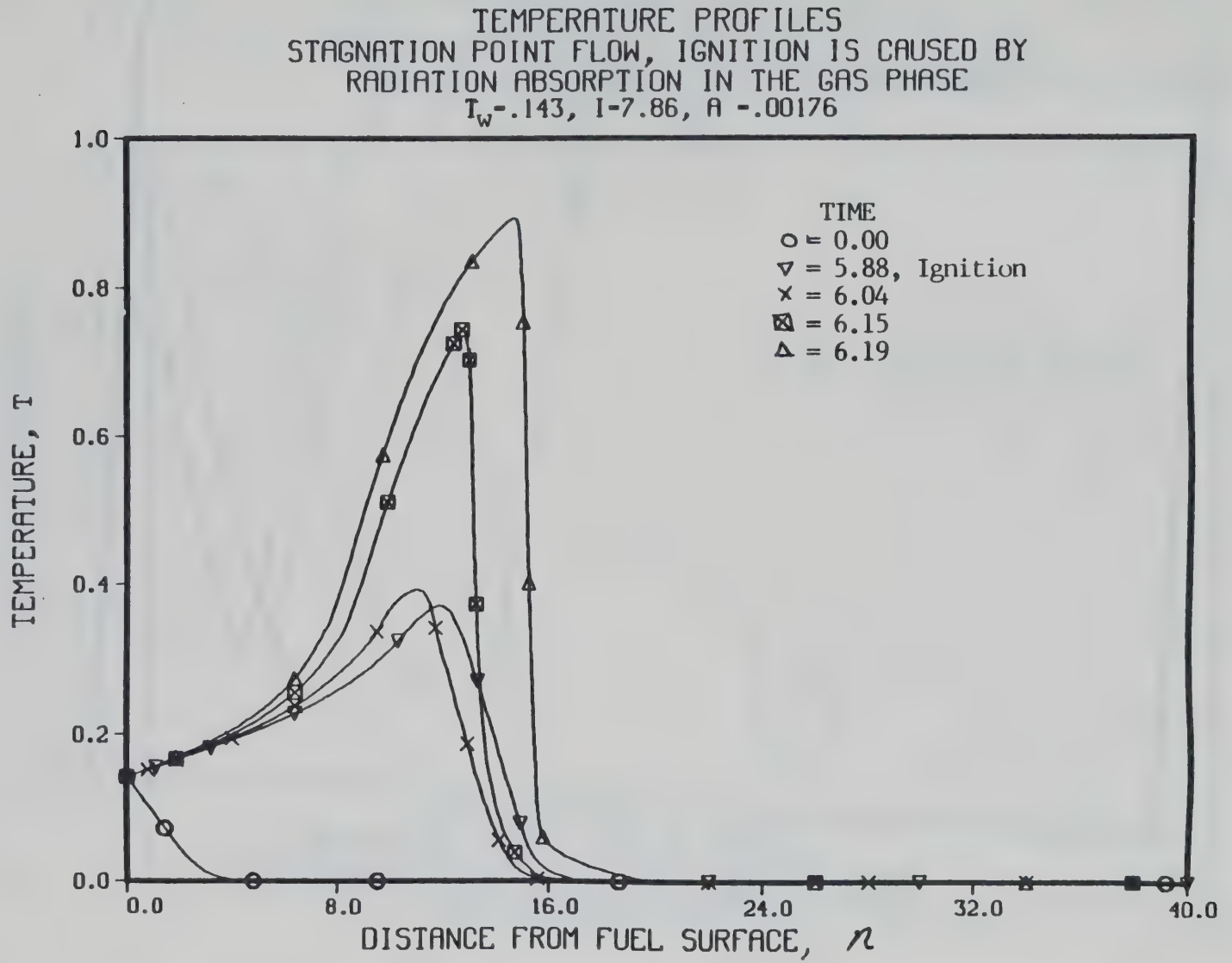
TEMPERATURE PROFILES
STAGNATION POINT FLOW, IGNITION IS CAUSED BY
RADIATION ABSORPTION IN THE GAS PHASE
T_w-.143, I-7.86, A -.00176
TIME
○ = 0.00
▽ = 5.88, Ignition
× = 6.04
⊠ = 6.15
△ = 6.19
TEMPERATURE, T
1.0
0.8
0.6
0.4
0.2
0.0
0.0
8.0
16.0
24.0
32.0
40.0
DISTANCE FROM FUEL SURFACE, η

Figure 4.2a

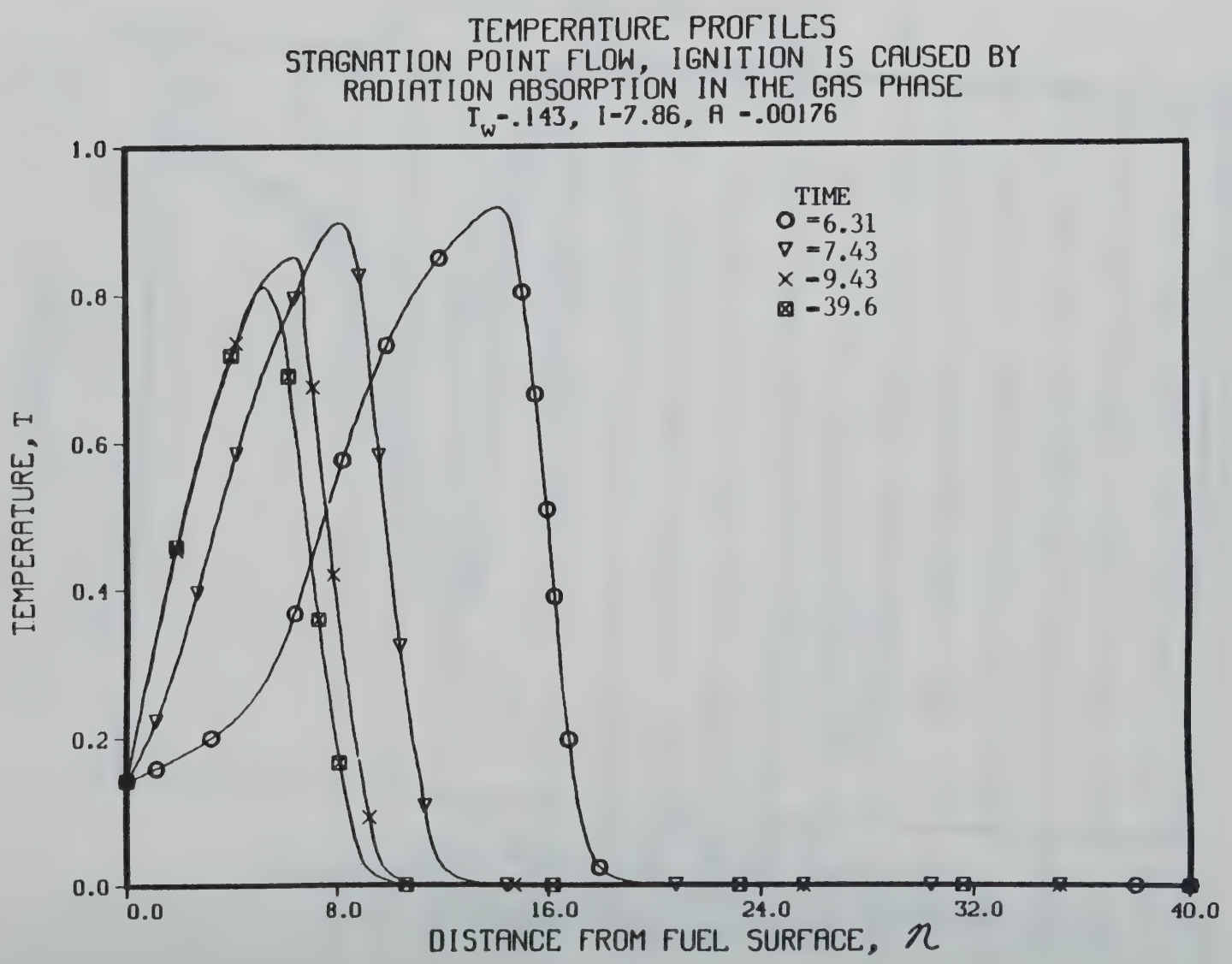
TEMPERATURE PROFILES
STAGNATION POINT FLOW, IGNITION IS CAUSED BY
RADIATION ABSORPTION IN THE GAS PHASE
T_w-.143, I-7.86, A -.00176
TIME
O =6.31
▽ =7.43
× -9.43
⊠ -39.6
TEMPERATURE, T
1.0
0.8
0.6
0.4
0.2
0.0
0.0
8.0
16.0
24.0
32.0
40.0
DISTANCE FROM FUEL SURFACE, η

Figure 4.2b

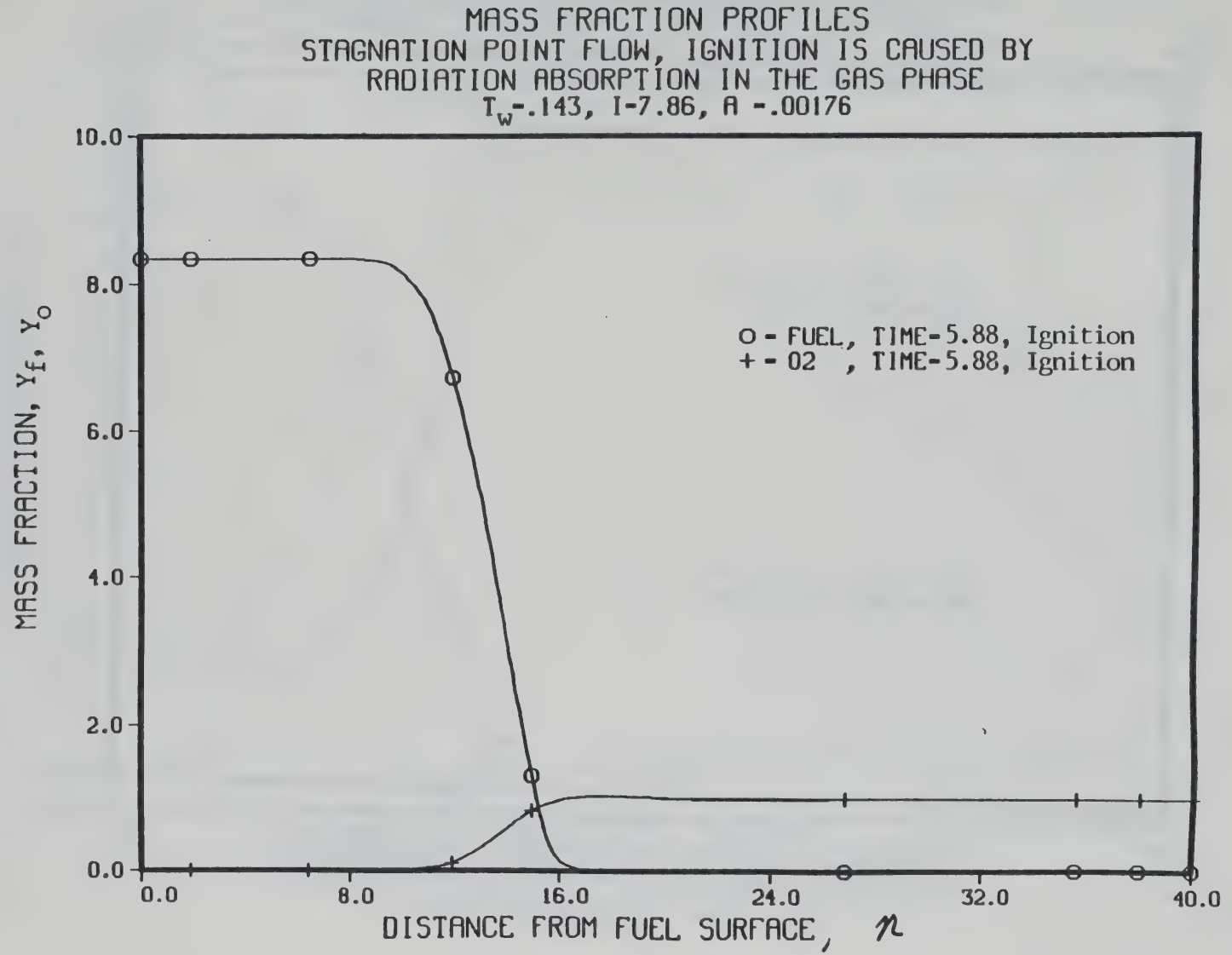
MASS FRACTION PROFILES
STAGNATION POINT FLOW, IGNITION IS CAUSED BY
RADIATION ABSORPTION IN THE GAS PHASE
T_w-.143, I-7.86, A -.00176
O - FUEL, TIME-5.88, Ignition
+ - 02 , TIME-5.88, Ignition
MASS FRACTION, Y_f, Y_o
DISTANCE FROM FUEL SURFACE, η
10.0
8.0
6.0
4.0
2.0
0.0
0.0
8.0
16.0
24.0
32.0
40.0

Figure 4.3a

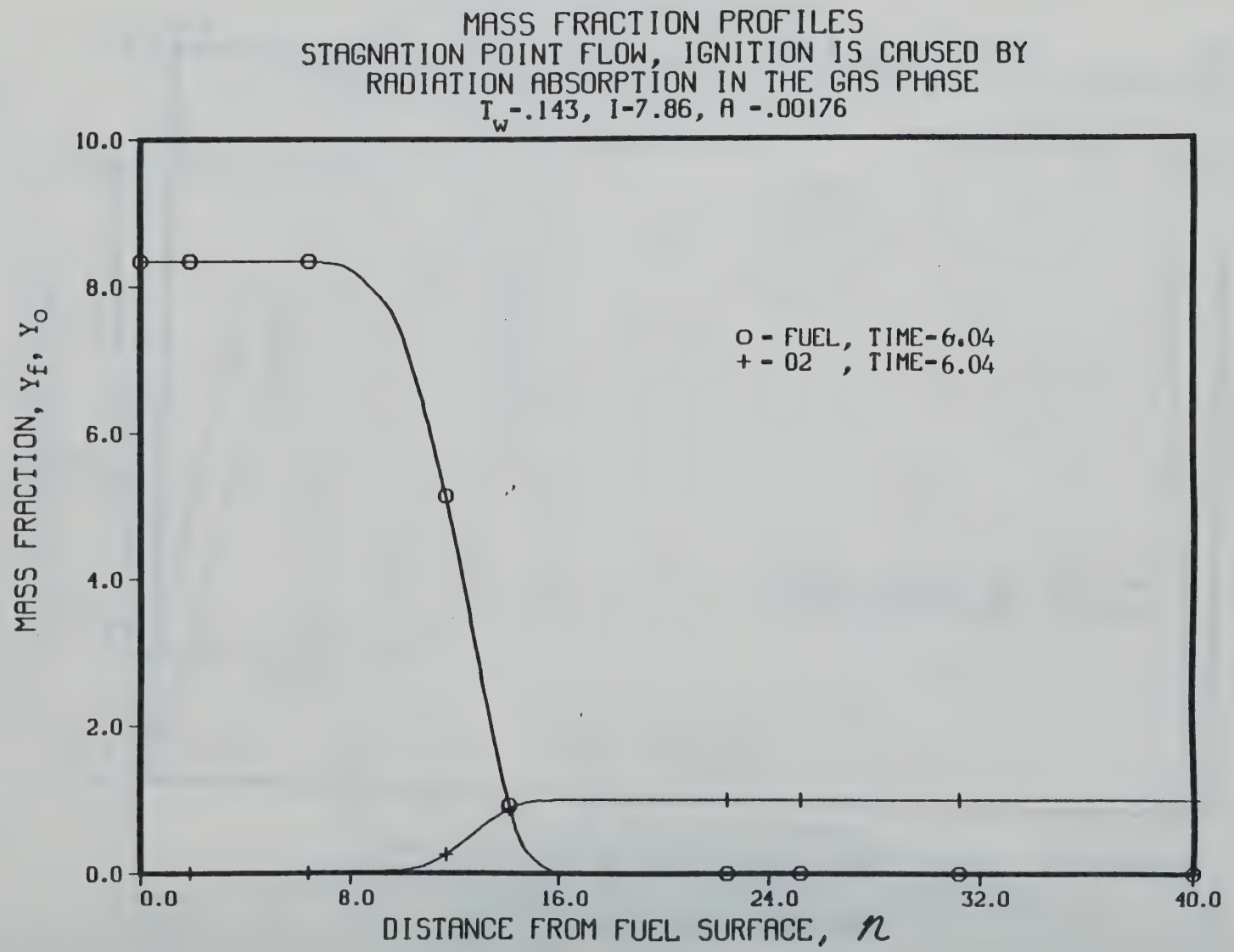
MASS FRACTION PROFILES
STAGNATION POINT FLOW, IGNITION IS CAUSED BY
RADIATION ABSORPTION IN THE GAS PHASE
T_w-.143, I-7.86, A -.00176
10.0
8.0
6.0
4.0
2.0
0.0
MASS FRACTION, Y_F, Y_O
o - FUEL, TIME-6.04
+ - 02 , TIME-6.04
0.0
8.0
16.0
24.0
32.0
40.0
DISTANCE FROM FUEL SURFACE, η

Figure 4.3b

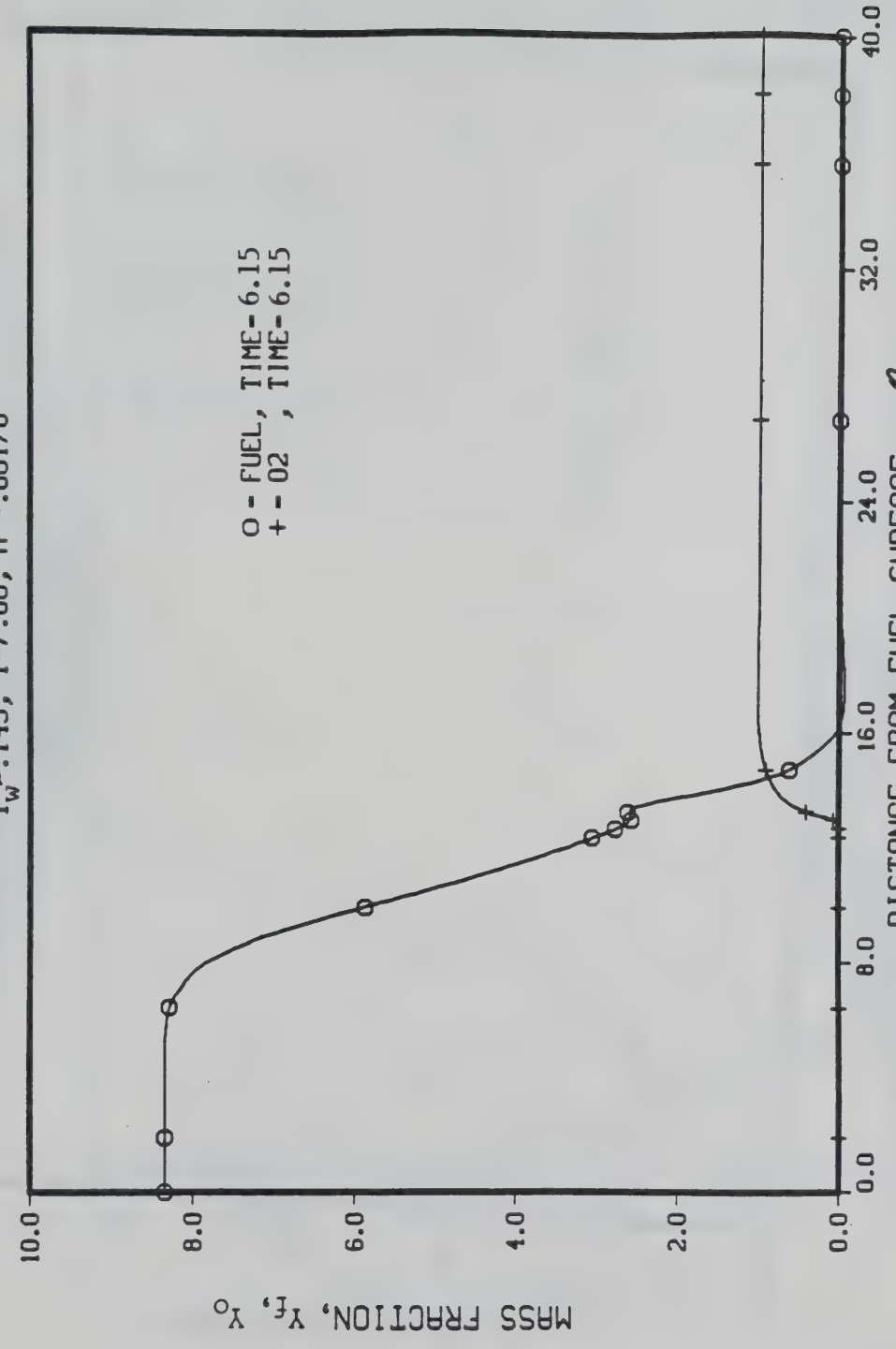
MASS FRACTION PROFILES
STAGNATION POINT FLOW, IGNITION IS CAUSED BY
RADIATION ABSORPTION IN THE GAS PHASE
T_w=.143, I-7.86, A =.00176
O - FUEL, TIME-6.15
+ - O2 , TIME-6.15
MASS FRACTION, Y_F, Y_O
DISTANCE FROM FUEL SURFACE, η
10.0
8.0
6.0
4.0
2.0
0.0
0.0
8.0
16.0
24.0
32.0
40.0

Figure 4.3c

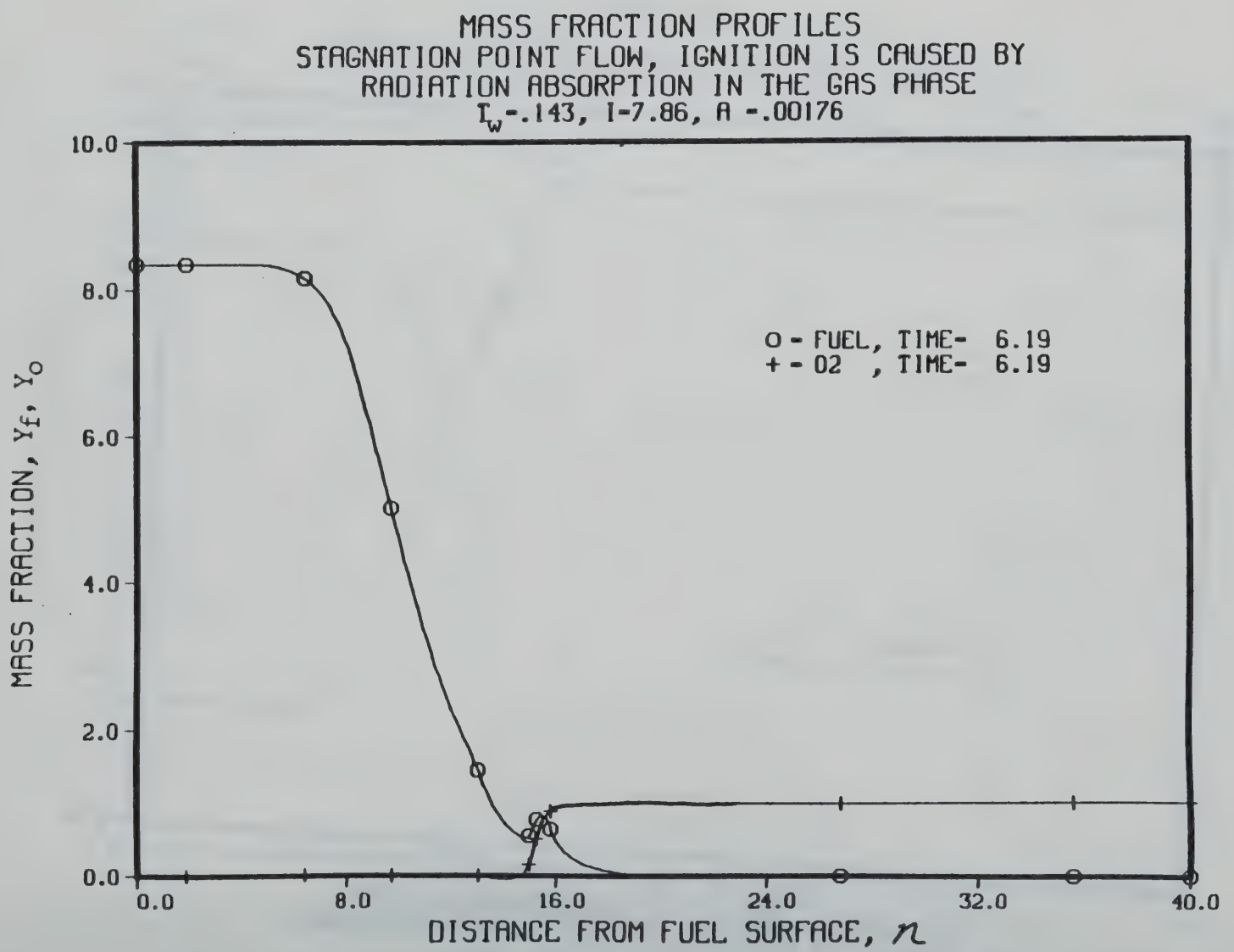
MASS FRACTION PROFILES
STAGNATION POINT FLOW, IGNITION IS CAUSED BY
RADIATION ABSORPTION IN THE GAS PHASE
I_w-.143, I-7.86, A -.00176
O - FUEL, TIME- 6.19
+ - 02 , TIME- 6.19
MASS FRACTION, Y_f, Y_O
DISTANCE FROM FUEL SURFACE, η
10.0
8.0
6.0
4.0
2.0
0.0
0.0
8.0
16.0
24.0
32.0
40.0

Figure 4.3d

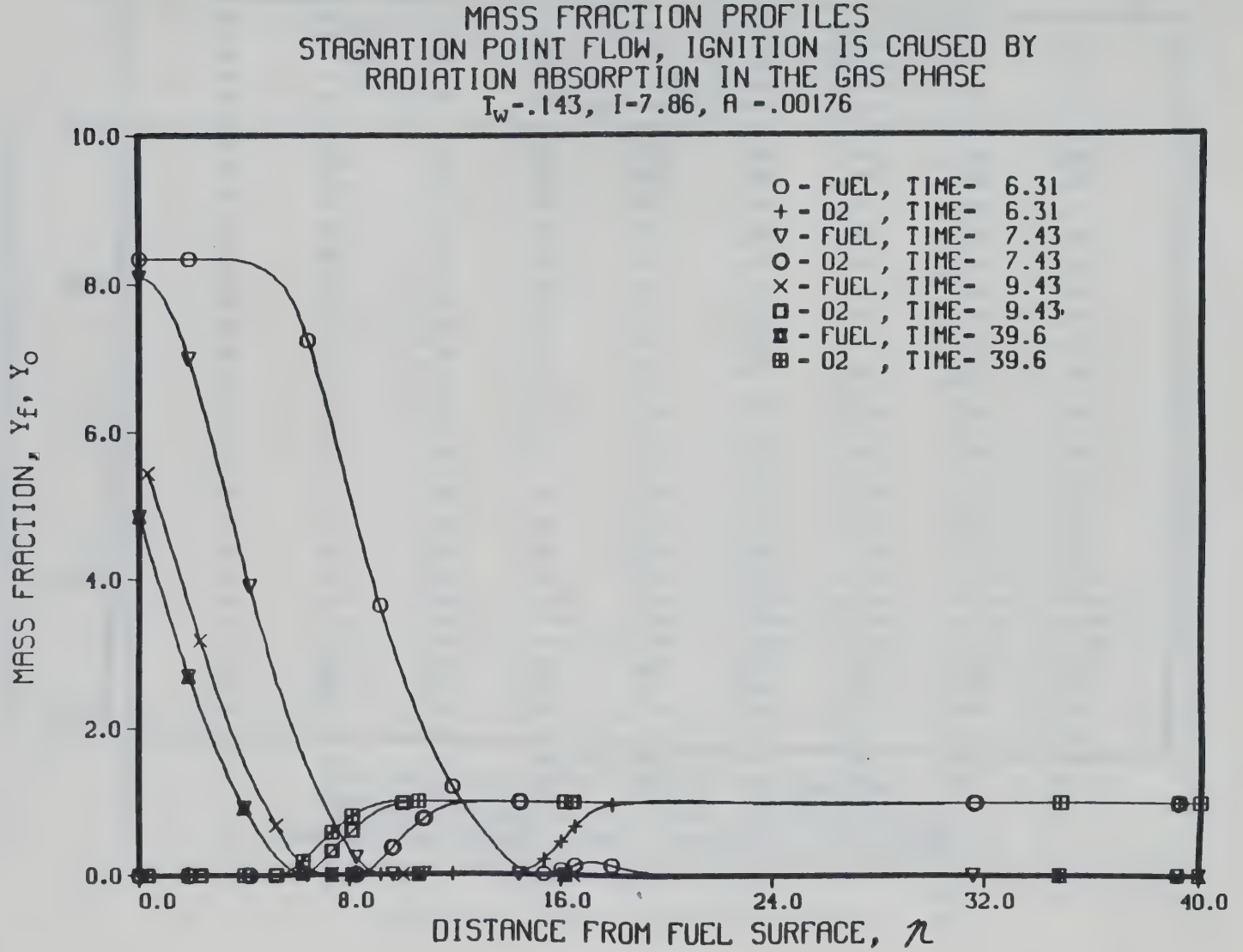
MASS FRACTION PROFILES
STAGNATION POINT FLOW, IGNITION IS CAUSED BY
RADIATION ABSORPTION IN THE GAS PHASE
T_w-.143, I-7.86, A -.00176
O - FUEL, TIME- 6.31
+ - O2 , TIME- 6.31
▽ - FUEL, TIME- 7.43
O - O2 , TIME- 7.43
× - FUEL, TIME- 9.43
□ - O2 , TIME- 9.43
⊠ - FUEL, TIME- 39.6
⊞ - O2 , TIME- 39.6
MASS FRACTION, Y_f, Y_O
10.0
8.0
6.0
4.0
2.0
0.0
0.0
8.0
16.0
24.0
32.0
40.0
DISTANCE FROM FUEL SURFACE, η

Figure 4.3e

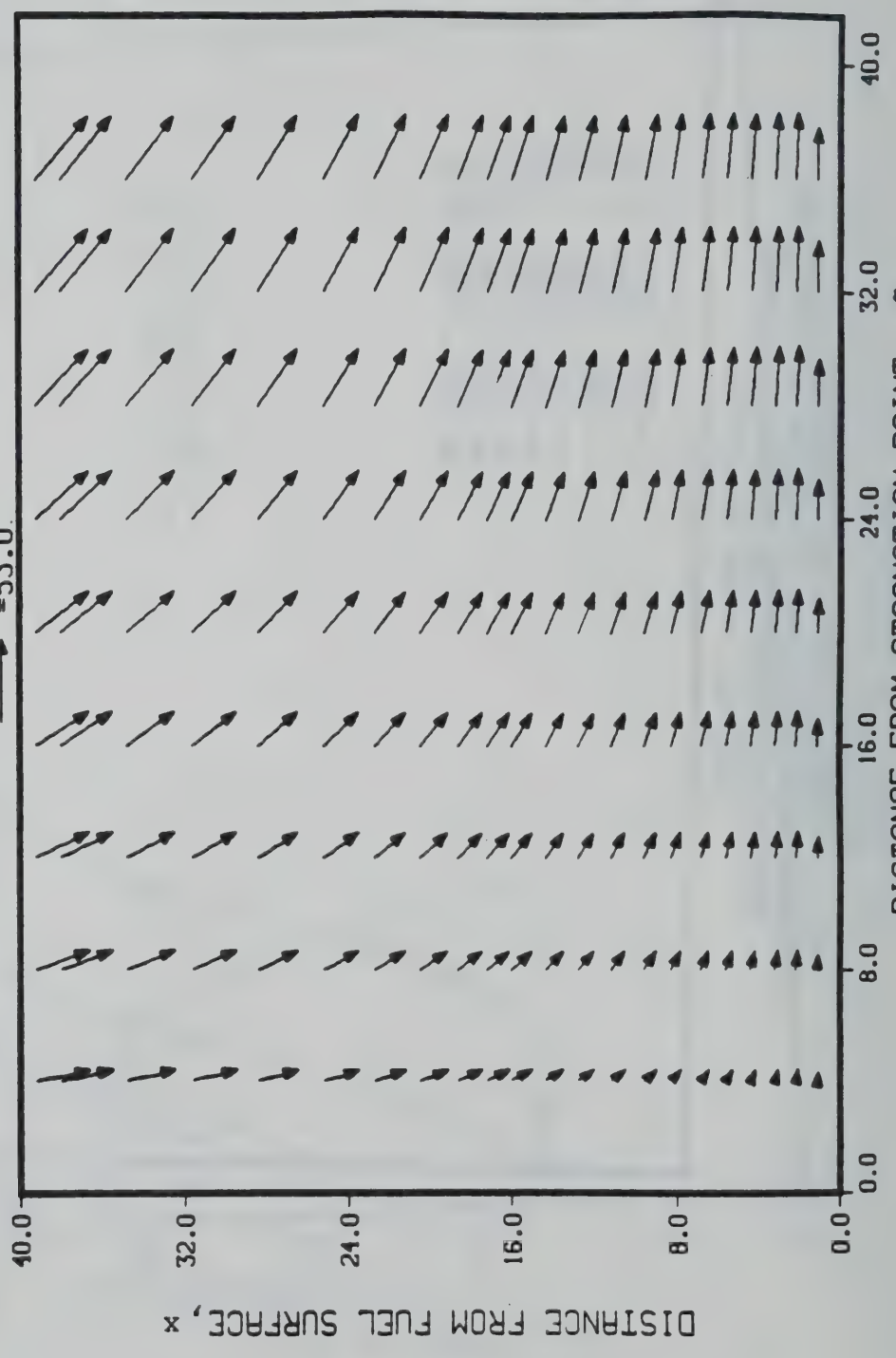
VELOCITY FIELD
STAGNATION POINT FLOW, IGNITION IS CAUSED BY
RADIATION ABSORPTION IN THE GAS PHASE
T_w=.143, I=7.86, A =.00176, TIME=0.00
=53.0
DISTANCE FROM FUEL SURFACE, x
DISTANCE FROM STAGNATION POINT, r
0.0
8.0
16.0
24.0
32.0
40.0

Figure 4.4a

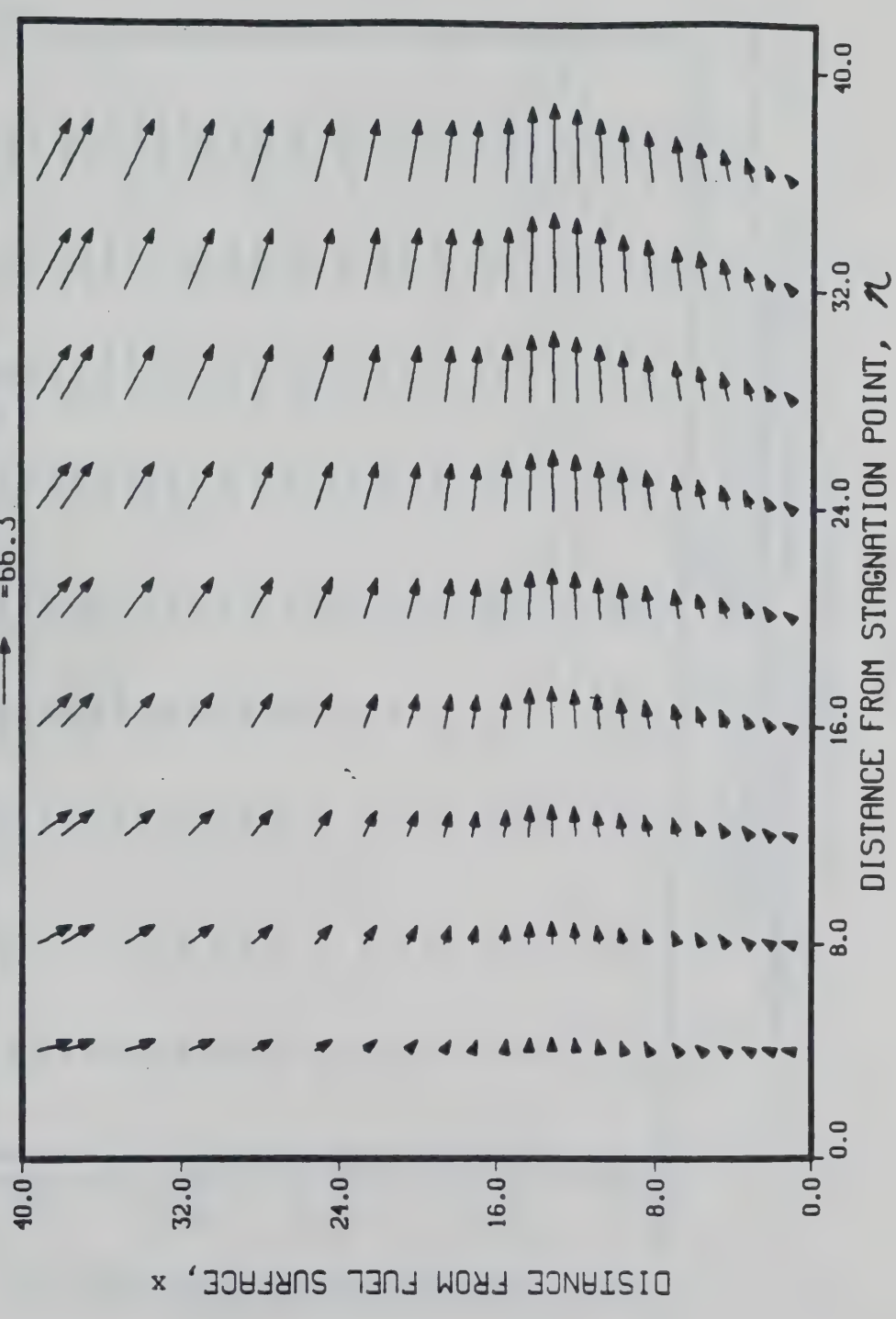
VELOCITY FIELD
STAGNATION POINT FLOW, IGNITION IS CAUSED BY
RADIATION ABSORPTION IN THE GAS PHASE
T_w=.143, I=7.86, A =.00176, TIME=5.88
=66.3
DISTANCE FROM FUEL SURFACE, x
DISTANCE FROM STAGNATION POINT, ξ
0.0
8.0
16.0
24.0
32.0
40.0

Figure 4.4b

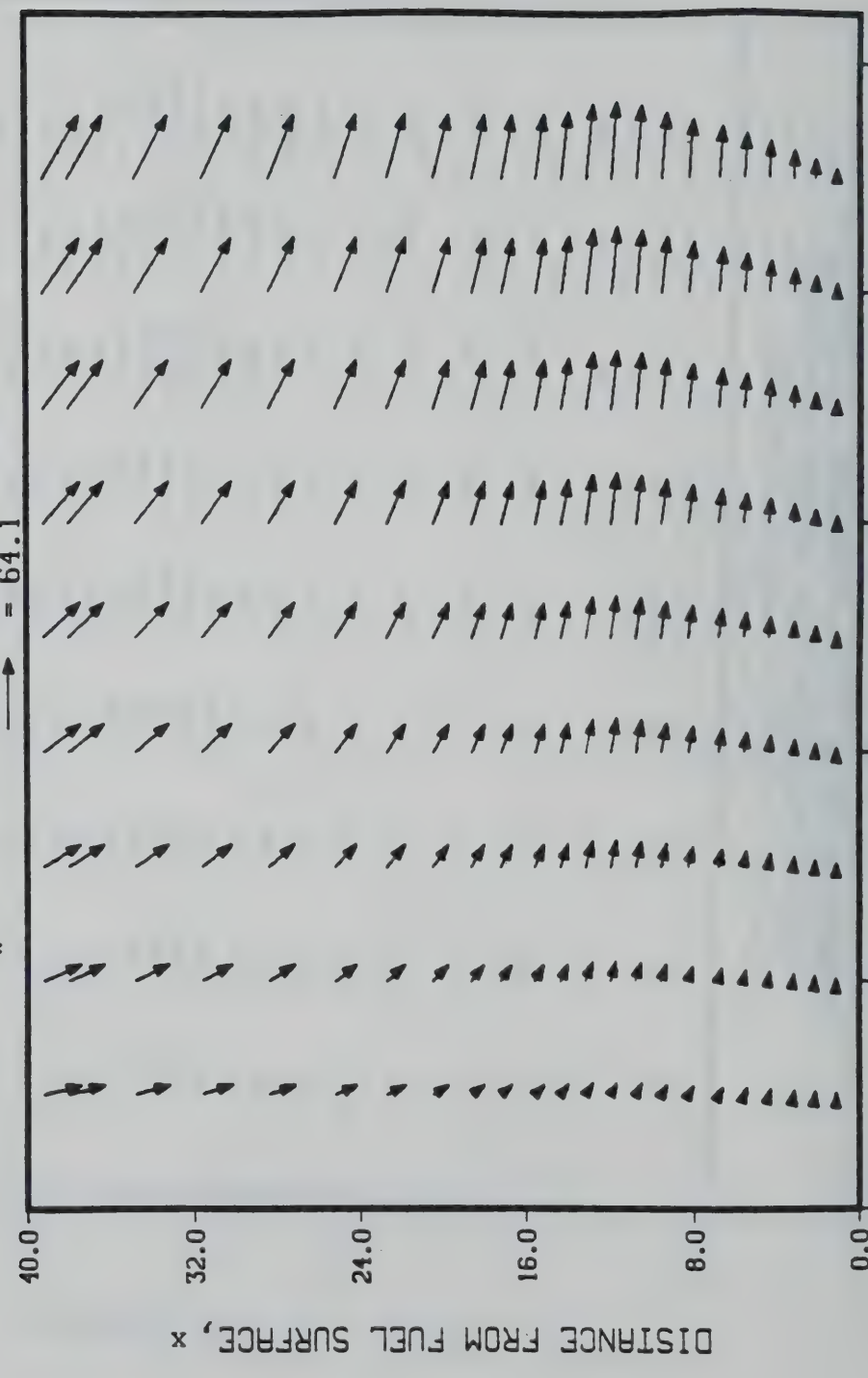
VELOCITY FIELD
STAGNATION POINT FLOW, IGNITION IS CAUSED BY
RADIATION ABSORPTION IN THE GAS PHASE
T_w=.143, I=7.86, A =.00176, TIME= 6.04
= 64.1
DISTANCE FROM FUEL SURFACE, x
DISTANCE FROM STAGNATION POINT, ℛ
0.0
8.0
16.0
24.0
32.0
40.0

Figure 4.4c

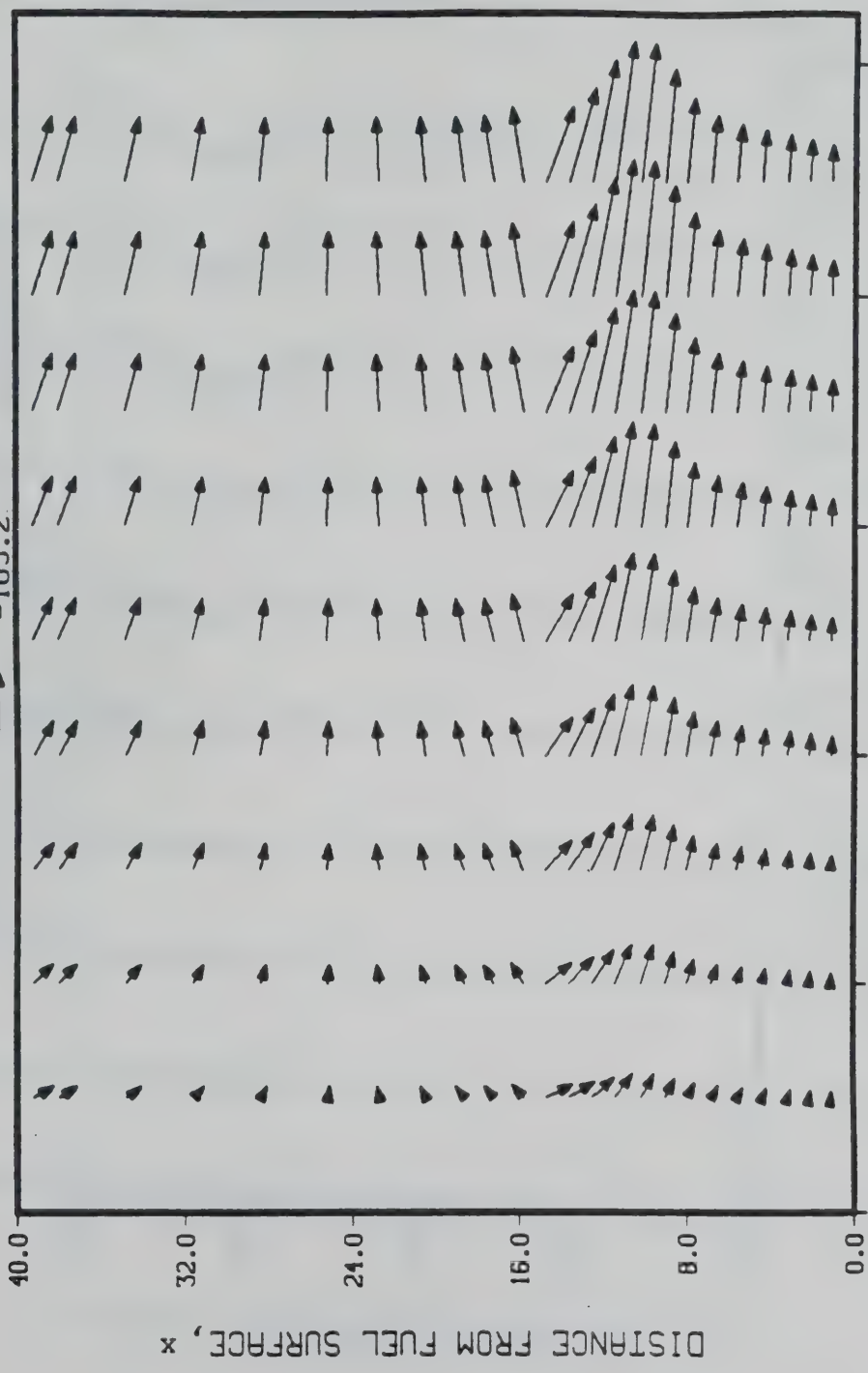
VELOCITY FIELD
STAGNATION POINT FLOW, IGNITION IS CAUSED BY
RADIATION ABSORPTION IN THE GAS PHASE
T_w=-.143, I=7.86, A =.00176, TIME=6.19
=103.2
DISTANCE FROM FUEL SURFACE, x
DISTANCE FROM STAGNATION POINT, ℳ
0.0
8.0
16.0
24.0
32.0
40.0

Figure 4.4d

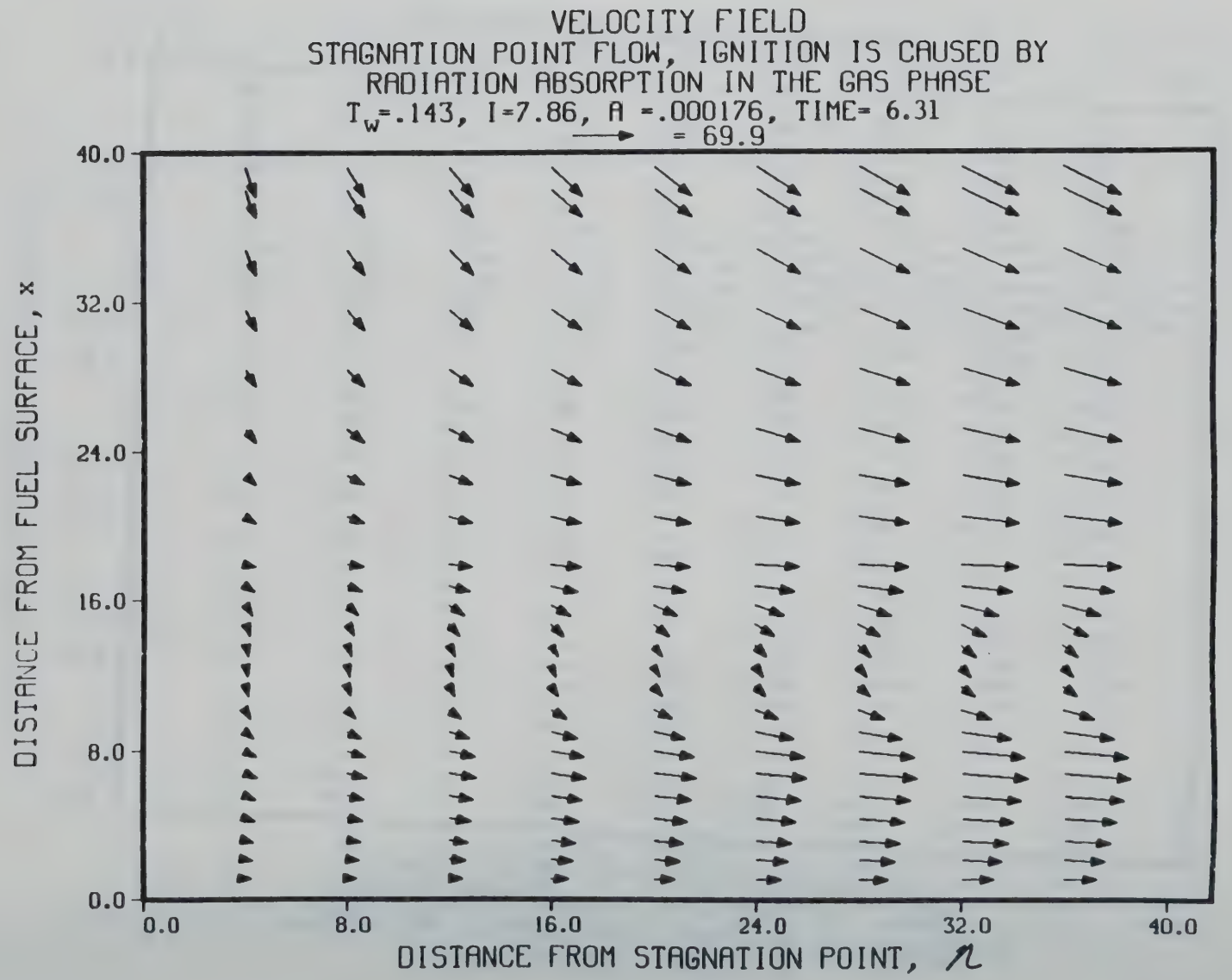
VELOCITY FIELD
STAGNATION POINT FLOW, IGNITION IS CAUSED BY
RADIATION ABSORPTION IN THE GAS PHASE
T_w=.143, I=7.86, A =.000176, TIME= 6.31
= 69.9
DISTANCE FROM FUEL SURFACE, x
DISTANCE FROM STAGNATION POINT, ξ
0.0
8.0
16.0
24.0
32.0
40.0

Figure 4.4e

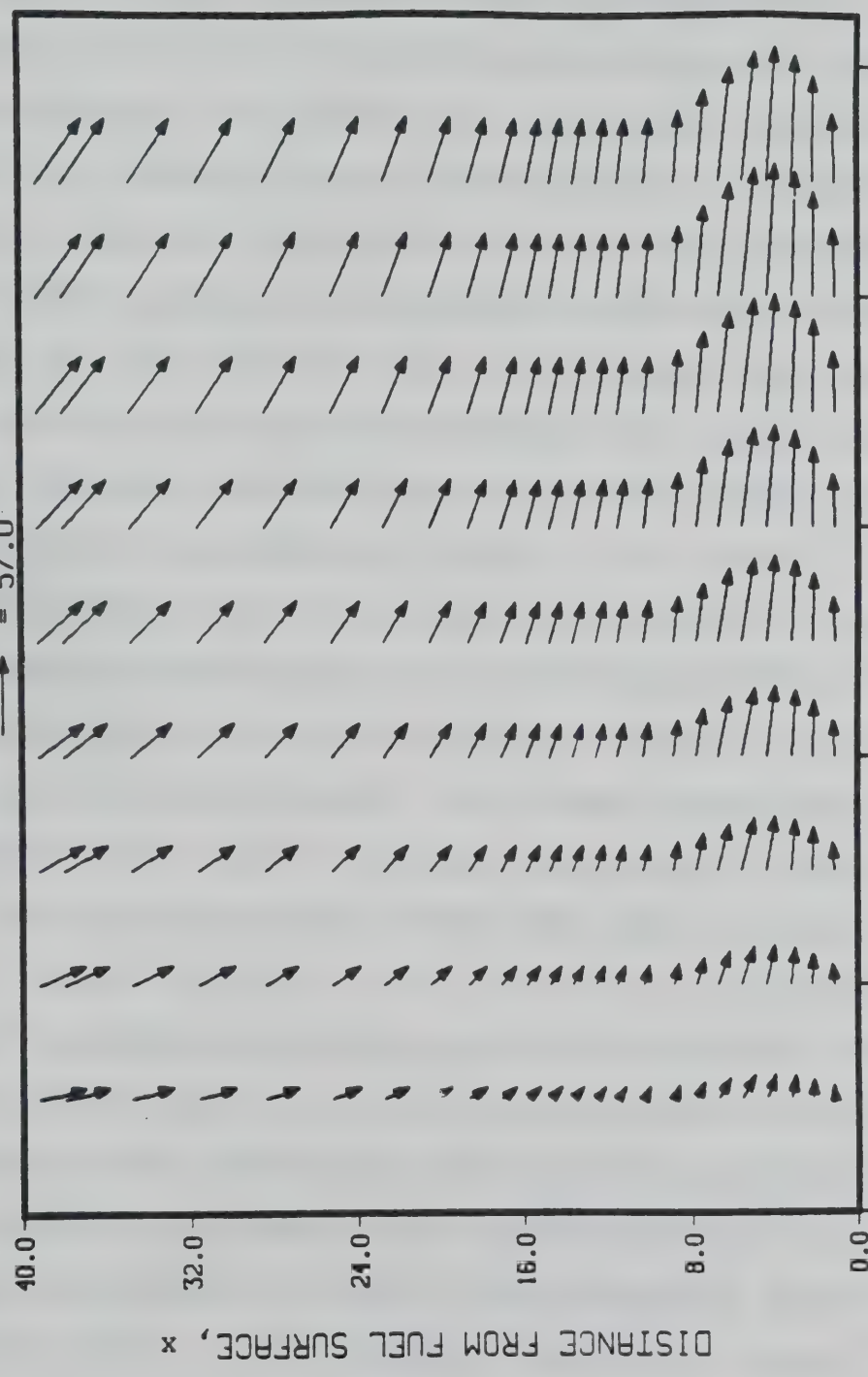
VELOCITY FIELD
STAGNATION POINT FLOW, IGNITION IS CAUSED BY
RADIATION ABSORPTION IN THE GAS PHASE
T_w=.143, I=7.86, A =.00176, TIME= 39.6
= 57.0
DISTANCE FROM FUEL SURFACE, x
DISTANCE FROM STAGNATION POINT, ℛ
0.0
8.0
16.0
24.0
32.0
40.0

Figure 4.4f

4.3.2 Results of the Parametric Study of Ignition Caused by Gas Phase Absorption

Two parametric studies are performed. The first study shows how the minimum radiation required for ignition varies with the incoming velocity and the second study analyzes how the intensity of radiation affects the ignition time. The results of the first study are shown in dimensional form in Fig. (4.5). It shows a linear relationship between the incoming velocity and the minimum incident intensity required for ignition. The results of this figure can be explained by noting that an increase in the velocity has two effects on the flow field. The first effect is to depress the fuel jet and cause a decrease in the residence time of the fuel. This decrease in residence time allows less time for heating of the fuel jet by radiation absorption. The second effect is to increase the velocities present in the interface region and, thus, to increase the convective cooling. Both of these effects combine to reduce temperatures in the interface region and must be offset by an adjustment in the intensity.

An increase in intensity has three effects. The first effect is to cause an overall decrease in the residence time of the fuel jet. The increase in intensity causes an increase in the injection velocity at the wall and also an increase in the height of the fuel jet. It can be shown that the increase in velocity at the wall is somewhat larger than the increase in jet height so that the residence will decrease on an overall

basis. The second effect is to increase the velocities near the interface region thus increasing the convective cooling. Both of these effect will tend to decrease the temperature of the gas in the interface region. The final effect is to increase the rate of radiant heating of the fuel vapor. This increase in radiant heating is the dominant effect and more than offsets the first two effects. Fig. (4.5) suggests that if the radiation intensity is increased in the proper linear proportion to the increase in velocity, then the increased rate of heating caused by the increase in intensity will exactly balance the decreases in residence time and the increases in convective cooling caused by the increases in velocity and the intensity.

The second parametric study, which is shown in Fig. (4.6), shows how the ignition times vary as the radiation intensity is increased with all other parameters remaining constant. As can be seen from the figure, the time to ignition asymptotically approaches infinity as the intensity approaches its minimum value. As the intensity is raised above the minimum value the time to ignition decreases in what appears to be an inverse fashion. The explanation for this curve is based upon the effect of increased intensity discussed above. Since the increased rate of heating caused by an increase in the intensity is dominant over the reduction in residence time and the increased convective cooling, the ignition time should decrease as shown in the figure.

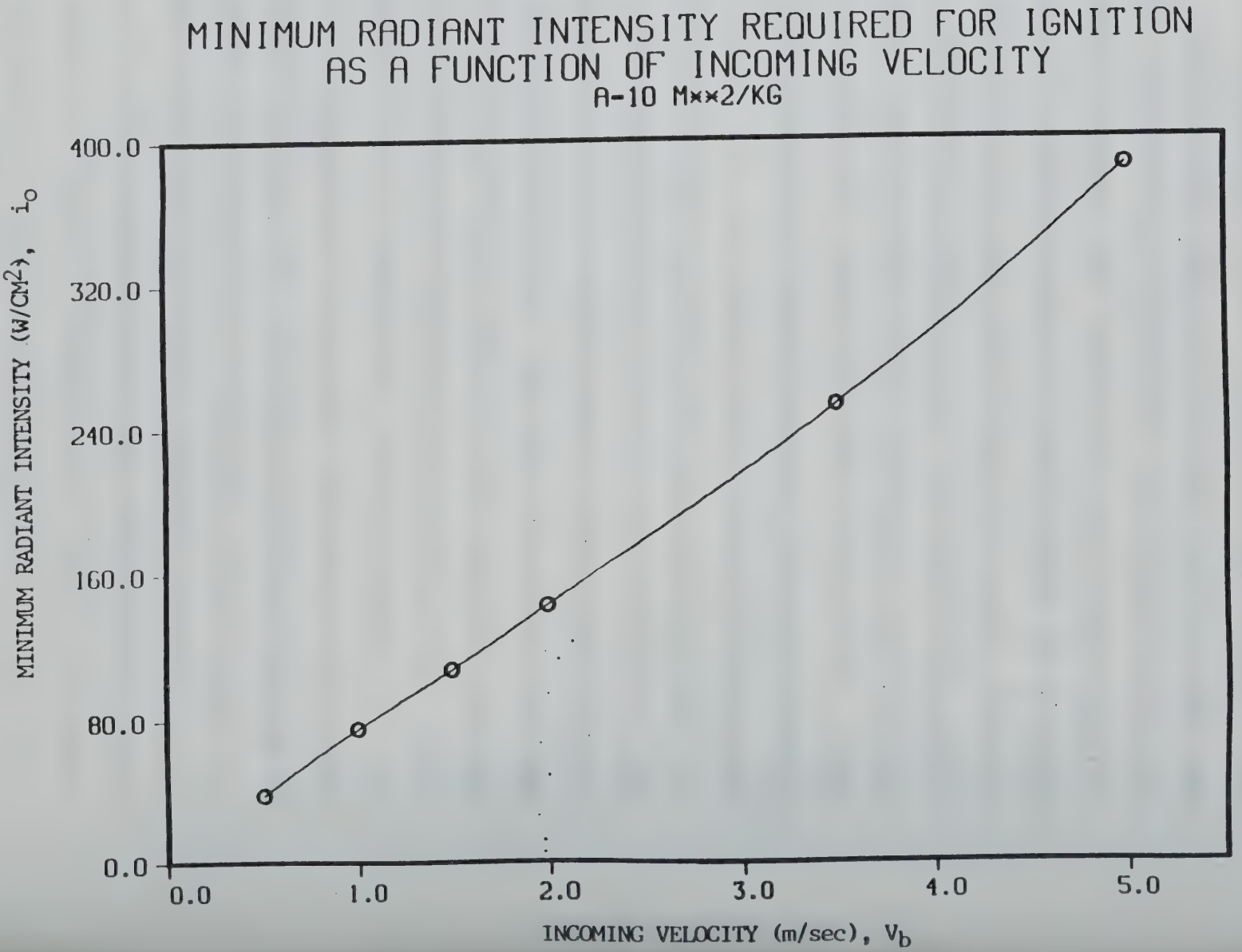
MINIMUM RADIANT INTENSITY REQUIRED FOR IGNITION
AS A FUNCTION OF INCOMING VELOCITY
A-10 M××2/KG
MINIMUM RADIANT INTENSITY (W/CM2), io
400.0
320.0
240.0
160.0
80.0
0.0
0.0
1.0
2.0
3.0
4.0
5.0
INCOMING VELOCITY (m/sec), Vb

Figure 4.5

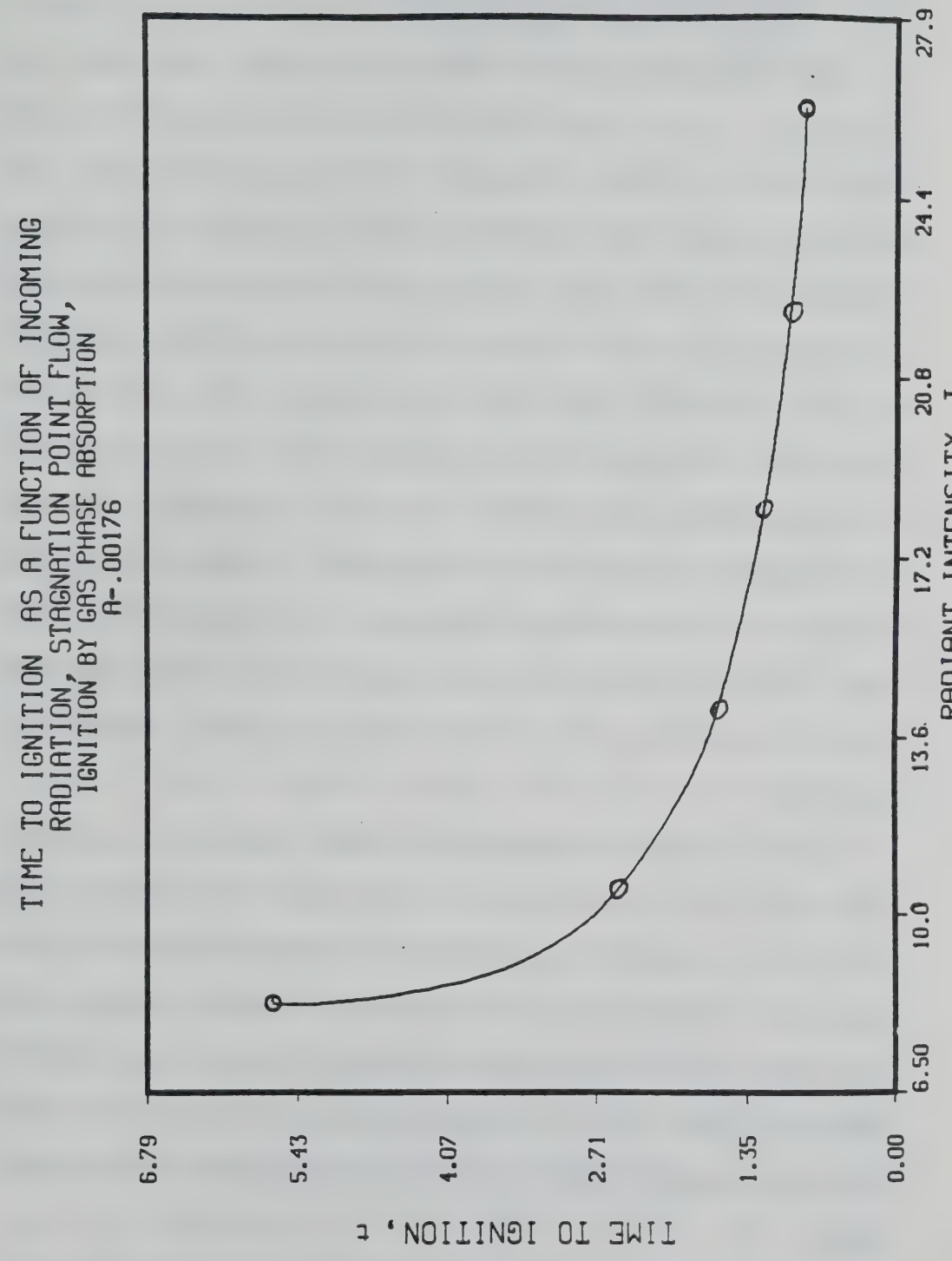
TIME TO IGNITION AS A FUNCTION OF INCOMING RADIATION, STAGNATION POINT FLOW, IGNITION BY GAS PHASE ABSORPTION
A=.00176
TIME TO IGNITION, τ
6.79
5.43
4.07
2.71
1.35
0.00
6.50
10.0
13.6
17.2
20.8
24.4
27.9
RADIANT INTENSITY, I

Figure 4.6

4.3.3 Results of the Ignition and Flame Propagation Study with Ignition Caused by a Hot Fuel Surface

The parameters which define this case are shown in dimensional form in Table (4.2) and in non-dimensional form in Table (4.3). The differences in parameters between the stagnation point flow case with ignition caused by gas phase absorption and this case parallel the differences between the one-dimensional cases. Again the absorption coefficient is set to zero and the wall temperature is increased. The total heat of combustion is reduced by approximately twenty percent hold down the maximum temperatures which occur in the problem. Finally, the intensity is reduced to 1.3 watts/cm^2, which is the minimum intensity required to cause ignition. If a value of intensity below this minimum value is used then a steady state boundary layer solution with fuel injection and no chemical reaction is obtained.

Like the stagnation point problem with ignition by gas phase absorption the results can be divided into five regimes based upon the strength of the chemical reaction and whether or not radiation is being applied to the wall. These five regimes are the same as in the gas phase absorption problem although the characteristics of each regime vary because of the different method of ignition used. The regimes are discussed in more detail next.

The first regime is the initial condition and is a

stagnation point flow which is composed entirely of air. It is exactly the same as in the gas phase absorption case except for changes in the momentum and thermal boundary layers caused by the increased wall temperature. This regime is illustrated in Figs. (4.7a), and (4.9a) at time, t=0.0.

The second regime is the pre-ignition regime and corresponds to when the radiant heat flux is applied to the wall. It occurs from time greater than t=0.0, and to times less than or equal to the time, t=0.377. It is illustrated in Figs. (4.7a), (4.8a), and (4.9b). This regime is significantly different from the second regime in the gas phase absorption case because the incident radiation is so weak. Instead of the opposed fuel jet flow, the boundary layer remains approximately intact with very weak fuel injection into it. Ignition takes place very close to the wall and at a location where there is a relatively high non-dimensional oxygen mass fraction of 0.60. Hence, after the chemical reaction becomes strong there will be a large and extremely short-lived spike in the power as shown in Fig. (3.7).

The beginning of the third regime occurs when ignition takes place and the radiation is turned off. The chemical reaction in this regime is weak and this regime is very similiar to the second regime except that fuel is no longer being injected at the wall because of the radiation. This phase last from times greater than t=0.377 to times less than t=0.425. On a large scale the temperature and mass fraction profiles and velocity fields look similiar to those shown for the second regime.

The fourth regime, which is characterized by the strong chemical reaction, begins at time, t=0.425 and last until approximately time ,t=0.450. It is illustrated in Figs. (4.7), (4.8b), (4.8c), (4.9c) and (4.9d). As in the gas phase absorption case, it is during this regime that a premixed flame front makes its appearance and propagates from the rich region to the lean region. It again serves to separate the fuel and the oxygen and to leave behind the diffusion flame at the stoichiometric point. Two differences between this case and the gas phase absorption case are that the flame propagation occurs much closer to the wall and, because of this closeness to the wall, more fuel vaporization takes place after ignition.

As in the previous case, the chemical reaction in this regime is strong enough to dominate the flow field. As can be seen in Fig. (4.9c) the expansion of gases from the reaction has pushed the incoming flow far back from the wall. A peculiar velocity field is again produced as the premixed flame front dies out and is shown in Fig. (4.9d). As can be seen from the figure, not only is there a region of reduced velocities in the low density region but also a region of back flow. This region of back flows occurs for the same reasons that the low velocities occurred in the gas phase absorption case.

The fifth and final regime occurs when the premixed flame front begins to die out leaving the diffusion flame. This regime occurs from time, t=0.450, and lasts until the steady state diffusion flame is obtained. It is illustrated in Figs. (4.7b),

(4.8d), (4.8e) and (4.9e). As in the gas phase absorption case, the incoming flow dominates because of the relatively weak chemical reaction, and the boundary layer flow is reestablished. In this regime the diffusion flame moves away from the wall towards its equilibrium position. However, because there is excess fuel behind the diffusion flame, the flame will slightly overshoot its equilibrium position. Since the incoming flow eventually flushes out the excess fuel the flame settles back into its equilibrium position and reaches a steady state. Because of the lower heat of combustion in this case, the diffusion flame is weaker with fuel and oxygen overlapping more, and the temperature being lower than in the gas phase absorption case.

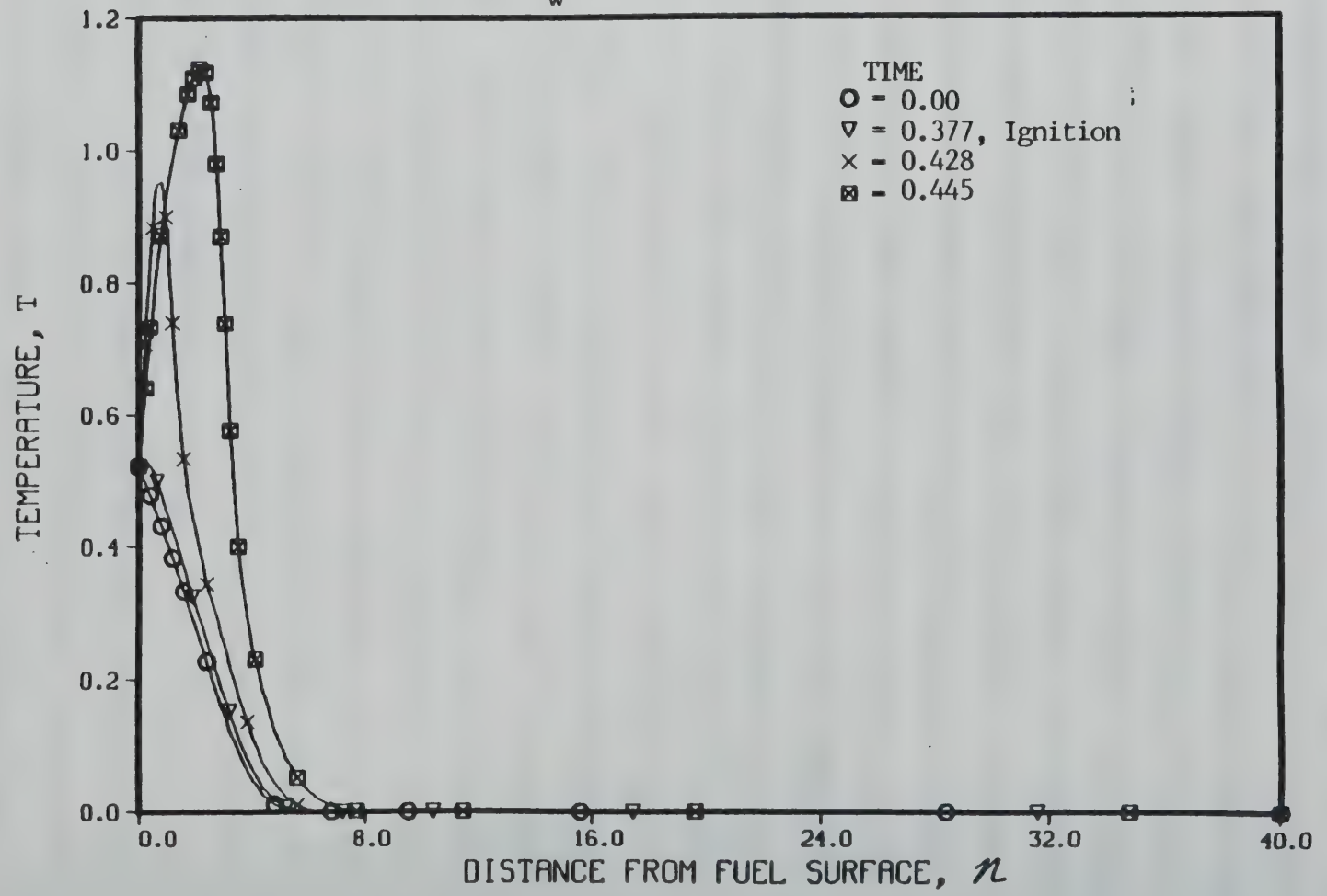
TEMPERATURE PROFILES
STAGNATION POINT FLOW, IGNITION IS CAUSED BY
A HIGH TEMPERATURE FUEL SURFACE
I_w-.523, I-.369, A -0.
TIME
O = 0.00
∇ = 0.377, Ignition
× = 0.428
⊠ = 0.445
TEMPERATURE, T
1.2
1.0
0.8
0.6
0.4
0.2
0.0
0.0
8.0
16.0
24.0
32.0
40.0
DISTANCE FROM FUEL SURFACE, η

Figure 4.7a

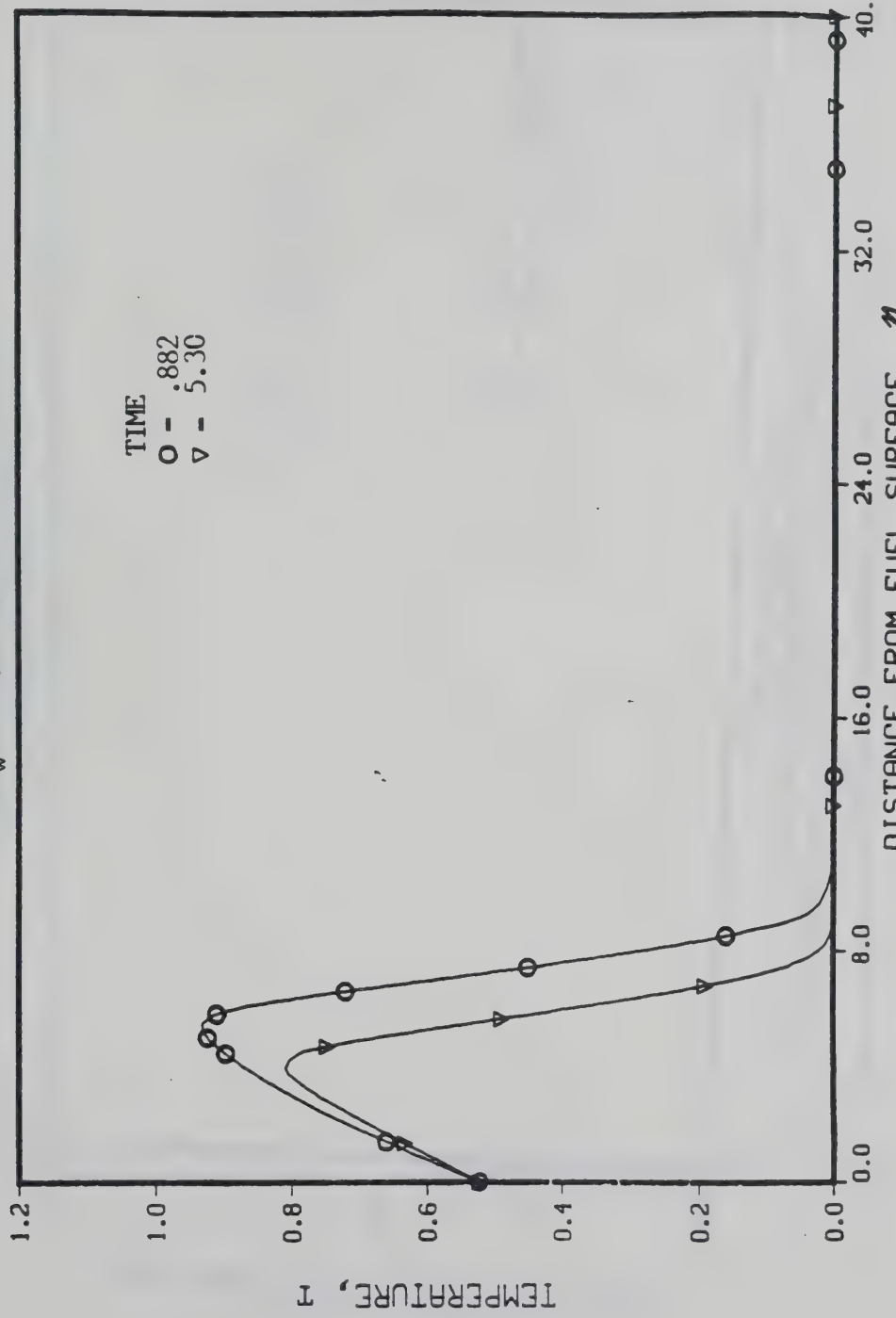
TEMPERATURE PROFILES
STAGNATION POINT FLOW, IGNITION IS CAUSED BY
A HIGH TEMPERATURE FUEL SURFACE
T_w=.523, I-.369, A -.0
TIME
o - .882
v - 5.30
TEMPERATURE, T
DISTANCE FROM FUEL SURFACE, η
0.0
0.2
0.4
0.6
0.8
1.0
1.2
0.0
8.0
16.0
24.0
32.0
40.0

Figure 4.7b

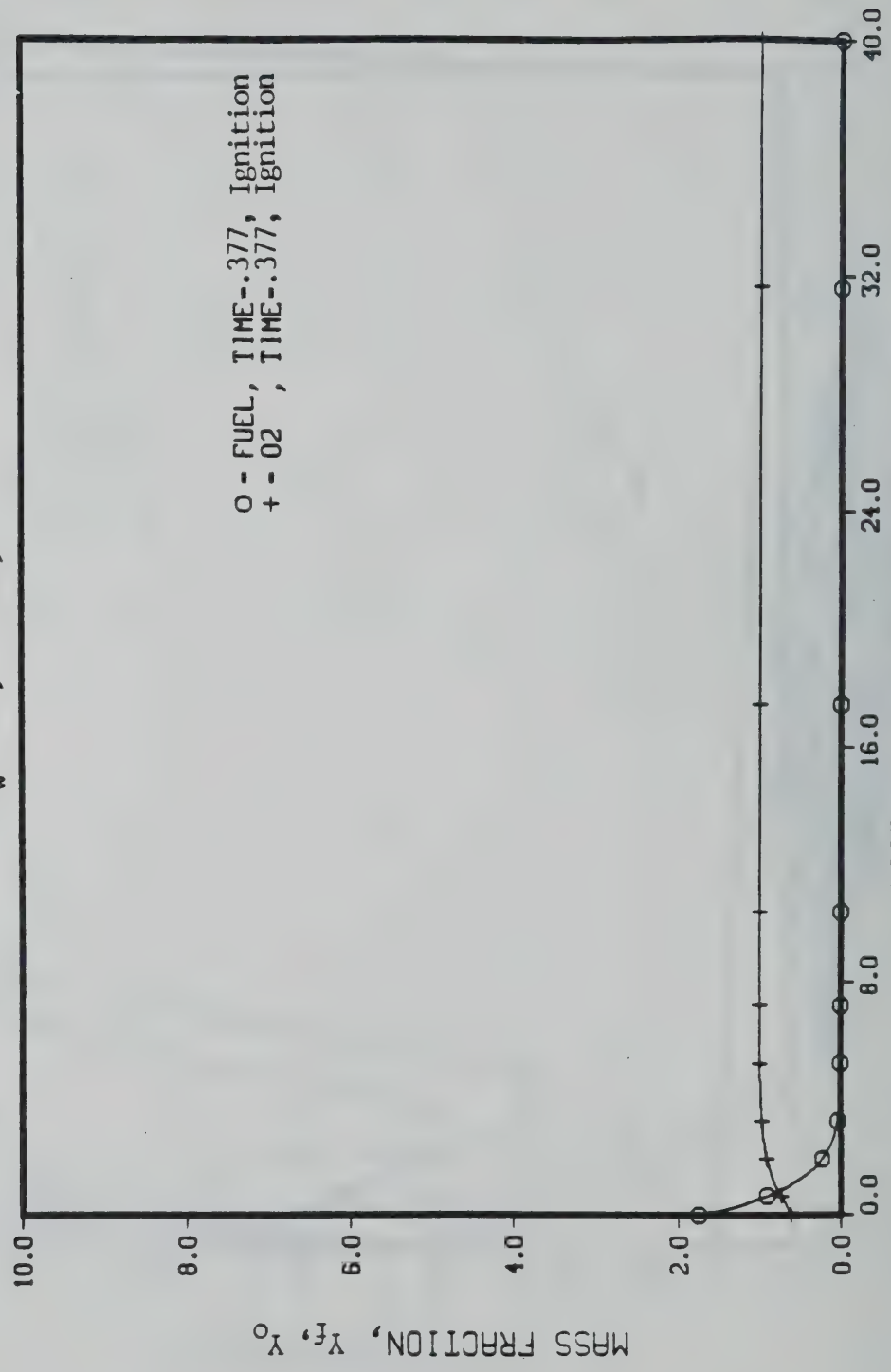
MASS FRACTION PROFILES
STAGNATION POINT FLOW, IGNITION IS CAUSED BY
A HIGH TEMPERATURE FUEL SURFACE
I_w=.523, I=.369, A =0.
O - FUEL, TIME=.377, Ignition
+ - O2 , TIME=.377, Ignition
MASS FRACTION, Y_F, Y_O
DISTANCE FROM FUEL SURFACE, η
10.0
8.0
6.0
4.0
2.0
0.0
0.0
8.0
16.0
24.0
32.0
40.0

Figure 4.8a

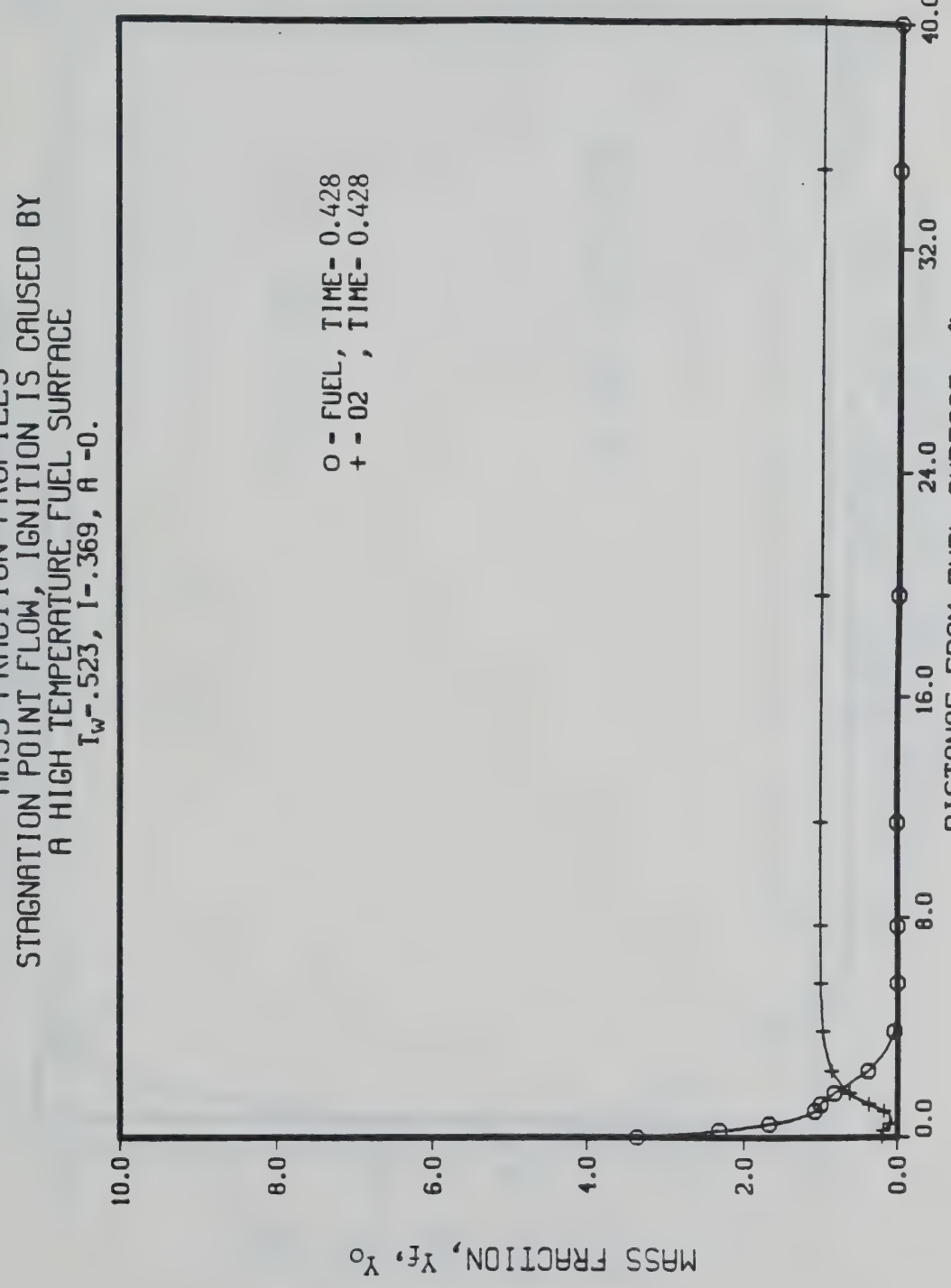
MASS FRACTION PROFILES
STAGNATION POINT FLOW, IGNITION IS CAUSED BY
A HIGH TEMPERATURE FUEL SURFACE
T_w=-.523, I=.369, A =0.
O - FUEL, TIME= 0.428
+ - O2 , TIME= 0.428
MASS FRACTION, Y_F, Y_O
DISTANCE FROM FUEL SURFACE, η
0.0
2.0
4.0
6.0
8.0
10.0
0.0
8.0
16.0
24.0
32.0
40.0

Figure 4.8b

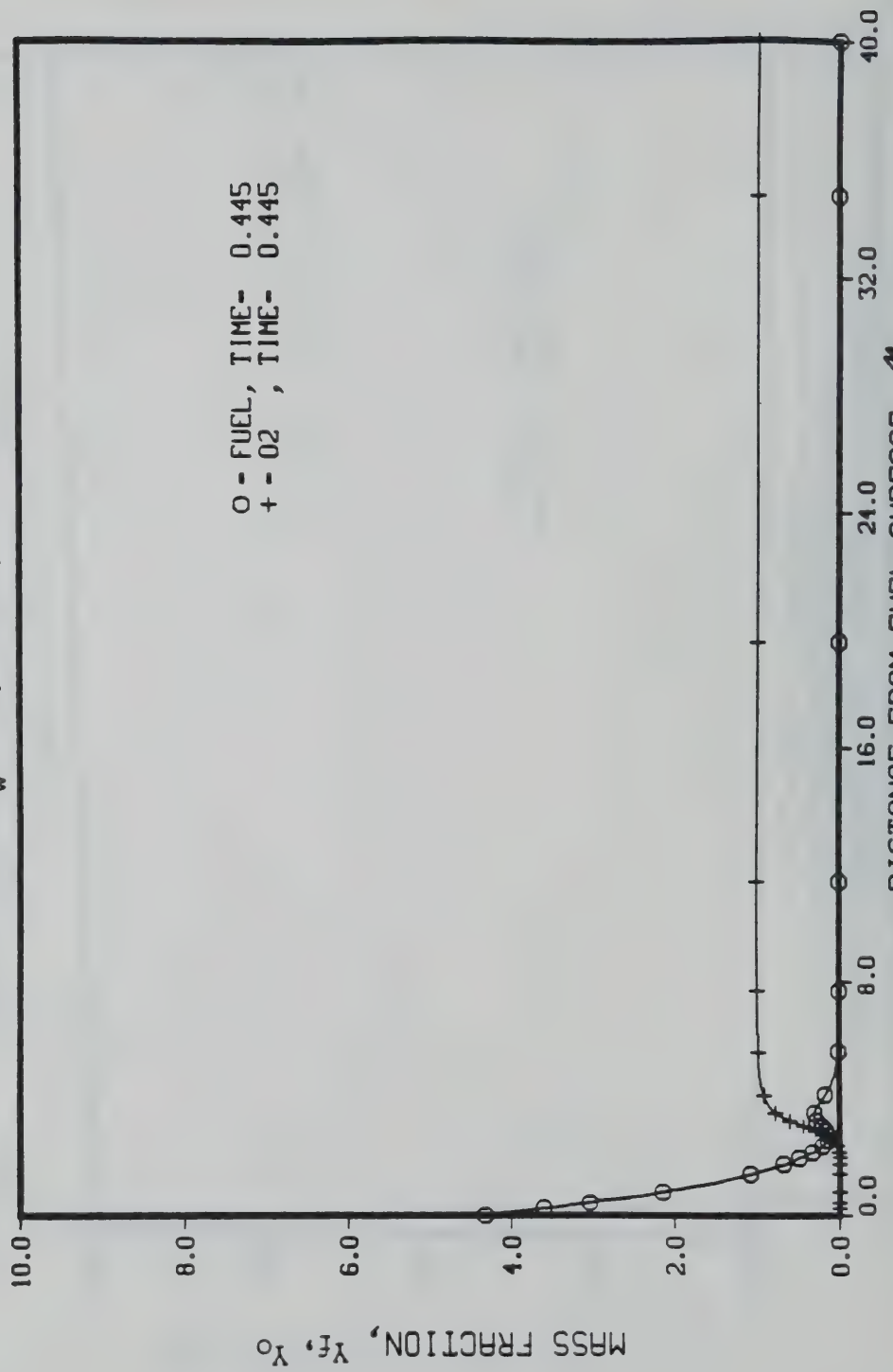
MASS FRACTION PROFILES
STAGNATION POINT FLOW, IGNITION IS CAUSED BY
A HIGH TEMPERATURE FUEL SURFACE
I_w=.523, I=.369, A =0.
O - FUEL, TIME- 0.445
+ - O2 , TIME- 0.445
MASS FRACTION, Y_F, Y_O
DISTANCE FROM FUEL SURFACE, η
0.0
2.0
4.0
6.0
8.0
10.0
0.0
8.0
16.0
21.0
32.0
40.0

Figure 4.8c

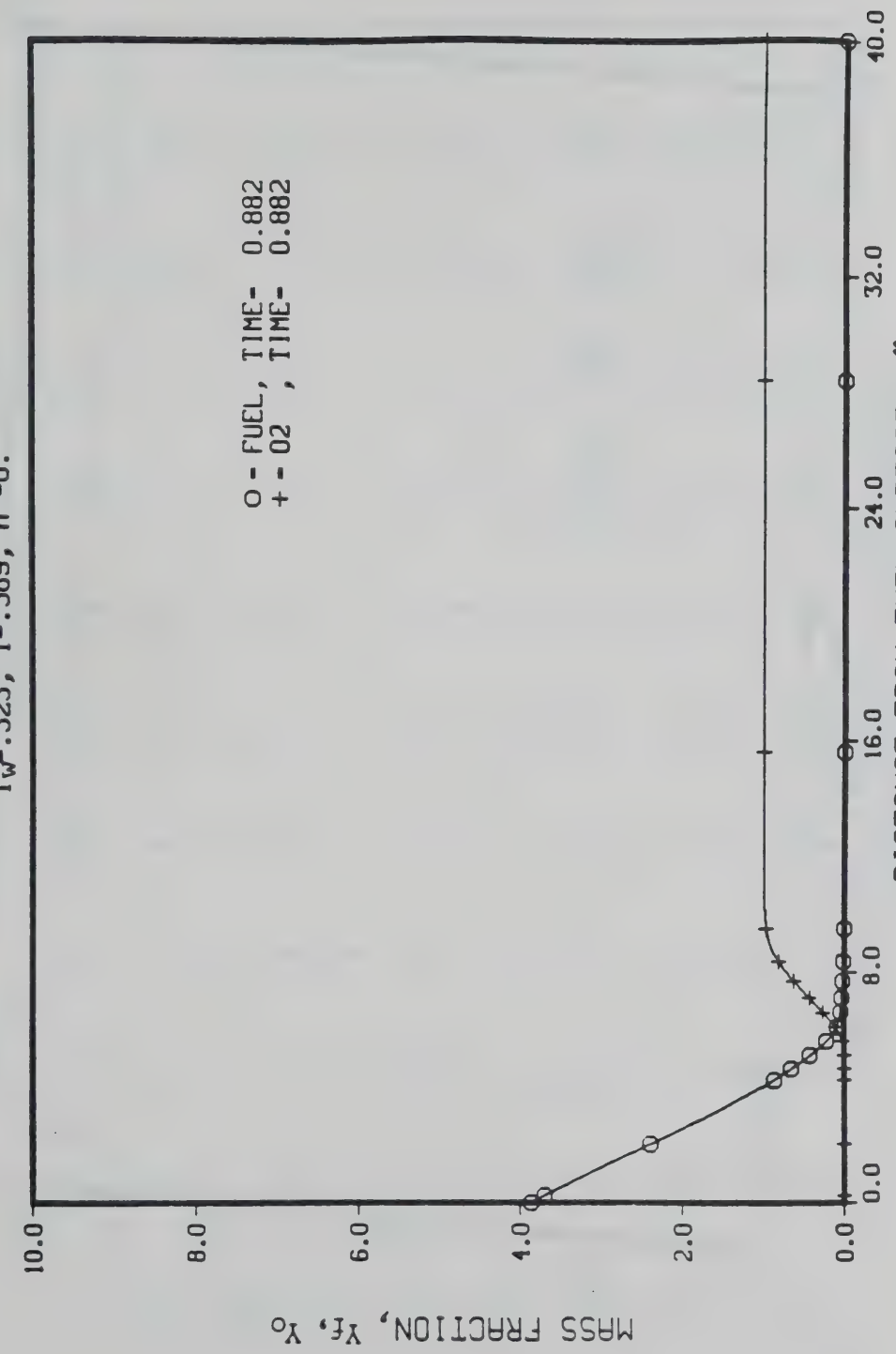
MASS FRACTION PROFILES
STAGNATION POINT FLOW, IGNITION IS CAUSED BY
A HIGH TEMPERATURE FUEL SURFACE
T_w=.523, I=.369, A =0.
O - FUEL, TIME- 0.882
+ - O2 , TIME- 0.882
MASS FRACTION, Y_F, Y_O
DISTANCE FROM FUEL SURFACE, η
10.0
8.0
6.0
4.0
2.0
0.0
0.0
8.0
16.0
24.0
32.0
40.0

Figure 4.8d

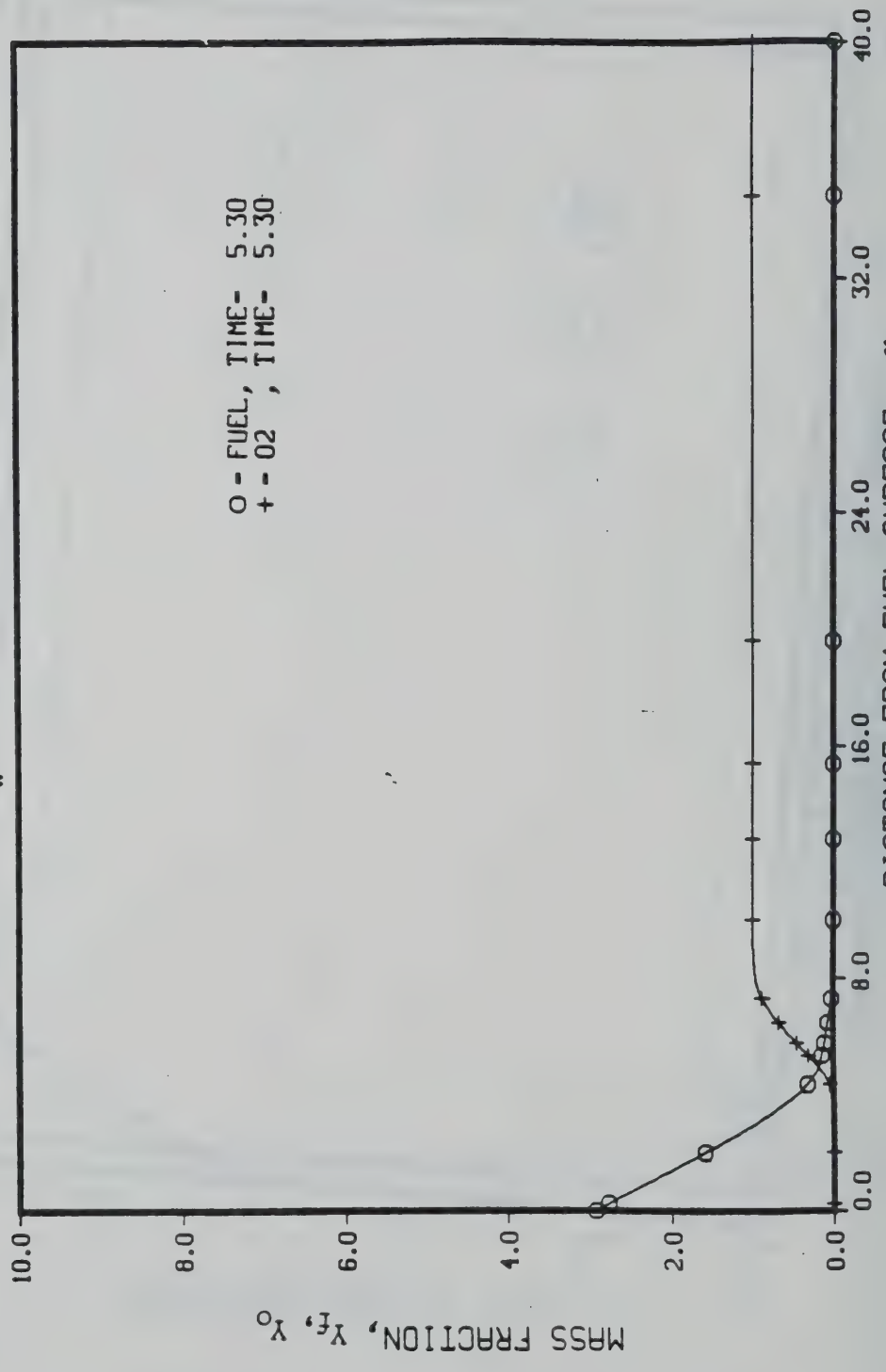
MASS FRACTION PROFILES
STAGNATION POINT FLOW, IGNITION IS CAUSED BY
A HIGH TEMPERATURE FUEL SURFACE
I_w=.523, I=.369, A =0.
O - FUEL, TIME- 5.30
+ - O2 , TIME- 5.30
MASS FRACTION, Y_F, Y_O
DISTANCE FROM FUEL SURFACE, η
0.0
2.0
4.0
6.0
8.0
10.0
0.0
8.0
16.0
24.0
32.0
40.0

Figure 4.8e

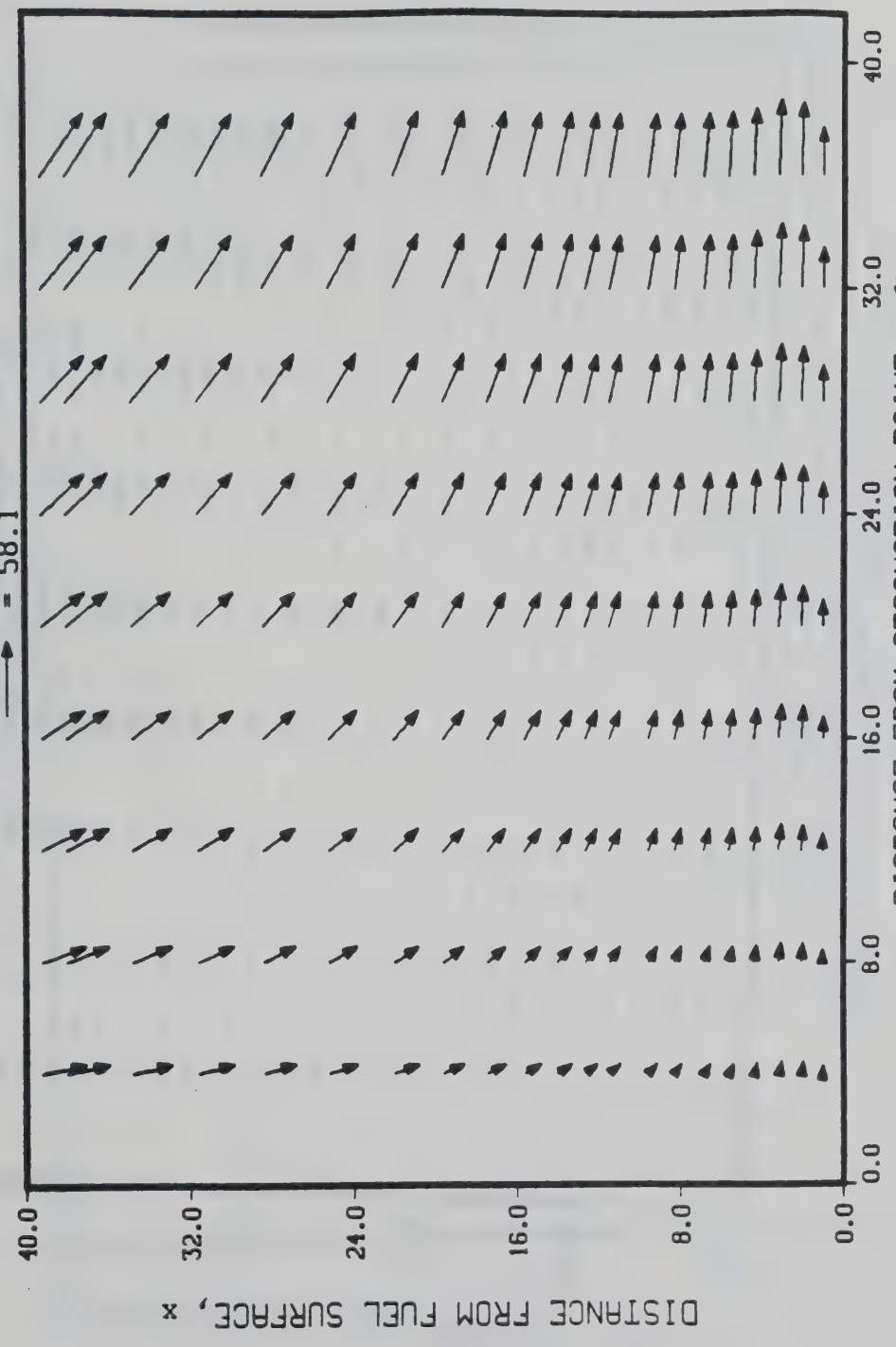
VELOCITY FIELD
STAGNATION POINT FLOW, IGNITION IS CAUSED BY
A HIGH TEMPERATURE FUEL SURFACE
T =.523, I=.369, A =0., TIME= 0.00
= 58.1
DISTANCE FROM FUEL SURFACE, x
DISTANCE FROM STAGNATION POINT, z
0.0
8.0
16.0
24.0
32.0
40.0

Figure 4.9a

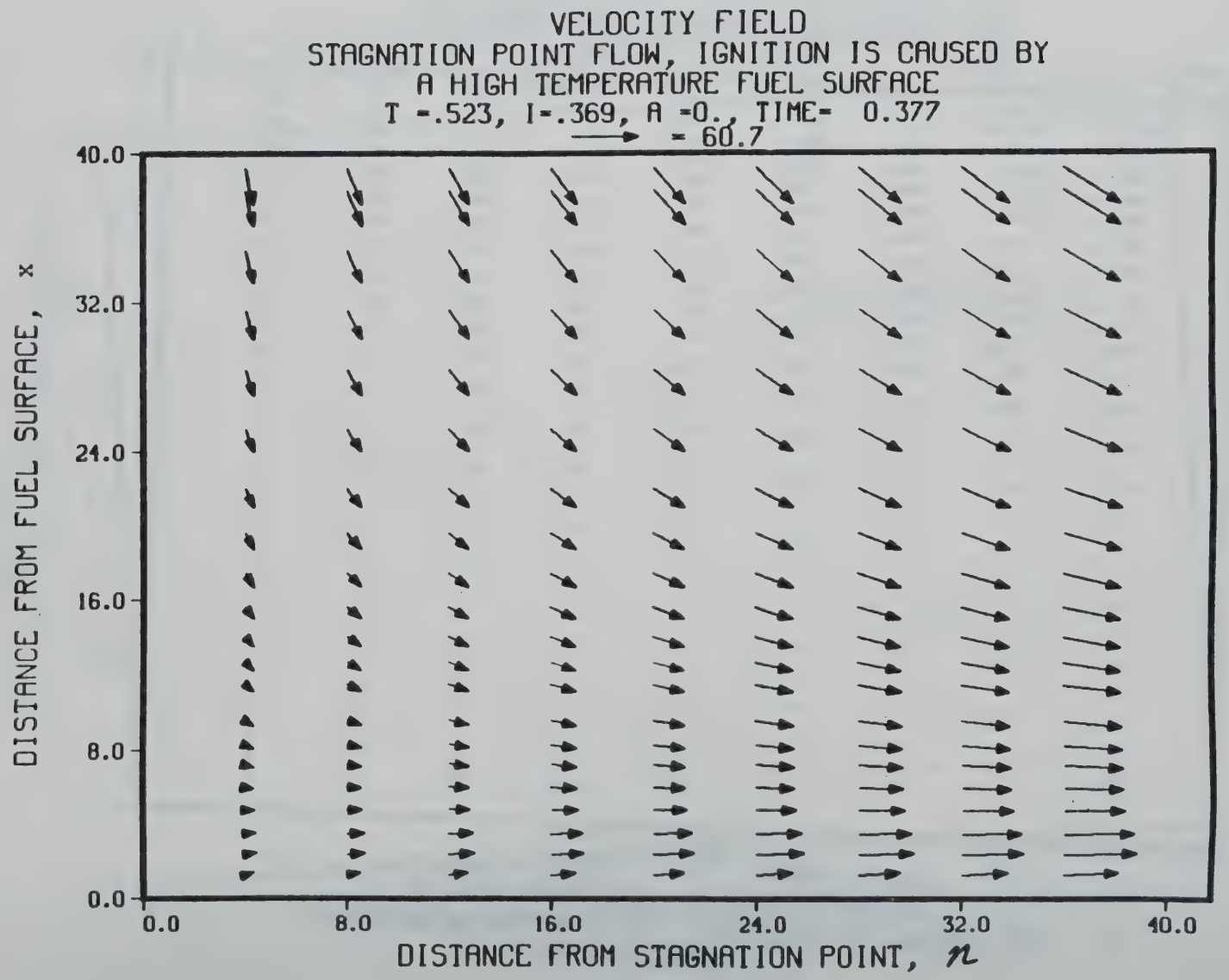
VELOCITY FIELD
STAGNATION POINT FLOW, IGNITION IS CAUSED BY
A HIGH TEMPERATURE FUEL SURFACE
T =.523, I=.369, A =0., TIME= 0.377
= 60.7
DISTANCE FROM FUEL SURFACE, x
40.0
32.0
24.0
16.0
8.0
0.0
0.0
8.0
16.0
24.0
32.0
40.0
DISTANCE FROM STAGNATION POINT, η

Figure 4.9b

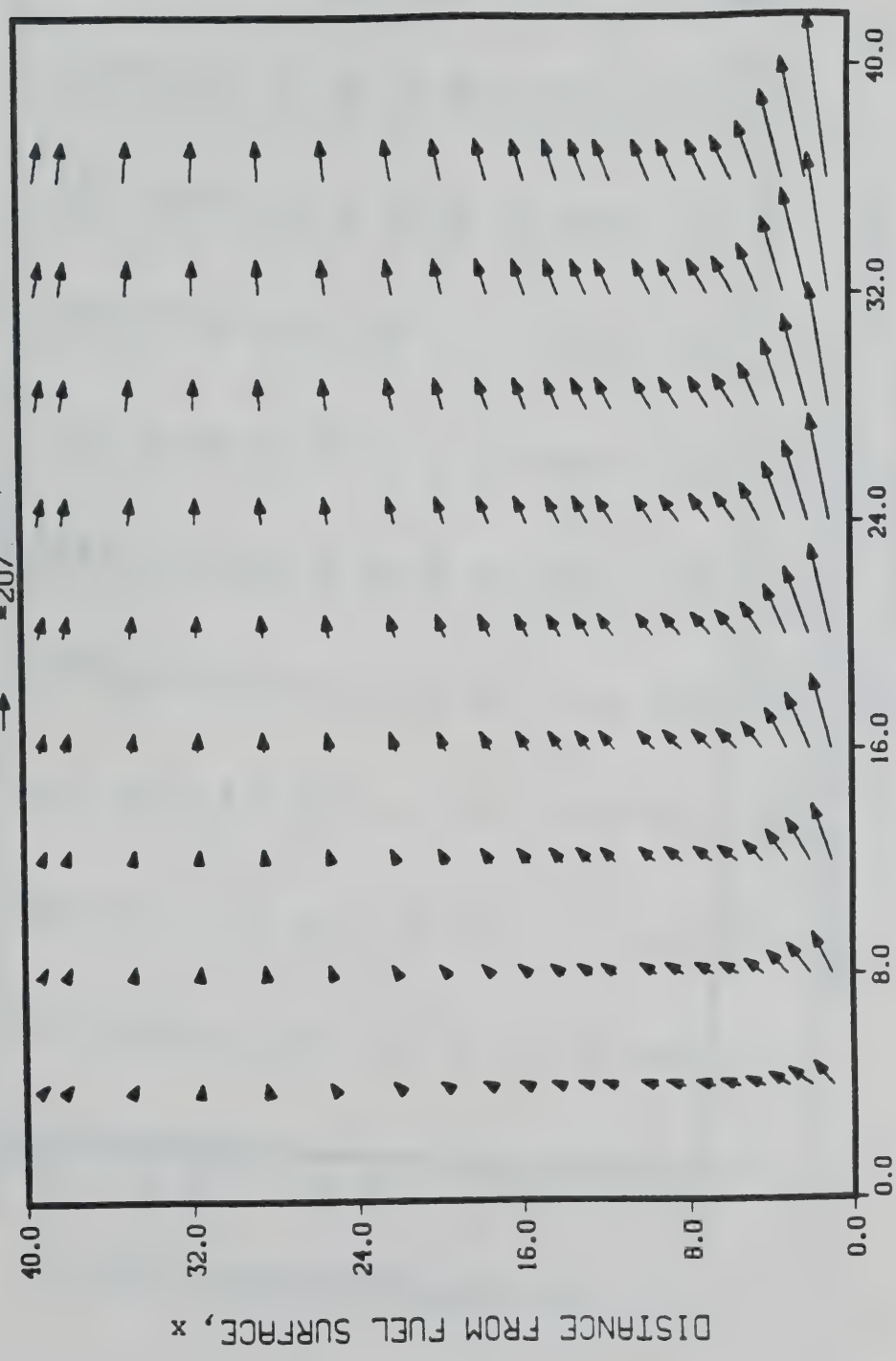
VELOCITY FIELD
STAGNATION POINT FLOW, IGNITION IS CAUSED BY
A HIGH TEMPERATURE FUEL SURFACE
T =.523, I=.369, A =0., TIME= 0.428
-20
DISTANCE FROM FUEL SURFACE, x
0.0
8.0
16.0
24.0
32.0
40.0
DISTANCE FROM STAGNATION POINT, ξ

Figure 4.9c

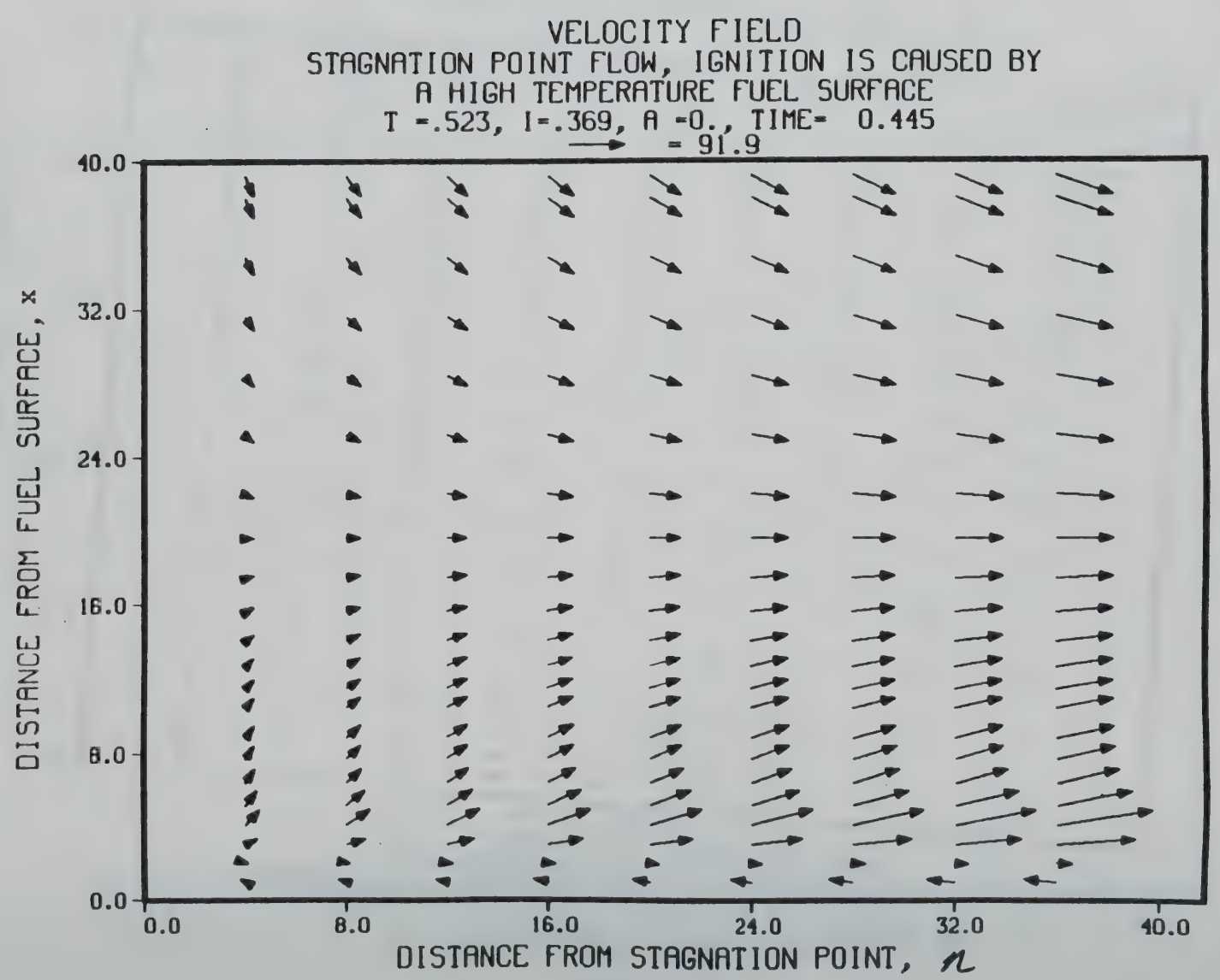
VELOCITY FIELD
STAGNATION POINT FLOW, IGNITION IS CAUSED BY
A HIGH TEMPERATURE FUEL SURFACE
T =.523, I=.369, A =0., TIME= 0.445
= 91.9
DISTANCE FROM FUEL SURFACE, x
0.0
8.0
16.0
24.0
32.0
40.0
DISTANCE FROM STAGNATION POINT, ξ

Figure 4.9d

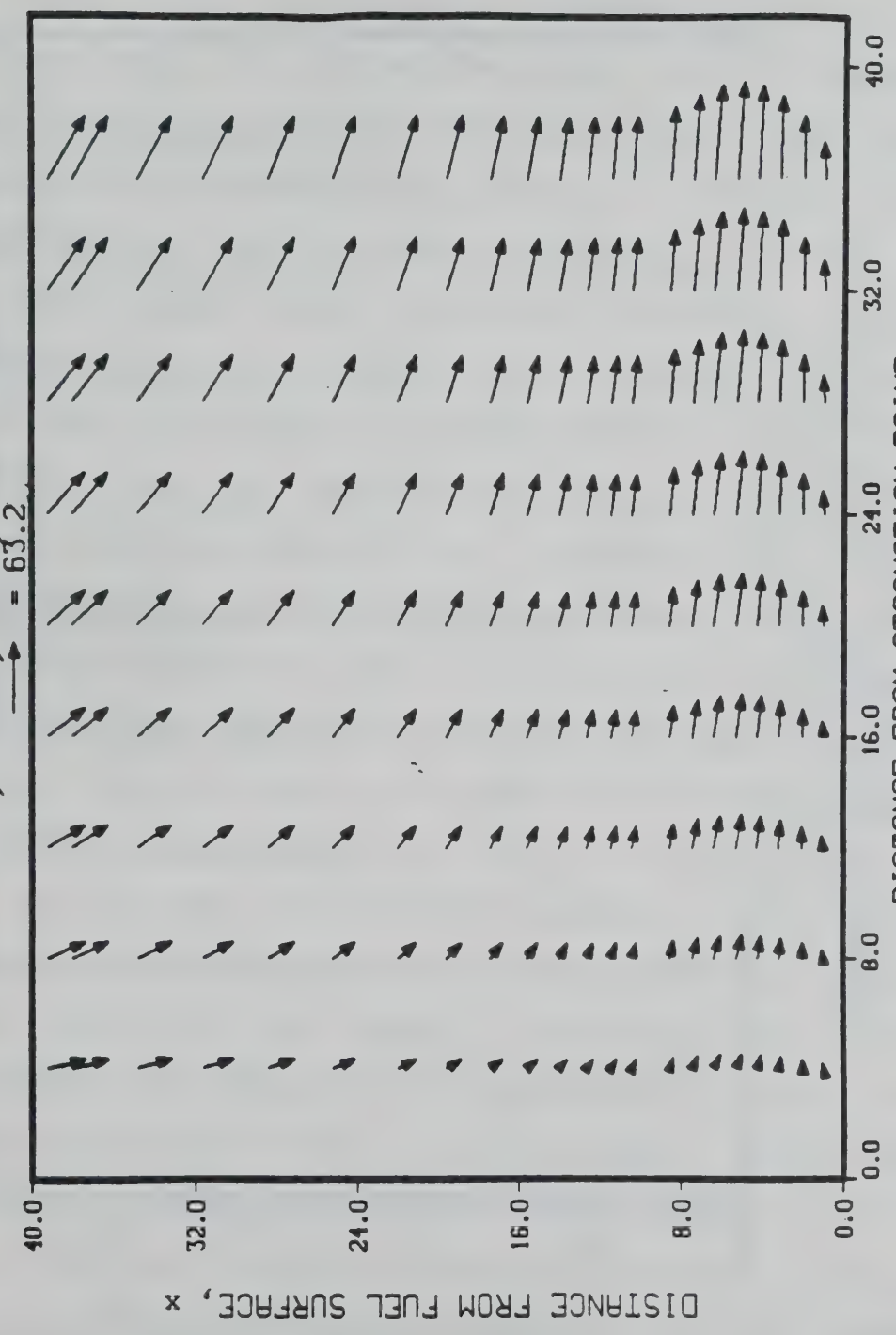
VELOCITY FIELD
STAGNATION POINT FLOW, IGNITION IS CAUSED BY
A HIGH TEMPERATURE FUEL SURFACE
T =.523, I=.369, A =0., TIME= 0.882
= 63.2
DISTANCE FROM FUEL SURFACE, x
DISTANCE FROM STAGNATION POINT, ℓ
0.0
8.0
16.0
24.0
32.0
40.0

Figure 4.9e

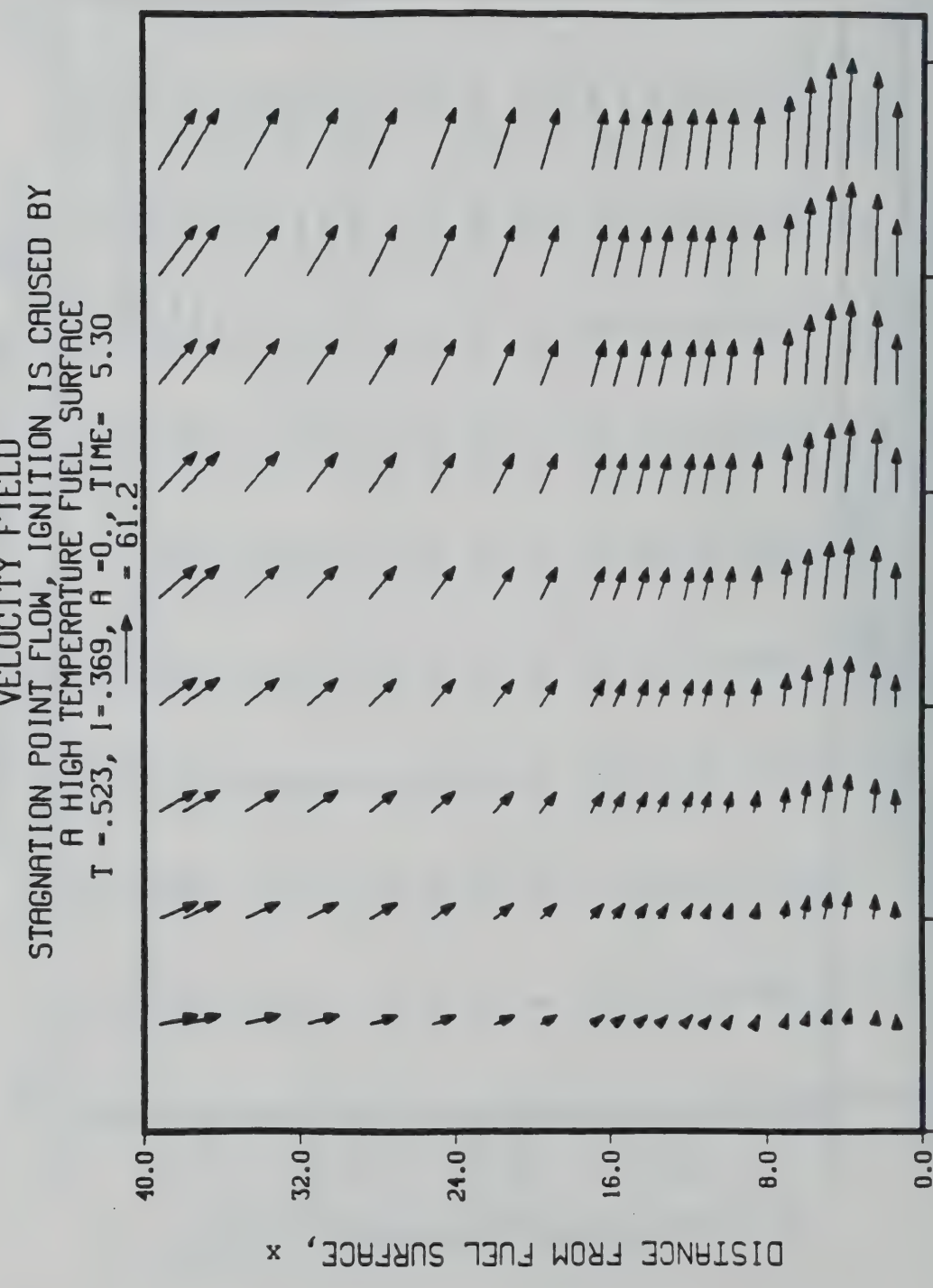
VELOCITY FIELD
STAGNATION POINT FLOW, IGNITION IS CAUSED BY
A HIGH TEMPERATURE FUEL SURFACE
T =.523, I=.369, A =0., TIME= 5.30
= 61.2
DISTANCE FROM FUEL SURFACE, x
DISTANCE FROM STAGNATION POINT, ℛ
0.0
8.0
16.0
24.0
32.0
40.0

Figure 4.9f

5. CONCLUSION

5.1 Summary

This study illustrates the relationships between the ignition regime, the premixed flame regime, and the diffusion flame regime which occur when considering the entire combustion process over a vaporizing fuel surface. Two different flow conditions over the fuel surface are analyzed: air which is initially stagnant and in a zero gravity environment, and air which is initially in a stagnation point flow pattern. For each flow condition two physically different methods of ignition are used. In the first method the flat plate is subjected to external radiation causing the fuel to vaporize. The fuel vapor then absorbs a fraction of the incoming radiation, becomes hot and causes the mixture to ignite. In the second method the flat plate is again subjected to radiation, but ignition occurs because the fuel surface is hot enough to ignite the vapor with no radiation being absorbed.

In all cases, the same general sequence of events occur. The first event is the application of the radiation which causes fuel vaporization and ignition. Ignition did not occur immediately upon application of the radiation, and during this delay there is time for the fuel and the oxygen to diffuse into one another creating a mixing region. Ignition eventually occurs in a rich part of the mixing region with the amount of power produced after ignition being determined by the oxygen concentration at the point of ignition. If the oxygen

concentration is high, as is the case of the hot wall ignition problems, the chemical power curve shows a large spike. If ignition occurs in a region with little oxygen, as is the case in the gas phase absorption ignition with realistic absorption coefficients, no chemical power spike occurs and the maximum chemical power is produced in the premixed region.

After ignition occurs, there is a period of weak chemical reaction. The reaction eventually becomes strong and leads to the development of a premixed flame front which moves away from the wall. The flame front begins travelling in the rich region where it leaves behind excess fuel, passes through a stoichiometric point and enters the lean region where excess oxygen is left behind. Hence, the premixed flame serves to separate the fuel and oxygen and to leave behind a diffusion flame at the stoichiometric point. For a brief period of time, a premixed flame front and diffusion flame exist .simultaneously. Eventually the premixed flame front enters a very lean region and dies out, leaving only the diffusion flame. In the one dimensional cases the diffusion flame moves away from the wall, weakens and also eventually dies out. In the stagnation point flow cases, the diffusion flame moves toward an equilibrium position and reaches a steady state.

The stagnation point flow cases also showed complex flow regimes which were often driven by the radiant heating or the chemical reaction. Because of the high radiant intensity used in the gas phase absorption case an opposing jet flow regime is

produced when the radiation is applied to the wall. The bottom jet is composed of fuel while the top jet is composed of air. In the hot wall ignition case, because of the low radiant intensity used, the boundary layer near the wall remains nearly intact. Immediately after ignition occurs and the radiation is removed, both cases show a boundary layer type of a flow with a weak chemical reaction present in the interface region between the fuel and the air. Later, in the premixed flame period, the chemical reaction is so strong that the expanding gases dominate the flow field and the incoming flow is pushed back. After the premixed flame dies out and the diffusion flame is left behind, the incoming stagnation point flow again dominates and the diffusion flame settles into a boundary layer near the wall.

5.2 Future Work

The scope of this thesis is restricted to analyzing overall processes and this limited the attention that could be devoted to any specific process. Certainly, a number of areas identified in this thesis deserve detailed study. Among these are the transition region which occurs immediately after ignition and before the premixed flame fronts develop, the passing of the premixed flame front through the stoichiometric point, and the slow extinction of the premixed flame front and its effect upon the flow field in the stagnation point flow cases.

Many of the assumptions made here can also be relaxed so that more realism is introduced. Perhaps the most limiting assumptions are that of single step chemistry and laminar flow.

Multiple step chemistry models are already available and their inclusion would not be difficult since all problems reduce to one spatial dimension. Also, once an accurate turbulence model is developed, it could be included. The overall model could then quite closely approximate a real combustion situation.

References

1. Kashiwagi, T., "A Radiative Ignition Model of a Solid Fuel," Combustion Science And Technology, Vol. 8, 1974, pp. 225-236.

2. Kumar, R. K., and Hermance, C. E., "Role of Gas-Phase Reactions During Radiant Ignition of Solid Propellants," Combustion Science and Technology, Vol.14, 1976, pp. 169-175.

3. Kumar, R. K., and Hermance, C. E., " Gas Phase Ignition Theory of a Heterogenous Solid Propellant," Combustion Science and Technology, Vol. 4, 1972, pp. 191-196.

4. Kindelan, M., and Williams, F. A., "Radiant Ignition of a Combustible Solid With Gas Phase Exothermicity," Acta Astronautica, Vol. 2, 1975, pp. 955-979.

5. Shannon, L. J., and Deverall L., "A Model of Solid Propellant Ignition in a Neutral Environment," AIAA Journal, Vol. 6, May 1968, pp.497-502.

6. Bradley, H., Jr., "A Unified Theory of Solid Propellant Ignition," NWC TP 5618, Parts 1-3, Naval Weapons Center, China Lake, Calif., Dec. 1975.

7. Price, E. W., and Bradley, H. H., "Theory of Ignition of Solid Propellants," AIAA Journal, Vol. 4, Sept. 1966, pp. 1153-1181.

8. Vilyunov, V., "A Gas Phase Model of the Ignition of Certain Solids in A Shock Tube," Combustion, Explosion, and Shock Waves, Vol. 8, 1972, pp. 284-289.

Flow Diffusion Flame Extensions," Eighteenth Symposium (International) on Combustion, The Combustion Institute, 1981, pp.1853-1860.

18. Holve, D. J., and Sawyer R. F., "Diffusion Controlled Combustion of Polymers," Fifthteenth Symposium (International) on Combustion, The Combustion Institute, 1974, pp. 351-361.

19. Seshadri, K., and Williams, F. A., "Structure and Extinction of Counterflow Diffusion Flames above Condensed Fuels: Comparison Between Poly(methMethacrylate) and its Liquid Monomer, Both Burning in Nitrogen-Air Mixture," Journal of Polymer Science: Polymer Chemistry Edition, Vol. 16, 1978, pp. 1755-1778.

20. Tsuji, H., and Yamaoka, I., "The Structure of Counterflow Diffusion Flames in the Forward Stagnation Region of a Porous Cylinder," Twelfth Symposium (International) on Combustion, The Combustion Institute, 1969, pp. 997-1005.

21. Tsuji, H., and Yamaoka, I., "Structure Analysis of Counterflow Diffusion Flames in the Forward Stagnation Region of a Porous Cylinder," Thirteenth Symposium (International) on Combustion, The Combustion Institute, 1971, pp. 723-731.

22. Pitz, W. J., Brown, N. J., and Sawyer, R. F., "The Structure of a Poly(ethylene) Opposed Flow Diffusion Flame", Eighthteenth Symposium (International) on Combustion. The Combustion Institute, 1981, pp.1871-1880.

23. Holve, D. J., and Sawyer, R. F., "Diffusion Controlled Combustion of Polymers," Fifthteenth Symposium (International)

9. Niioka, T., and Williams, F. A., "Relationship between Theory and Experiment for Radiant Ignition of Solids," Combustion Science and Technology, Vol. 16, 1977, pp. 47-58.

10. Niioka, T., "Ignition Time in the Stretched Flow Field," Eighthteenth Symposium (International) on Combustion, The Combustion Institute, 1980, pp. 1807-1813.

11. Alkidas, A., and Durbetaki, P., "Ignition Characteristics of a Stagnation Point Combustible Mixture," Combustion Science and Technology, Vol. 3, 1971, pp. 187-194.

12. Krishnamurthy, L., "On Gas Phase Ignition of Diffusion Flames in the Stagnation Point Boundary Layer," Acta Astronautica, Vol. 3, 1976, pp.935-942.

13. Chen, T., and Toong, T., "Laminar Boundary Layer Wedge Flows with Evaporation and Combustion," Heterogeneous Combustion: Progress in Astronautics and Aeronautics, Vol. 15, Academic Press, New York, 1964, pp. 643-664.

14. Krishnamurthy, L., and Williams, F., "A Flame Sheet in the Stagnation Point Boundary Layer of a Condensed Fuel," Paper 73-10, Western States Section/The Combustion Institute, April, 1973.

15. Linan, A., "The Asymptotic Structure of Counterflow Diffusion Flames for Large Activation Energies," Acta Atronautica, Vol. 1, pp. 1007-1039.

16. Kinoshita, C. M., and Pagni, P. J., "Stagnation Point Combustion with Radiation," Eighteenth Symposium(International) on Combustion, The Combustion Institute, 1981, p. 1415.

17. Kinoshita, C. M., Pagni, P. J., and Beier, R. A., "Opposed

on Combustion, The Combustion Institute, 1975, pp. 351-361.

24. Mathews, R. D., and Sawyer, R. F., "Limiting Oxygen Index Measurement and Interpretation in an Opposed Flow Diffusion Flame", Journal of Fire and Flammability, Vol. 7, 1976, pp.200-216.

25. Kashiwagi, T., "Experimental Observation of Radiative Ignition Mechanisms," Combustion and Flame, Vol. 34, 1979, p. 231.

26. Kashiwagi, T., "Ignition of a Liquid Fuel Under High Intensity Radiation," Combustion Science and Technology, Vol. 21, 1980, p. 131.

27. Kashiwagi, T., "Effects of Attenuation of Radiation on Surface Temperature for Radiative Ignition," Combustion Science an Technology, Vol.20, 1979, p. 225.

28. Kashiwagi, T., "Effects of Sample Orientation on Radiative Ignition," Combustion and Flame, Vol.44, 1982, p. 223.

29. Kashiwagi, T., "A Study of Oxygen Effects on Non-flaming Transient Gasification of PMMA and PE During Thermal Radiation", Nineteenth Symposium (International) on Combustion, The Combustion Institute, 1982, p. 1511.

30. Yoshizawa, Y., and Kubota, H., "Experimental Study of Gas Phase Ignition of Celluose under Thermal Radiation," Nineteenth Symposium (International) on Combustion, The Combustion Institute, 1982, pp.787-795.

31. Mutoh, N., Toshisuki, H., and Akita, K., "Experimental Study of Radiative Ignition of Polymethylmethacrylate,"

Seventeenth Symposium (International) on Combustion, The Combustion Institute, 1978, p. 1183.

32. Williams, F. A., Combustion Theory, The Benjamin/Cummings Publishing Company, Inc., Menlo Park, 1985.

33. Otey, G., and Dwyer, H. A., "Numerical Study of the Interaction of Fast Chemistry and Diffusion", AIAA Journal, Volume 17, 1979, p. 606.

34. Dwyer, H. A., and Sanders, B. R., and Raiszadek, F., "Ignition and Flame Propagation Studies with Adaptive Numerical Grids," Combustion and Flame, Vol. 52, 1983, pp. 11-23.

35. Dwyer, H. A., Kee R. J., and Sanders B. R., "Adaptive Grid Method for Problems in Fluid Mechanics and Heat Transfer", AIAA Journal, Volume 18, 1980, p. 1205.

36. Chorin, J. A., "Flame Advection and Propagation Algorithms," Journal of Computational Physics, Vol. 35, 1980, pp. 1-11.

37. Patankar, S. V., Numerical Heat Transfer and Fluid Flow, McGraw-Hill Book Co., New York, 1980.

38. Brosmer, M. A., and Tien, C. L., "Radiative Energy Blockage in Large Pool Fires," Combustion Science and Technology, Vol. 51, 1986, p. 21.

39. Brosmer, M. A., and Tien, C. L., "Thermal Radiation Properties of Propylene," Combustion and Flame, Vol. 61, 1986, pp. 177-190.

40. Mao, C. P., Kodama, H., and Fernandez-Pello, A. C., "Convective Structure of a Diffusion Flame Over a Flat

Combustible Surface", Combustion and Flame, Vol. 57, 1984, p.209.

41. Westbrook, C. K., and Dryer, F. L., "Chemical Kinetic Modeling of Hydrocarbon Combustion," Prog. Energy Combustion Science, Vol. 10, 1984, pp.1-57.

42. Kanury, A. M., Introduction to Combustion Phenomena, Gordon and Breach Co., London, 1975.

43. Drysdale, D., An Introduction to Fire Dynamics, John Wiley and Sons, Chichester, 1985.

44. Schlichting, H., Boundary-Layer Theory, Mcgraw-Hill Book Company, New York, 1968.

45. Pagni, P. J., Diffusion Flame Analyses, Fire Safety Journal, Vol. 3, 1980/1981, pp. 273-285.

List of Tables

List of Figures

problem. Ignition is caused by a hot fuel surface. 115

NIST-114A
(REV. 3-90)

U.S. DEPARTMENT OF COMMERCE
NATIONAL INSTITUTE OF STANDARDS AND TECHNOLOGY

BIBLIOGRAPHIC DATA SHEET

1. PUBLICATION OR REPORT NUMBER
NIST-GCR-92-604

2. PERFORMING ORGANIZATION REPORT NUMBER

3. PUBLICATION DATE
March 1992

4. TITLE AND SUBTITLE

Ignition and Flame Propagation Studies Over a Flat Fuel Surface

5. AUTHOR(S)

Bryan Thomas Amos

6. PERFORMING ORGANIZATION (IF JOINT OR OTHER THAN NIST, SEE INSTRUCTIONS)

University of California
Dept. of Mechanical Engineering
Berkeley, CA 94720

7. CONTRACT/GRANT NUMBER
NIST Grant 60NANB7D737

8. TYPE OF REPORT AND PERIOD COVERED
September 23, 1987

9. SPONSORING ORGANIZATION NAME AND COMPLETE ADDRESS (STREET, CITY, STATE, ZIP)

Building and Fire Research Laboratory
National Institute of Standards & Technology
U.S. Department of Commerce
Gaithersburg, MD 20899

10. SUPPLEMENTARY NOTES

11. ABSTRACT (A 200-WORD OR LESS FACTUAL SUMMARY OF MOST SIGNIFICANT INFORMATION. IF DOCUMENT INCLUDES A SIGNIFICANT BIBLIOGRAPHY OR LITERATURE SURVEY, MENTION IT HERE.)

Numerical studies are performed which show the evolution of the combustion process over a flat fuel surface subjected to an external source of radiation. Ignition is caused either by the high temperature of the fuel surface or by radiation absorption by the fuel vapor. The surface is assumed to be either in a zero gravity, initially stagnant air environment or in a stagnation point flow field. Regardless of the source of ignition considered or the type of the flow field, the same sequence of events is predicted. This sequence of events begins with a pre-ignition, radiation dominated phase in which fuel and air mix above the fuel surface. After ignition occurs, there is a period of weak chemical reaction, which is followed by a period of stronger reaction in which a premixed flame front develops. Before dying out the premixed flame front separates the fuel from the oxygen and leaves behind a diffusion flame. The combustion and radiation processes are shown to have a large effect on the flow field in the stagnation point flow cases. For the case in which ignition is caused by gas phase absorption, the radiation required to cause ignition is so high that an opposed jet flow is created. In the case in which ignition is caused by the hot surface, the radiation is lower and the boundary layer remains almost intact. For both types of ignition the premixed flame fronts produced heat fast enough that the expanding gas is able to drive the incoming flow back from the fuel surface. After the premixed flame front dies out leaving the diffusion flame the incoming flow again dominates and a boundary layer reappears.

12. KEY WORDS (6 TO 12 ENTRIES; ALPHABETICAL ORDER; CAPITALIZE ONLY PROPER NAMES; AND SEPARATE KEY WORDS BY SEMICOLONS)

combustion; diffusion flames; fuels; ignition; premixed flames; radiation; surface temperature

13. AVAILABILITY

X	UNLIMITED
	FOR OFFICIAL DISTRIBUTION. DO NOT RELEASE TO NATIONAL TECHNICAL INFORMATION SERVICE (NTIS).
	ORDER FROM SUPERINTENDENT OF DOCUMENTS, U.S. GOVERNMENT PRINTING OFFICE, WASHINGTON, DC 20402.
X	ORDER FROM NATIONAL TECHNICAL INFORMATION SERVICE (NTIS), SPRINGFIELD, VA 22161.

14. NUMBER OF PRINTED PAGES
148

15. PRICE
A07

ELECTRONIC FORM